

New Views of Lunar Geoscience: An Introduction and Overview

Harald Hiesinger and James W. Head III

*Department of Geological Sciences
Brown University
Box 1846
Providence, Rhode Island, 02912, U.S.A.
Harald_Hiesinger@Brown.edu James_Head_III@Brown.edu*

1. INTRODUCTION

Beyond the Earth, the Moon is the only planetary body for which we have samples from known locations. The analysis of these samples gives us “ground-truth” for numerous remote sensing studies of the physical and chemical properties of the Moon and they are invaluable for our fundamental understanding of lunar origin and evolution. Prior to the return of the Apollo 11 samples, the Moon was thought by many to be a primitive undifferentiated body (e.g., Urey 1966), a concept shattered by the data returned from the Apollo and Luna missions. Ever since, new data have helped to address some of our questions, but of course, they also produced new questions. In this chapter we provide a summary of knowledge about lunar geologic processes and we describe major scientific advancements of the last decade that are mainly related to the most recent lunar missions such as Galileo, Clementine, and Lunar Prospector.

1.1. The Moon in the planetary context

Compared to terrestrial planets, the Moon is unique in terms of its bulk density, its size, and its origin (Fig. 1.1a-c), all of which have profound effects on its thermal evolution and the formation of a secondary crust (Fig. 1.1d). Numerous planetary scientists considered the Moon as an endmember among the planetary bodies in our solar system because its lithosphere has been relatively cool, rigid, and intact throughout most of geological time (a “one-plate” planet), and its surface has not been affected by plate recycling, an atmosphere, water, or life. Therefore the Moon recorded and preserved evidence for geologic processes that were active over the last 4–4.5 b.y. and offers us the unique opportunity to look back into geologic times for which evidence on Earth has long been erased (Fig. 1.1c,d). Impact cratering, an exterior process, is considered the most important surface process on the Moon. Internal processes, such as volcanism and tectonism, also have played an important role.

The Moon represents a keystone in the understanding of the terrestrial planets. For the Moon we have a data set for geology, geochemistry, mineralogy, petrology, chronology, and internal structure that is unequaled for any planetary body other than the Earth. These data are fundamental to understanding planetary surface processes and the geologic evolution of a planet, and are essential to linking these processes with the internal and thermal evolution. The Moon thus provides a planetary process and evolutionary perspective.

Specifically, for important planetary processes such as impact cratering, the Moon records and preserves information about depths of excavation, the role of oblique impact, modification stages, composition and production of impact melt, ejecta emplacement dynamics, and the role of volatile-element addition. By virtue of the lunar samples returned from known geological units, the Moon also provides the foundation of crater size-frequency distribution chronologies

for the solar system. These data are key to further understanding the importance of this fundamental process in shaping planetary crusts, particularly early in solar-system history. For example, from crater counts it is apparent that the impactor flux was much higher in the early history of the Moon, the period of the “heavy bombardment,” which lasted until ~ 3.8 b.y. ago (e.g., Melosh 1989; Neukum et al. 2001).

The Moon also provides key information about planetary magmatic activity. We have a general picture of many aspects of plutonism (intrusion) and volcanism (extrusion), and can assess the role of magmatism as a major crust building and resurfacing process throughout history. The ages, distribution, and volumes of volcanic materials provide a record of the distribution of mantle melting processes in space and time. Furthermore, the detailed record coupled with the samples permit an assessment of the processes in a manner that can be used to infer similar processes on other planets. These data have provided a picture of the role of magmatic activity during the heavy bombardment (intrusion, extrusion, cryptomaria), and more recently in lunar history, the mare stratigraphic record, the distribution of basalt types, and the implied spatial and temporal distribution of melting. Stratigraphic information and crater ages are also providing an emerging picture of volcanic volumes and fluxes. In addition, the Moon allows us to assess a wide range of eruption styles, including pyroclastics and their petrogenetic significance.

The Moon provides a type locality for tectonic activity on a one-plate planet. Tectonic processes and tectonic activity can be understood in the context of the complete lunar data set, including the internal structure and thermal evolution data. Graben illustrate deformation associated with mascon loading, and wrinkle ridges appear to document the change in the net state of stress in the lithosphere from initially extensional to contractional in early lunar history. Finally we are able to link individual tectonic features to the lunar thermal evolution.

1.2. Lunar missions of the last decade

Several spacecraft visited the Moon during the 1990s and returned new data that have significantly expanded our knowledge about lunar topography, composition, internal structure,

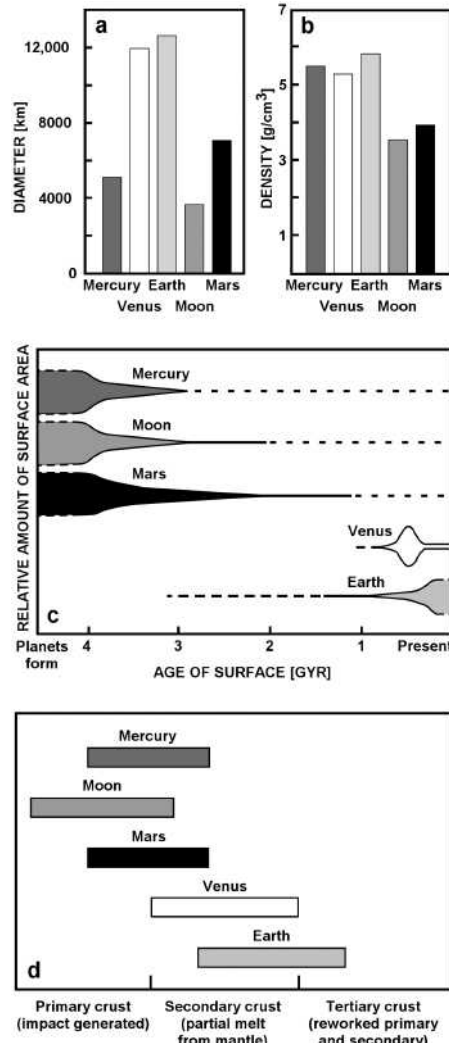


Figure 1.1. Comparison of the Moon with terrestrial planets in terms of (a) diameter, (b) bulk density, (c) surface age, and (d) types of crust (Used by permission of Sky Publishing, after Head 1999, *The New Solar System*, 4th ed., Fig. 1, p. 157, Fig. 18, p. 171, Fig. 20, p. 173).

magnetic field, and the impact flux in the inner solar system. This is only a partial list of specific fields for which a better understanding exists now compared to a decade ago. The results of these missions will be highlighted throughout various chapters of this volume.

In 1990 and 1992, the Galileo spacecraft used the Earth/Moon system for gravity assist maneuvers to gain enough momentum for its travel to Jupiter. During the first flyby, Galileo imaged the western nearside and parts of the farside that were not illuminated during the Apollo missions, thus becoming the first spacecraft to obtain multispectral images of the Moon since Mariner 10 days (Head et al. 1993). The images from the SSI camera (e.g., Belton et al. 1992) led to investigations of the crustal diversity of the western hemisphere, the geology of several lunar impact basins such as the Orientale basin and South Pole-Aitken basin, the western maria and their related deposits, and the post-Imbrium impact craters (e.g., Greeley et al. 1993; Head et al. 1993; McEwen et al. 1993; Pieters et al. 1993a). During the second flyby, Galileo took multispectral images from the north-central nearside (e.g., Belton et al. 1994) that allowed detailed studies, for example, of the Humboldtianum basin, a large impact structure only partially visible from Earth.

In 1994, Clementine spent two months in lunar orbit and acquired a global data set of just under two million digital images at visible and near-infrared wavelengths, which allowed detailed mapping of the lunar major mineralogy (i.e., mafic silicates and ilmenite) and rock types (Nozette et al. 1994). Clementine, which was originally intended to observe asteroid Geographos, had four cameras on board and mapped the Moon in 11 colors at an average surface resolution of ~200 m. Most widely used and best calibrated are data from the UV/VIS camera, which provided information in 5 narrow-band filters and 1 broad-band filter that have been used to derive the major mineralogy and global composition (FeO , TiO_2) of the lunar surface (e.g., Lucey et al. 1994, 1995, 1996, 1997, 1998, 2000; McEwen et al. 1994; Pieters et al. 1994; Shoemaker et al. 1994; Blewett et al. 1997; Giguere et al. 2000; Gillis et al. 2003). UV/VIS data have also been used to study specific lunar surface features in great detail (e.g., Staid et al. 1996; Hawke et al. 1999; Li and Mustard 2000; Staid and Pieters 2001), identify hidden mare deposits (e.g., Antonenko and Yingst 2002), estimate the thickness of mare basalts (e.g., Budney and Lucey 1998), and to investigate the structure and composition of the lunar crust (e.g., Tompkins et al. 1994, 2000; Neumann et al. 1996; Wieczorek and Phillips 1998, 2000; Jolliff et al. 2000). In addition, Clementine carried a laser altimeter, which provided the first global view of lunar topography (Zuber et al. 1994) and although the resolution of these data was not optimal, several previously unmapped impact basins were revealed (Spudis et al. 1994). Clementine also gave us the first look, albeit preliminary, at the global lunar gravity field (Zuber et al. 1994; Lemoine et al. 1997), which provided new insights into the internal structure and thermal evolution of the Moon. The new Clementine data gave us the first total view of the South Pole-Aitken basin, the oldest discernible impact structure on the Moon, which is ~2500 km in diameter and about 13 km deep (Spudis et al. 1994; Pieters et al. 2001; Petro and Pieters 2004). This basin is larger and deeper than the Hellas basin on Mars (Spudis 1993; Smith et al. 1999) and is the largest and deepest impact crater yet discovered in the solar system.

Lunar Prospector was launched in 1998 and was the first NASA-supported lunar mission in 25 years (Binder 1998). The main goal of the Lunar Prospector mission was to map the surface abundances of a series of key elements such as H, U, Th, K, O, Si, Mg, Fe, Ti, Al, and Ca with special emphasis on the detection of polar water-ice deposits. For this purpose, Lunar Prospector had several spectrometers on board, including a gamma-ray spectrometer, a neutron spectrometer, an alpha-particle spectrometer, a magnetometer/electron reflectometer, and a Doppler gravity experiment. The interpretation of high radar reflectivities and high polarization ratios associated with permanently shaded craters in the polar areas of Mercury (e.g., Slade et al. 1992) as water-ice deposits suggested that similar deposits might also exist on the Moon (Arnold 1979). Although an initial analysis of the Clementine bistatic radar data was consistent

with an occurrence of water-ice near the poles (e.g., Nozette et al. 1996), more detailed studies of the same data suggest that this interpretation is not unique (e.g., Simpson and Tyler 1999, Nozette et al. 2001, Vondrak and Crider 2003). Feldman et al. (1998, 2001) concluded that Lunar Prospector data are consistent with deposits of hydrogen in the form of water ice in the permanently shaded craters of the lunar poles. Lunar Prospector provided for the first time an entire suite of global elemental abundance maps, although at various resolutions. These maps are described in detail elsewhere (e.g., Lawrence et al. 1998, 2000, 2001, 2002; Feldman et al. 1999, 2001; Elphic et al. 2000; Maurice et al. 2001; Lawson et al. 2002; Prettyman et al. 2002) and in Chapter 2. Another important Lunar Prospector contribution is to completely outline a large area on the lunar nearside with high thorium concentrations (e.g., Lawrence et al. 1998) and to show the uniqueness of this terrane, the formation of which is enigmatic (see Chapters 2, 3, and 4). Lunar Prospector improved our knowledge of the global gravity field of the Moon and detected several new areas with large mass concentrations, so-called “mascons” (e.g., Konopliv et al. 1998, 2001). Finally, Lunar Prospector measured the lunar crustal magnetic field and provided further evidence that basin-forming impacts magnetize the lunar crust at their antipodes (e.g., Lin et al. 1988; Halekas et al. 2001; Hood et al. 2001).

1.3. Origin and evolution of the Moon

Numerous models, summarized in Hartmann et al. (1986), have been proposed for the origin of the Moon, including fission from Earth (e.g., Darwin 1879; Binder 1980), formation along with Earth as a sister planet (e.g., Schmidt 1959), and gravitational capture of a body formed elsewhere in the solar system (e.g., Gerstenkorn 1955). Today it is widely accepted that the Moon formed early in solar-system history when a Mars-sized object collided with the proto-Earth (Fig. 1.2a), ejecting crust and upper mantle material (Fig. 1.2b), which re-accreted in Earth orbit (Fig. 1.2c,d) (e.g., Hartmann and Davis 1975; Cameron and Ward 1976; Hartmann et al. 1986; Kipp and Melosh 1986; see Chapter 4). In order to create a Moon with the observed geochemical characteristics (see Chapter 7), the impactor’s iron and siderophile elements must have been concentrated into a core before the collision. While this core became incorporated into the Earth’s mantle, the outer portions of the impactor and the ejected terrestrial material accreted to the Moon.

Over the last decade significant improvements in numerical modelling of the origin and accretion of the Moon have been made and additional information can be found in Canup (2004), Canup et al. (2001), Levison et al. (2001), Agnor et al. (1999), Cameron and Canup (1998), Cameron (1997), Canup and Esposito (1996), Tonks and Melosh (1992, 1993), Cameron and Benz (1991), and Benz et al. (1986, 1987). Energy release associated with the large impact and accretion produced large-scale melting, that is a magma ocean, accompanied by density segregation of crystals from the melt and formation of a low-density, plagioclase-rich crust (Fig. 1.3). Chapter 4 regards the initial differentiation of the Moon in detail, including the magma ocean concept and alternative models. Figure 1.4 is an interpretative diagram of the thermal evolution of the Moon, which is discussed in detail in Chapter 4.

Seismic and remotely sensed data, as well as the lunar samples, suggest that the Moon has been differentiated into a crust, mantle, and possibly a small core, although higher resolution seismic data that come from a global (rather than just the nearside as in the Apollo Seismic Experiment) seismometer network are required for definitive conclusions. The formation of a globally continuous low-density crust is thought to be responsible for the lack of plate tectonics on the Moon, leading to dominantly conductive cooling through this layer and producing a globally continuous lithosphere (i.e., a one-plate planet) instead of multiple laterally moving and subducting plates as on Earth. It is currently thought that during and several hundred million years after the solidification of the magma ocean, a massive influx of projectiles, termed the “heavy bombardment,” impacted on the Moon (e.g., Ryder et al. 2000; Ryder 2002; see Chapter 5). The exact timing of the heavy bombardment remains an open question. This

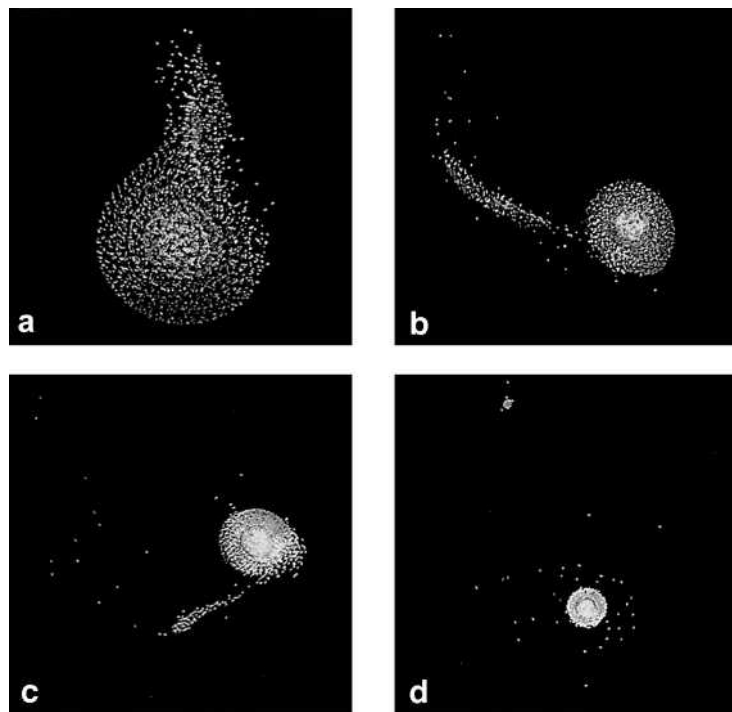


Figure 1.2. Computer simulation of the formation of the Moon. A Mars-size body impacts on proto-Earth (a), ejects crustal and mantle material (b-c), which later accretes to the Moon in Earth orbit (d). (Used by permission of Sky Publishing, in Spudis 1990, *The New Solar System*, 3rd ed., Fig. 14, p. 51).

heavy bombardment formed numerous craters and basins and obscured most evidence for early volcanism. Most evidence for volcanic flooding is only preserved since the waning stages of the heavy bombardment (3.8–3.7 Ga) when lavas could retain observable morphologies and were no longer covered and modified by regional impact-ejecta deposits. By about 2.0–1.5 Ga, basaltic lavas covered the surface to the presently observed extent (~17%) and made up ~1% of the volume of the lunar crust (Head 1976). Virtually no major internal geologic activity has occurred for the last 1.5 Ga.

1.4. Internal structure of the Moon

Since the publication of the Lunar Source Book (Heiken et al. 1991), new Clementine and Lunar Prospector data have provided improved models of the topography and internal structure of the Moon (e.g., Zuber et al. 1994; Smith et al. 1997; Konopliv et al. 1998, 2001; Wieczorek and Phillips 1998; Arkani-Hamed et al. 1999), which are discussed in Chapter 3.

A decade ago, topographic data were only available for limited areas of the Moon, that is, the areas covered by the Apollo laser altimeter and stereo imagery as well as by earth-based radar interferometry (e.g., Zisk 1978; Wu and Moore 1980). The Clementine topographic map of Zuber et al. (1994) was the first reliable global characterization of surface elevations on the Moon. Compared to data derived during the Lunar Orbiter missions (e.g., Müller and Sjogren 1968, 1969), Clementine also significantly improved knowledge of the lunar gravity field (e.g., Zuber et al. 1994), although for a variety of reasons these data are still subject to relatively large errors. From an assessment of the combined Clementine data, the lunar highlands appear to be in a state of near-isostatic compensation; however, basin structures show a wide range

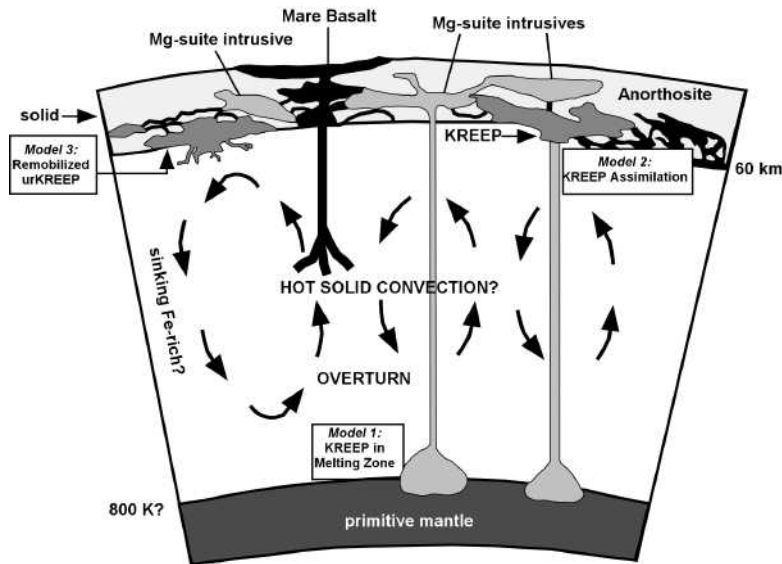


Figure 1.3. Pre-Lunar Prospector schematic cross section through the magma ocean down to ~800 km depth. An ~60 km thick crust of anorthosite forms from buoyant plagioclase cumulates. Also shown are three models for the origin of the younger Mg-suite rocks. In model 1 KREEP is delivered to depth by convective overturn and mixing with Mg-rich ultramafic cumulates. Model 2 is the same as model 1 with the exception that KREEP is assimilated at the base of the crust. Model 3 involves mobilization of urKREEP caused by decompressional melting triggered by basin-forming impact events (After Papike et al. 1998, *Planetary Materials*, Fig. 4, p. 5-5).

of compensation states that do not correlate with basin size or age (Zuber et al. 1994). Crustal thinning was observed beneath all resolvable basin structures and it was concluded that the structure and thermal history of the Moon are more complex than was appreciated ten years ago. Using Clementine data, the crustal thickness was modeled as ranging between ~20 and ~120 km, averaging at ~61 km (e.g., Neumann et al. 1996; Arkani-Hamed 1998; Khan et al. 2000; Wieczorek et al. 2001; Logonné et al. 2003; Wieczorek 2003). The average farside crust was estimated to be ~12 km thicker than on the nearside. Using Clementine data, von Frese et al. (1997) estimated a minimum crustal thickness of ~17 km beneath the Orientale basin, and Arkani-Hamed (1998) derived crustal thicknesses of 30–40 km beneath the mascon basins except for Crisium and Orientale where they estimated a thickness of ~20 km. Recently, from reinvestigation of Apollo seismic data, crustal thicknesses as low as 30 ± 2.5 km have been inferred for some regions of the nearside crust, and the region of thinnest crust is found to be located beneath Crisium (e.g., Khan et al. 2000; Wieczorek et al. 2001; Logonné et al. 2003; Wieczorek 2003). Using Lunar Prospector data, Konopliv et al. (1998) detected three new large mass concentrations (mascons) beneath Mare Humboldtianum, Mendel-Rydberg, and Schiller-Zucchinus, and possibly several others on the lunar farside (Konopliv et al. 2001).

Seismic data collected by seismometers emplaced by the Apollo astronauts revealed apparent divisions within the mantle at ~270 and ~500 km (e.g., Goins et al. 1978; Nakamura 1983). Below ~1000 km P- and S-waves are attenuated, suggesting minor partial melting. Because only P-waves are able to move through the core, it is reasonable to assume that the core is at least partially molten (Hood and Zuber 2000). Work by Khan et al. (2000), reanalyzing Apollo seismic data, resulted in a more detailed lunar velocity structure than was previously obtainable. On the basis of their reinterpretation, they found that the velocity increases from the surface to the base

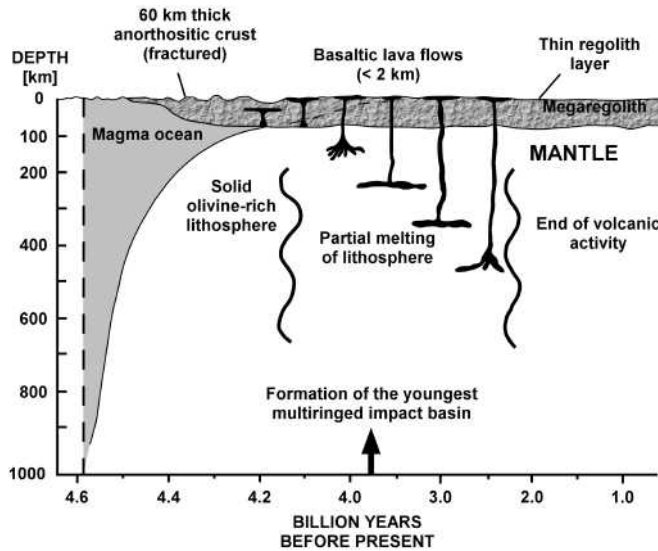


Figure 1.4. Evolution of lunar magma ocean, crust and mantle as a function of time. Simplified geological cross section of the outer 1000 km of the Moon showing (1) the evolution of the magma ocean by fractional crystallization (formation of olivine-rich residual mantle and plagioclase-rich flotation crust), (2) the simultaneous impact brecciation of the crust (megaregolith and regolith) and (3) the later partial melting of the mantle and the formation of chemically distinct basaltic lavas due to mineralogical zoning of the mantle established about 4.3 Ga. Timescale not linear. (Used by permission of Kluwer Academic Publishers, after Stöffler and Ryder 2001, *Chronology and Evolution of Mars*, Fig. 2, p. 11).

of the crust at 45 ± 5 km. Velocities remain constant throughout the upper mantle extending to 560 ± 15 km depth but are about 1 km/s higher in the middle mantle (Fig. 1.5). This work, coupled with that of Nakamura (2003, 2005), also resulted in an improvement in locating the origin of moonquakes. Shallow moonquakes were found to originate at ~ 50 – 220 km depths, deep moonquakes are located in 850–1000 km depth with a rather sharp lower boundary. Finally, Lognonné et al. (2003) presented a new seismic model for the Moon based upon a complete reprocessing of the Apollo lunar seismic data that suggested that the crust-mantle boundary is at ~ 30 km depth, with a pyroxenitic mantle. This model utilized electrical conductivity observations to suggest a liquid Fe core was not possible, but that their model was compatible with the Moon having a Fe–S liquid core. However, with the Apollo seismometers only located over a relatively small area on the lunar nearside, definitive conclusions about the global interior structure of the Moon based upon seismic data, including core size and composition, remain illusive.

The improved normalized polar moment of inertia provides an upper bound of the core radius, with core-free scenarios possible. The polar moment of inertia data were interpreted by Konopliv et al. (1998) to be consistent with an iron core of 220–450 km radius. However, moment of inertia data are also consistent with a core-free Moon (e.g., Kuskov and Konrod 2000). Support for the existence of a core comes from Lunar Prospector magnetometer data that indicate a core size of 340 km (Hood et al. 1999; Khan et al. 2004) and from analysis of laser ranging data, which indicates a liquid core having a radius less than 374 km (Williams et al. 2001a). The internal structure of the Moon is considered in more detail in Chapter 3.

1.5. Diversity of lunar rocks

The 6 Apollo missions returned 381.7 kg of lunar rocks or 2196 individual samples, and the Luna missions brought 276 g of lunar regolith to Earth (Table 1.1). Figure 1.6a is a view of the

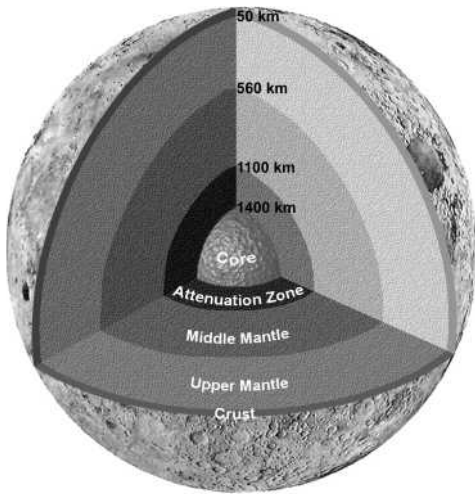


Figure 1.5. Model of the internal structure of the Moon. The thickness of the crust and mantle are based on work by Khan et al. (2000), the size of the core is based on work by Konopliv et al. (1998) and Hood et al. (1999).

The lunar experience has shown the utility of samples from other planets for comparative planetology. For example, samples from Mars will provide a record of the history of water on the surface of that planet, samples from Mercury will record whether there was active basaltic volcanism in its past, samples from Venus will be key to understanding its evolution and its heat- and volatile-loss mechanisms, and additional samples of the Moon, for example from the South Pole-Aitken basin, will lead to a better understanding of its internal structure, thermal evolution, and geologic history (see Chapters 3, 5 and 7). Here we provide only a very brief summary of the returned samples and point the reader to extensive summaries (and references therein) in BVSP (1981), Taylor et al. (1991), Haskin and Warren (1991), Papike et al. (1998), and in the following chapters.

Lunar materials can be classified on the basis of texture and composition into four distinct groups: (1) pristine highland rocks that are primordial igneous rocks, uncontaminated by impact mixing; (2) pristine basaltic volcanic rocks, including lava flows and pyroclastic deposits; (3) polymict clastic breccias, impact melt rocks, and thermally metamorphosed granulitic breccias; and (4) the lunar regolith. Details on the classification are given in Tables 1.1 and 1.2. A detailed discussion of lunar rock types is given in Chapters 2 and 3.

Pristine highland rocks can be subdivided into two major chemical groups based on their molar $\text{Na}/(\text{Na}+\text{Ca})$ content versus the molar $\text{Mg}/(\text{Mg}+\text{Fe})$ content of their bulk rock compositions (e.g., Warner et al. 1976; Papike et al. 1998). The ferroan anorthosites yield ages in the range 4.5–4.3 Ga; the magnesian-suite rocks (high Mg/Fe) are, as a group, somewhat younger (4.43–4.17 Ga) (Taylor et al. 1993) and contain dunites, troctolites, norites, and gabbro-norites. A less abundant alkali suite contains similar rock types, but enriched in alkali and other trace elements, and extending to somewhat younger ages. This rather simple picture has been complicated by more recent work (e.g., see Shearer and Newsom 2000). The magnesian suite may mark the transition between magmatism associated with the magma ocean and serial magmatism. This transition period may have occurred as early as 30 Ma (Shearer and Newsom 2000) or as late as 200 Ma after the formation of the magma ocean (Solomon and Longhi

lunar nearside and shows the location of the Apollo and Luna landing sites from which the samples originated, as well as the names and locations of major impact structures and maria. Figure 1.6b shows the lunar farside with several impact basins, including the largest basin, South Pole-Aitken. The importance of the returned samples, which are the only extraterrestrial samples that were specifically selected by humans, cannot be overemphasized. The returned samples have allowed scientists to study in great detail the age, mineralogy, chemistry, and petrology of lunar rocks as well as their physical properties (Fig. 1.7) and, maybe most importantly, the samples have allowed remotely sensed data to be properly calibrated, interpreted, and expanded to areas where no samples have been returned. Having lunar samples on Earth makes the Moon a true and unique keystone in our understanding of the entire solar system.

1977; Longhi 1980). The duration of magnesian-suite emplacement into the crust is also an open issue. The absence of magnesian-suite rocks with ages similar to products of the younger episodes of KREEP basaltic magmatism can be explained by a lack of deep sampling after 3.9 Ga due to a decrease in impact flux. “KREEPy” rocks are enriched in potassium (K), rare-earth elements (REE), and phosphorus (P), and are recognized in many breccias owing to the unique chemical signature. Recent Lunar Prospector data indicate that KREEP-rich rocks are most abundant around the Imbrium basin. For a more detailed description of these rock types

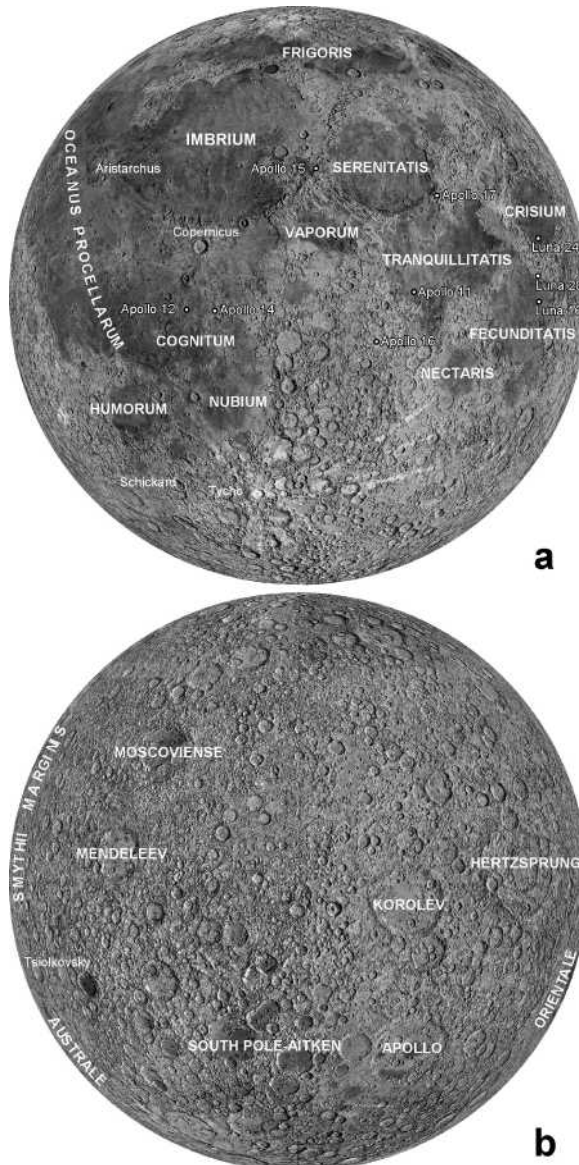


Figure 1.6. Global views of the Moon (USGS shaded relief map) which show the location of the Apollo and Luna landing sites, basins, and other prominent morphologic features; (a) nearside, (b) farside.

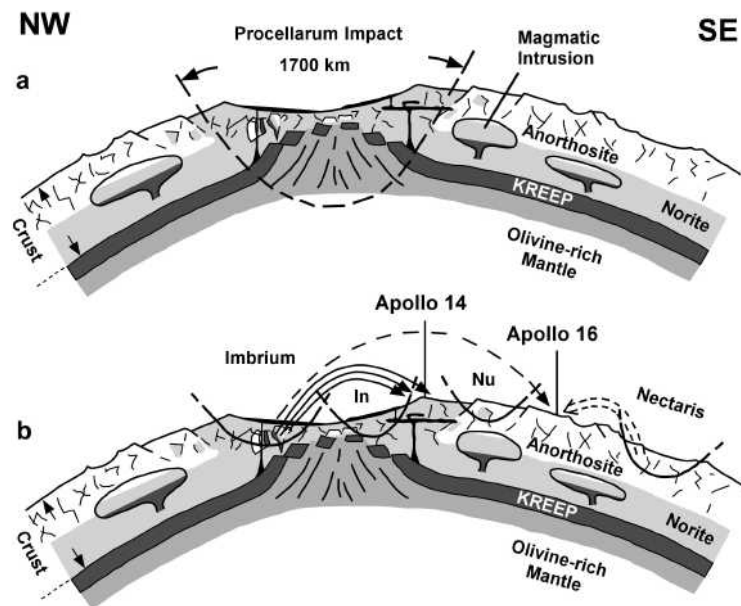


Figure 1.7. Conceptual cross sections of lunar crust and upper mantle at two different early stages. (a) Simplified cross section of lunar crust and upper mantle ~4.2 Ga shortly after the formation of a hypothetical Procellarum impact basin, which would have uplifted lower crust and upper mantle, bringing material from the layer of residual melt (ur-KREEP) and from some layered intrusive plutons containing Mg-suite igneous rocks near the surface. (b) Simplified cross section as in (a) but at ~3.8 Ga, shortly after the formation of the Imbrium impact basin, explaining the widespread occurrence of KREEP-rich lithologies around this basin; note that the Apollo 14 and 16 landing sites collected mainly Imbrium ejecta and Nectaris and Imbrium ejecta, respectively; In = Insularum basin, Nu = Nubium basin; Figures adapted from Stöffler (1990).

see Chapters 2 and 3. Most highland rocks were formed during the early differentiation of the Moon when upward separation of buoyant plagioclase within a magma ocean produced a thick anorthositic crust (see Chapter 4). Taylor et al. (1993) estimated that the magnesian-suite rocks make up ~20% of the uppermost 60 km of the crust; the rest is composed of ferroan anorthosite. Studies conducted since Lunar Prospector, however, suggest a more restricted provenance for the magnesian and alkali suite rocks (e.g., Jolliff et al. 2000; Korotev 2000; see Chapter 3). Non-volcanic rocks and the breccias and regolith derived from them cover about 83% of the lunar surface and are likely to represent over 90% of the volume of the crust (Head 1976).

Mare basalts are variably enriched in FeO and TiO₂, depleted in Al₂O₃, and have higher CaO/Al₂O₃ ratios than highland rocks (Taylor et al. 1991). Mineralogically, mare basalts are enriched in olivine and/or pyroxene, especially clinopyroxene, and depleted in plagioclase compared to highland rocks. Mare basalts originate from remelting of mantle cumulates produced in the early differentiation of the Moon. KREEP basalts, with enriched concentrations of incompatible elements, differ fundamentally from mare basalts and are thought to have formed by remelting or assimilation by mantle melts of late-stage magma-ocean residua, so-called urKREEP (Warren and Wasson 1979; see Chapter 4). Several classification schemes exist for lunar mare basalts based on their petrography, mineralogy, and chemistry (e.g., Neal and Taylor 1992; Papike et al. 1998). For example, using TiO₂ contents, mare basalts have been classified into three groups: high-Ti basalts (>9 wt% TiO₂), low-Ti basalts (1.5–9 wt% TiO₂), and very low-Ti (VLT) basalts (<1.5 wt% TiO₂) (Taylor et al. 1991).

Table 1.1. Classification of lunar rocks and statistics of samples at the lunar landing sites.

Sample Summary	A 11	A 12	A 14	A 15	A 16	A 17	L 16	L 20	L 24
Number of samples	58	69	227	370	731	741	1 core	1 core	1 core
Total mass (kg)	21.6	34.3	42.3	77.3	95.7	110.5	0.101	~0.05	0.17
Wt% of rocks >10 mm	44.9	80.6	67.3	74.7	72.3	65.9	-	-	-
plutonic	2	<1	<1	<1	12	5			
volcanic (basalt)	20	79	9	38	<1	29			
impactite	23	2	58	36	62	32			
Wt% soil fines < 10 mm	34.6	16.8	30.6	17	19.3	26.7	100	100	100
Wt% drill cores	0.4	1.2	0.9	6	7.4	6.6	100	100	100
IGNEOUS ROCKS (FIRST GENERATION)									
<i>Plutonic rocks</i>									
Anorthosite	Granite						Basalts		
Gabbronorite	Quartz monzodiorite						Aluminous basalt		
Troctolite	Monzogabbro						KREEP-basalt		
Dunite							Mare basalt		
Norite							Basaltic glass		
METAMORPHIC ROCKS (SECOND GENERATION)									
<i>Recrystallized rocks/breccias</i>									
Granulites	Polymict (<i>impact</i>) breccias						Impact melt rocks, clast-bearing, feldspathic		
Granulitic breccias							Impact melt rocks, clast bearing, mafic		
<i>Monomict (<i>impact</i>) breccias</i>							Impact melt rocks, clast-free		
Cataclastic plutonic rocks							Fragmental (lithic) breccias		
Cataclastic metamorphic rocks							Impact glass		
POLYMIXT IMPACT BRECCIAS (THIRD GENERATION)									
<i>Fragmental (lithic) breccias</i>									
Regolith breccias									
Impact glass									

Data from Heiken et al. (1991); weight percentages of the total weight of all samples of each mission given in italics; *Wt.% of total of rocks > 10 mm; from Stöfler and Ryder (2001).

The TiO_2 content, which is the most useful discriminator to classify lunar mare basalts, can be derived from remotely sensed data. The TiO_2 concentrations of the lunar samples have been studied extensively (e.g., Papike et al. 1976; Papike and Vaniman 1978; Neal and Taylor 1992; Papike et al. 1998) and numerous attempts have been made to expand this knowledge with remote-sensing techniques in order to derive global maps of the major mineralogy/chemistry of the Moon (e.g., Charette et al. 1974; Johnson et al. 1991; Melendrez et al. 1994; Shkuratov et al. 1999; Lucey et al. 2000; Giguere et al. 2000). From the Apollo and Luna samples, an early reading of the data suggested that Ti-poor basalts were generally younger than Ti-rich basalts, and models were proposed in which lunar mare volcanism began with high- TiO_2 content but decreased with time, and that this was coupled to depth of melting (e.g., Taylor 1982). However remote-sensing data indicate that young basalts exist with high TiO_2 concentrations (e.g., Pieters et al. 1980) and lunar basaltic meteorites have been found that are very low in Ti content and are old (mostly >3 Ga) (Cohen et al. 2000a). Based on Clementine data, Lucey et al. (2000) produced maps of the iron and titanium concentrations of the lunar surface. Combining these maps with crater size-frequency distribution ages, Hiesinger et al. (2001) found no distinct correlation between the deposit age and the composition. Instead, FeO and TiO_2 concentrations appear to vary independently with time, and generally eruptions of TiO_2 -rich and TiO_2 -poor basalts have occurred contemporaneously, as is the case for basalts with varying FeO contents.

Lunar impact breccias are produced by single or multiple impacts and are a mixture of materials derived from different locations and different kinds of bedrock (Table 1.2). They contain various proportions of clastic rock fragments and impact melts, and show a wide variety of textures, grain sizes, and chemical compositions. A widely adopted classification of breccias was presented by Stöffler et al. (1980), who discriminated between fragmental, glassy melt, crystalline melt, clast-poor impact melt, granulitic, dimict, and regolith breccias. A detailed discussion of these breccias is provided in Taylor et al. (1991), Papike et al. (1998), and in subsequent chapters of this volume.

“Lunar regolith” usually refers to the fine-grained fraction (mostly <1 cm) of unconsolidated surface material. The term “soil” has often been misused in the literature to describe this material. Lunar regolith ranges in composition from basaltic to anorthositic (with a small meteoritic component usually $<2\%$), has an average grain size of ~ 60 – 80 μm , and consists of mainly five particle types: mineral fragments, pristine crystalline rock fragments, breccia fragments, glasses, and agglutinates (McKay et al. 1991). Agglutinates are aggregates of smaller particles welded together by glasses produced in micrometeorite impacts, which also produces an auto-reduction of FeO to metallic Fe, increasing the abundance in nanophase iron in the more “mature” regolith (see Chapter 2). Lunar regolith exhibits variations in maturity, a quality which is roughly proportional to the time the soil is exposed to micrometeorite bombardment and the agglutinate abundances. With the exception of a few small-scale exposures of bedrock, lunar regolith covers more or less the entire lunar surface. Thus, understanding the optical properties, for example the effects of grain size and maturity of the lunar regolith, is extremely important for optical remote-sensing techniques (see Chapter 2) such as the mapping of TiO_2 and FeO abundances (e.g., Pieters 1993b; Lucey et al. 2000; Taylor 2002).

1.6. Lunar meteorites

Since about 1980, more than 36 meteorites have been recovered, mostly from Antarctica and the Sahara desert, that have proven to be pieces of the Moon delivered to Earth as debris from large impacts. Extensive work has been done on the lunar meteorites (e.g., see Warren 1994; Korotev et al. 1996, 2003a,b). In contrast to martian meteorites, which are mostly igneous rocks from terrains younger than 1.3 Ga (McSween 1999), the lunar meteorites are mostly samples of the very old highlands, though some basaltic lavas from the maria are present in the collection. Ages derived by ^{40}Ar - ^{39}Ar techniques of 31 impact-melt clasts in lunar meteorites range from ~ 2.43 – 4.12 Ga with most of the meteorites being older than 3 Ga (Cohen et al.

Table 1.2. Classification of impactites according to a provisional proposal by the IUGS Subcommission of the Systematics of Metamorphic Rocks (SCMR), Subgroup “Impactites” (Stöffler and Grieve 1994, 1996).

I. CLASSIFICATION OF IMPACTITES FROM SINGLE IMPACTS

Proximal impactites

<i>Shocked rocks^a</i>	<i>Impact melt rocks^b</i>	<i>Impact breccias</i>
4–6 stages of progressively increasing shock metamorphism ^d	Clast-rich Clast-poor Clast-free	Cataclastic (monomict) breccia Lithic breccia (without melt particles) ^c Suevite (with melt particles) ^c

Distal impactites

<i>Consolidated</i>	<i>Unconsolidated</i>
Tektite*	Air fall bed
Microtektite*	
Microkrystite*	

II. CLASSIFICATION OF IMPACTITES FROM MULTIPLE IMPACTS¹

<i>Impact detritus</i> (unconsolidated impactoclastic debris)	<i>Shock lithified impact detritus</i> (consolidated impactoclastic debris)	
Regolith ²	Regolith breccias ² (breccias with matrix melt and melt particles)	Lithic (“fragmental” ³) breccias (breccias without matrix melt and melt particles)

^a either as clasts in polymict breccias and impact melt rocks or as zones in the crater basement

^b may be subclassified into glassy, hypocrystalline, and holocrystalline varieties

^c generally polymict but can be monomict in a single lithology target

^d depending on type of rock (see Table 1.4)

* impact melt with very minor or minor admixed shocked and unshocked clasts

¹ best known from lunar rocks (Apollo and Luna) and from lunar and asteroidal meteorites

² contain solar wind gases

³ previously used for lunar rocks and meteorites

2000a). These ages have been attributed to seven different impact events ranging in age from 2.76 to 3.92 Ga (Cohen et al. 2000a). Most of the lunar meteorites are feldspathic regolith breccias or impact-melt breccias, and there is evidence that some of the lunar meteorites might share the same source crater. For example Warren (1994) proposed that Asuka-881757 and Y-793169 (most probable) and Y-793274 and EET875721 were derived from the same source crater, respectively. Similarly, Arai and Warren (1999) found that QUE94281 is remarkably similar to Y-793274 and interpreted this as evidence for a shared launch. Warren (1994) also suggested that some lunar meteorites were launched from <3.2 m depth within the last 1 million years. In addition to the Apollo and Luna sample collection lunar meteorites are “new” samples, which provide significant new information about the Moon because they potentially represent areas not sampled by the Apollo and Luna missions. Unlike the returned samples, however, the lunar meteorites do contain a terrestrial weathering component.

1.7. The stratigraphic system of the Moon

Numerous attempts have been made to subdivide the history of the Moon into time-stratigraphic systems (e.g., Shoemaker and Hackman 1962; Shoemaker 1964; McCauley 1967,

Wilhelms 1970, Stuart-Alexander and Wilhelms 1975; Wilhelms 1987). The basic idea is to use the ejecta blankets of large basins and craters as global marker horizons, similar to time-stratigraphic units on Earth, in order to establish a relative stratigraphy of the Moon. The most widely accepted stratigraphy is based on work by Wilhelms (1987), who divided the lunar history into five time intervals, the pre-Nectarian (oldest), the Nectarian, the Imbrian, the Eratosthenian, and the Copernican System (Fig. 1.8). Assigning absolute ages to these stratigraphic periods is controversial and depends mostly on an interpretation of which sample represents the “true” age of a specific impact event, i.e., the Imbrium or Nectaris event (Fig. 1.9) (e.g., Baldwin 1974, 1987; Jessberger et al. 1974; Nunes et al. 1974; Schaefer and Husain 1974; Maurer et al. 1978; Neukum 1983; Wilhelms 1987; Stöffler and Ryder 2001). Detailed discussions of this issue occur elsewhere (e.g., Spudis 1996; Hiesinger et al. 2000; and in Chapter 5). The chronostratigraphic systems such as *Imbrian*, *Eratosthenian*, and *Copernican* were defined in different ways that couple measured ages of samples to specific key lunar impact events (e.g., Wilhelms 1987; Neukum and Ivanov 1994; Stöffler and Ryder 2001). For example, the beginning of the Eratosthenian system, 3.2 Ga, is based on the measured ages of basalts onto which ejecta from the crater Eratosthenes (which has no rays) are superposed. However, the stratigraphies vary

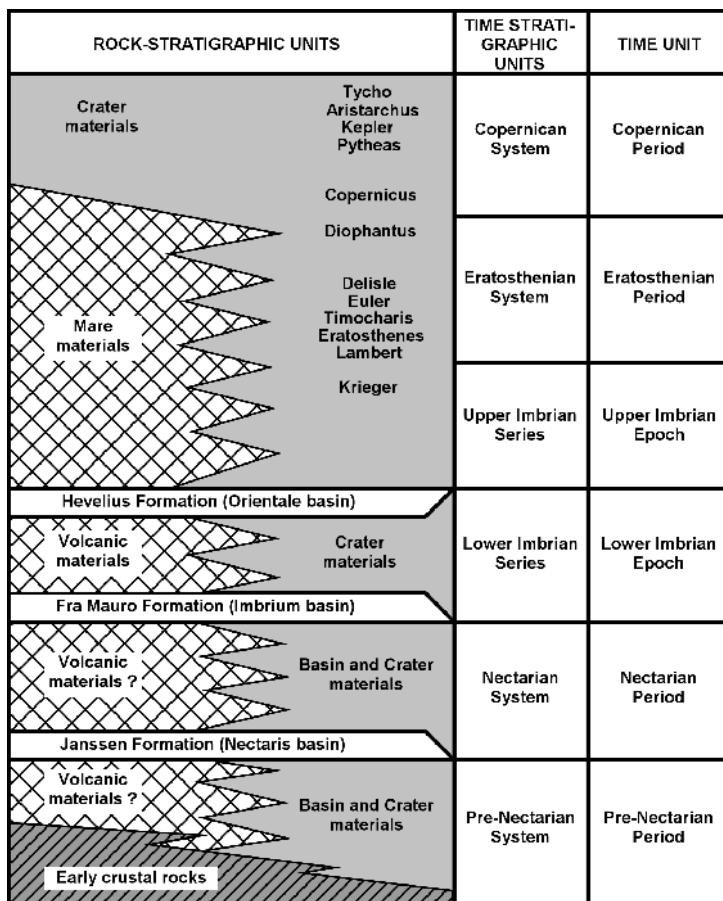


Figure 1.8. The stratigraphic system of the Moon. (Courtesy of the U. S. Geological Survey, after Wilhelms 1987, *The Geologic History of the Moon*, Fig. 7.1, p. 121).

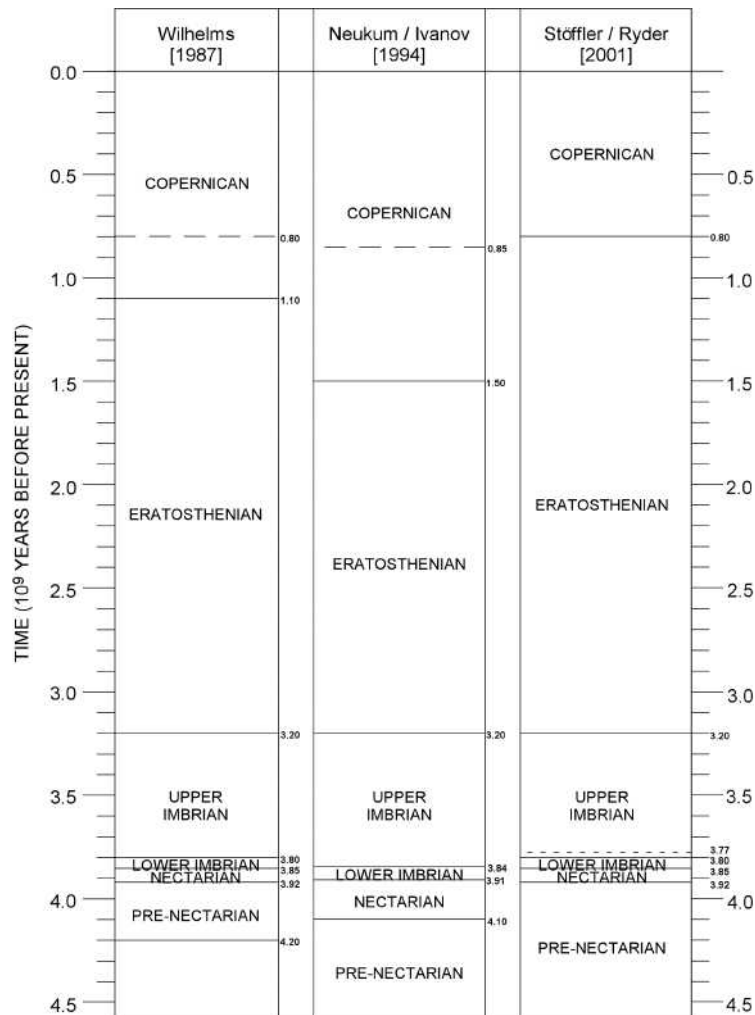


Figure 1.9. Comparison of stratigraphies of Wilhelms (1987), Neukum and Ivanov (1994, and Stöffler and Ryder (2001). Dashed lines in the stratigraphies of Wilhelms (1987) and Neukum and Ivanov (1994) indicate radiometric ages, which these authors attribute to the formation of the crater Copernicus. In Stöffler and Ryder (2001) two formation ages for the Imbrium basin have been proposed, that is, 3.85 Ga and 3.77 Ga (dashed line).

substantially in their definition of the beginning of the Copernican system i.e., 0.8–1.5 b.y., based on different interpretations of the age of Copernicus. A detailed and updated review of the available sample data and their stratigraphic interpretations is given in Chapter 5.

On the basis of Wilhelms' (1987) work, the pre-Nectarian Period spans from the time of accretion (~4.5 b.y.) to ~3.92 b.y., the time of the formation of the Nectaris basin, which is based on the ages of impact-melt breccia from Apollo 16. The pre-Nectarian Period is characterized by an intense impact bombardment that melted and mixed the lunar surface to significant depth. This bombardment is accompanied by the differentiation of a feldspathic crust and a more mafic mantle from a magma ocean prior to about 4.4–4.3 b.y. ago. The age of the Nectaris basin

of ~3.92 b.y. was tentatively inferred from samples of the Apollo 16 landing site, but recently this has been challenged by Haskin et al. (1998, 2003), who argued that these samples may represent Imbrium ejecta. Accepting the age of 3.92, then the Nectarian Period lasted from ~3.92 b.y. until ~3.85 b.y. when the Imbrium impact occurred. However, Stöffler and Ryder (2001) presented arguments for two distinctly different ages of the Imbrium event, one 3.77 (Stöffler), the other 3.85 b.y. (Ryder). During the Nectarian Period, continued heavy impact bombardment resulted in the formation of a number of large impact basins, of which two were sampled (Serenitatis, Crisium). There is also evidence for early volcanism during the Nectarian but the extent remains undetermined.

Wilhelms (1987) subdivided the Imbrian Period into Early (~3.85–3.8 b.y.) and Late Imbrian Epochs (~3.8–3.2 b.y.). During the Early Imbrian, two major impact basins (Imbrium, Orientale) were formed that had profound effects on the subsequent and present day appearance of the Moon. Cessation of giant impacts during the Late Imbrian enabled mare basalts that were continuously extruded, finally to remain preserved on the surface (Fig. 1.10). Wilhelms (1987) argued that Imbrian mare basalts probably lie beneath the entire area now covered with mare basalts.

The Eratosthenian Period, which began at ~3.2 b.y. ago and lasted for ~2.1 b.y., is characterized by continued volcanic eruptions and interfingering of volcanic deposits with crater materials. However, both impact rates and volcanic activity declined drastically during the Eratosthenian Period.

The beginning of the Copernican Period has not been accurately dated on either an absolute or a relative time scale. Apollo 12 samples, thought to represent ray material from Copernicus,

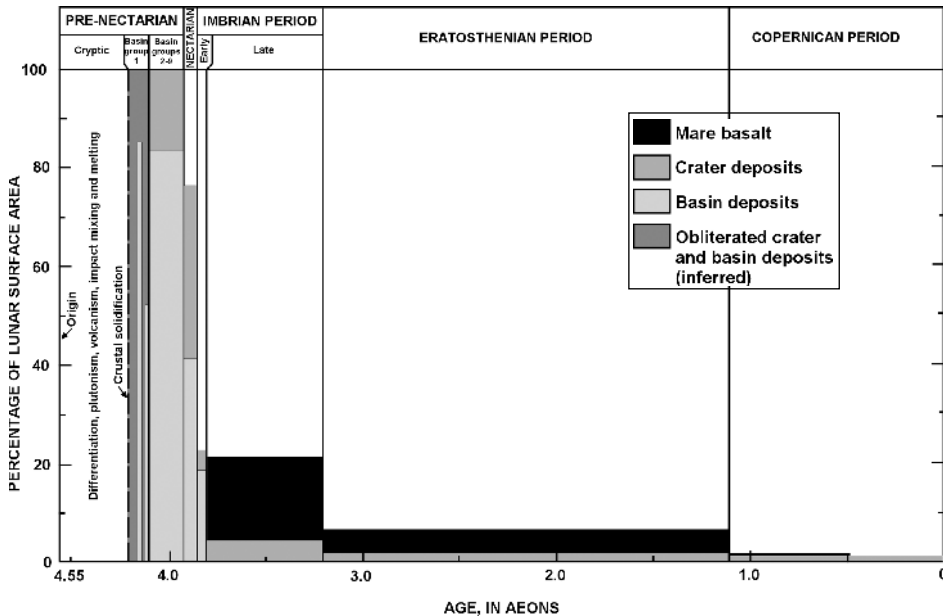


Figure 1.10. Stratigraphy of the Moon (after Wilhelms, 1987). The vertical axis indicates the surface area inferred to have been originally covered by each group of deposits. Basin and crater deposits are assumed to extend one diameter from the crater (i.e., the continuous ejecta), mare deposits of each age are assumed to extend beneath the entire area of the younger maria. Procellarum and South Pole-Aitken basin (pre-Nectarian group 1) are shown diagrammatically as narrow vertical bars. (Courtesy of the U. S. Geological Survey, after Wilhelms 1987, *The Geologic History of the Moon*, Fig. 14.3, p. 277).

yield an uncertain age of 0.81 b.y.; crater frequencies suggest an age of 1.1 b.y. This age is extremely important to know accurately because it provides a guideline for the interpretation of rayed craters in general and of the length required for impact gardening to homogenize ray material and substrate, thus erasing the ray signature. Volcanism finally stopped during the Copernican Period, and mare units younger than ~1.5 b.y. are known only from a few regions (e.g., Schultz and Spudis 1983; Hiesinger et al. 2000, 2003). Impacts, mostly of small scale, still occur on the Moon and are responsible for the formation of the uppermost layer of comminuted rock and glass particles, termed the regolith. Figure 1.11 shows conceptually the various evolutionary stages of the Moon, depicting how the Moon might have looked (a) 3.8–3.9 b.y. ago, (b) 3.0 b.y. ago, and (c) today.

2. GEOLOGIC PROCESSES

The next sections are intended as brief descriptions and syntheses of lunar processes and surface features that are crucial for understanding the geologic history and evolution of the Moon. An introduction to impact cratering, followed by introductions to volcanism and tectonism summarize important basic concepts, provide background knowledge, and set the stage for the following chapters.

2.1. Impact processes

2.1.1. Origin of craters. Although craters on the Moon were once thought to be mostly volcanic in origin (e.g., Dana 1846; Spurr 1944, 1945, 1948, 1949), we know today that most of these craters were formed by impact processes. The Moon has been struck by 15–20 km/sec projectiles that range over 35 orders of magnitude in mass from microscopic dust particles of 10^{-15} g to asteroids as massive as 10^{20} g. The associated kinetic energies vary from a fraction of an erg to $\sim 10^{32}$ erg per individual impact and can exceed the total internal energy of 10^{26} – 10^{27} erg that is released by the Earth during one year (Lammlein et al. 1974). A non-trivial amount of meteoritic material has been added since the solidification of the Moon's crust. For example, Chyba (1991) estimated addition of $\sim 10^{20}$ kg of material from impacts, with perhaps half of it retained (compared to a lunar mass: 7.35×10^{22} kg). An extensive review

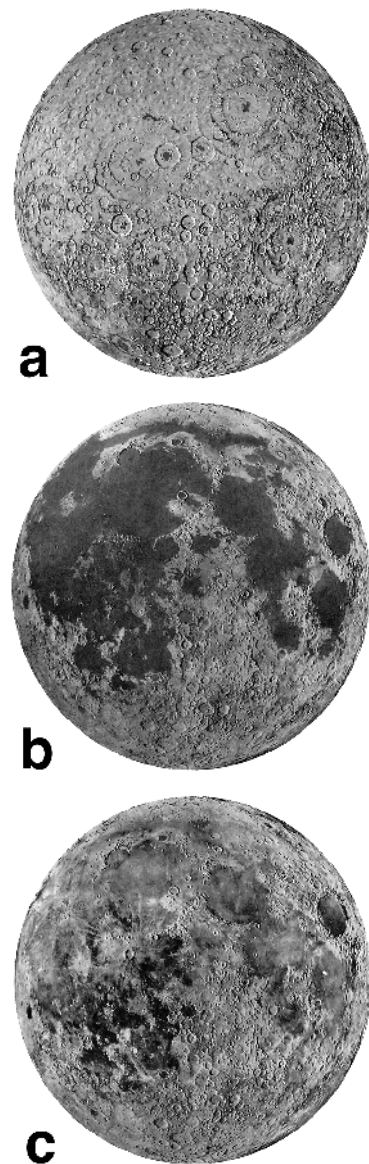


Figure 1.11. Artist conception of the evolution of the nearside of the Moon. (a) Surface of the Moon as it probably appeared after the formation of most of the lunar impact basins but before the formation of the Imbrium basin 3.8–3.9 Ga; (b) features as they probably appeared after the emplacement of most of the extensive mare floods 3.0 Ga, (c) the present appearance of the Moon. [After Fig. 2.7, p. 20–21 in *Lunar Source Book*, edited by Heiken et al. (1991). Artist: Don Davis].

of impact cratering as a geologic process was provided by Melosh (1989), including discussions on the influence of an atmosphere and different gravities, impact angles, and velocities.

2.1.2. Morphology of craters. From examination of the morphology of lunar impact craters in different size ranges, it is apparent that with increasing diameter, craters become proportionally shallower (e.g., Pike 1980) and develop more complex floor and rim morphologies, including the formation of multiple rings and central peaks (Fig. 1.12a–h). Impact crater morphologies can be characterized as (1) simple craters, (2) complex craters, and (3) basins. Simple craters are usually bowl-shaped, with rounded or small flat floors, smooth rims, and no wall terraces. With increasing diameter, simple craters transition into complex craters showing terraces and crenulated rims, zones of broad-scale inward slumping, and uplifted central peaks protruding through a wide, flat floor. On the Moon this transition from simple to complex craters occurs at about 15–20 km (Pike 1977). The diameter of this transition scales to $1/g$ for planetary surfaces when strength is not strain-rate dependent (O'Keefe and Ahrens 1993, 1994). At diameters in excess of 100 km, peak rings occur on the crater floor, defining the transition from craters to basins (Hartmann and Kuiper 1962). Central-peak basins with a fragmentary ring of peaks, such as in crater Compton, are found in the 140–175 km diameter range and are transitional to peak-ring basins, which have a well-developed ring but lack a central peak. Peak-ring basins like the Schrödinger basin are generally 175–450 km in diameter. Finally, multiring basins on the Moon, such as the Orientale basin, are larger than 400 km and have up to six concentric rings. Spudis (1993) reviewed the geology of lunar multiring impact basins; for a more detailed discussion of morphologic parameters of lunar craters and basins such as crater diameter/depth ratios etc., see for example Pike (1977, 1980) and Williams and Zuber (1998). A discussion of the influence of a planet's curvature on the shape of impact craters is provided, for example, by Fujiwara et al. (1993). The effects of target porosities are discussed by Love et al. (1993) and the influence of impact angle on crater shape are discussed in Burchell and Mackay (1998).

On the Moon, an airless body with most “erosion” related to impact processes, we can observe a large number of craters over a wide range of sizes, degradation stages, and morphologies. The large number of lunar impact craters and their characteristics provide excellent statistics for detailed quantitative studies of crater morphologies (e.g., Pike 1980), which can be used for comparison with other planetary bodies, such as Mercury, Mars, Venus, the asteroids, or the moons of the outer planets. Studies of terrestrial impact craters complement the investigations of lunar craters. On Earth, erosional processes can remove most of the surface features of impact craters (e.g., ejecta blankets, crater rims) and expose deeper levels within or beneath the original crater. This allows a three-dimensional study of large-scale impact craters not possible on other planets or in the laboratory. As a result, many fundamental concepts of cratering mechanics have been established on terrestrial impact structures and then applied to craters elsewhere in the solar system.

2.1.3. Cratering mechanics. An understanding of the observed variety of lunar impact crater morphologies requires a basic knowledge of cratering mechanics. On the basis of observations and modelling of lunar impact crater morphologies, we now know that the morphology of a crater is strongly dependent on the interaction of stress waves with free surfaces as well as upon the thermodynamics of the stress wave itself (e.g., Melosh 1989). Rocks that were formed during the impact process, i.e., the breccias returned by the Apollo missions, provide key information on the cratering process. For example, from these samples we can estimate the temperature and pressure regimes to which the breccias were exposed during their formation.

The mechanics of impacts that produce small, simple craters have been extensively studied and are relatively well understood from observations of experimental craters. During the very first stages of an impact, the projectile's kinetic energy is transformed into shock waves that travel forward into the target surface and backward into the projectile. Within the target, the

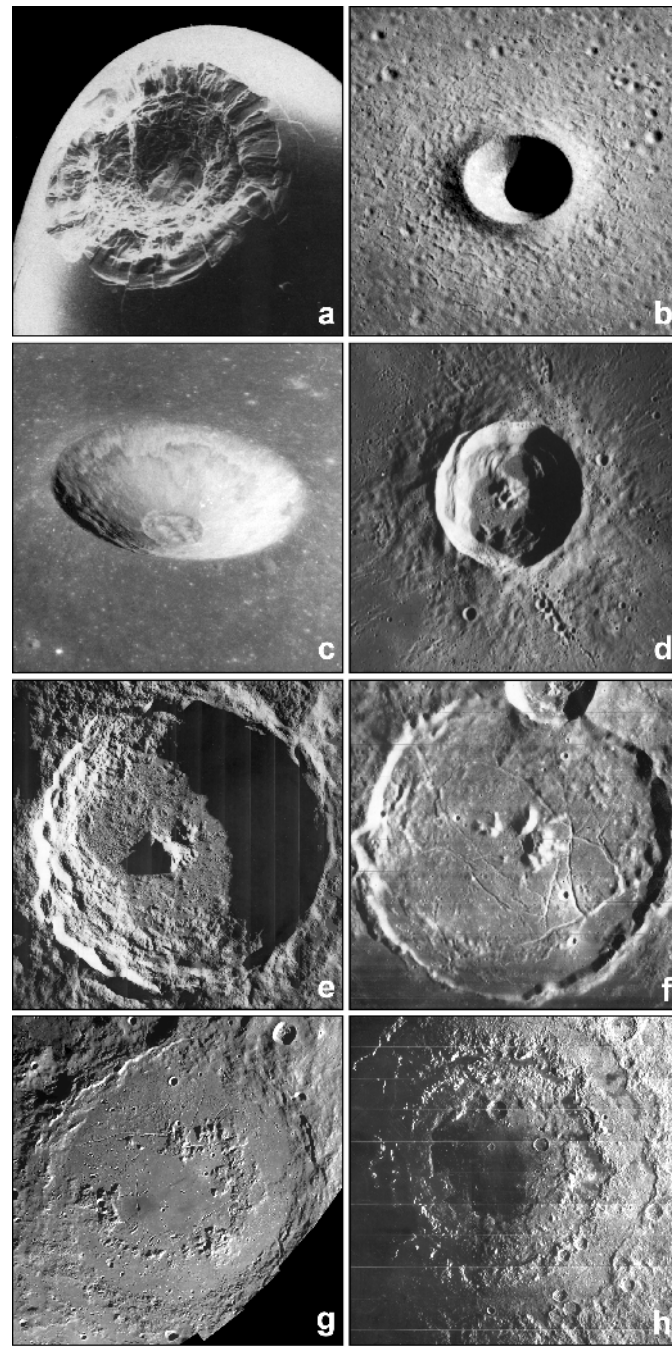


Figure 1.12. Morphologies of craters and basins; (a) micro crater on a lunar glass spherule (<1 mm), (b) bowl-shaped crater (Linné, 2.5 km, Apollo 15 frame P-9353), (c) transitional crater (Taruntius, 8.5 km, Apollo 10 frame H-4253), (d) complex crater (Euler, 28 km, Apollo 17 frame M-2923), (e) central peak crater (Tycho, 85 km, LO V M-125), (f) floor-fractured crater (Gassendi, 110 km, LO IV 143H2), (g) central peak ring basin (Schrödinger, 320 km, Clementine mosaic), (h) multi-ringed basin (Orientale, 930 km, LO IV M-187).

shock wave causes particle motion, which accelerates the impacted material radially downward and outward. At the same time the return shock wave decelerates the projectile. During this phase, the specific energies of the highly compressed target and projectile are increased, and after the passage of the shock wave, adiabatic decompression causes the release of this energy in the form of heat. Because pressure release associated with hypervelocity impacts can be up to several hundred GPa, large volumes of the target and virtually the entire projectile are melted and vaporized. Unloading from the high-pressure levels is initiated by the rarefaction waves that form as the shock wave reaches free surfaces such as the backside of the projectile or the ground surface at some distance from the impact point. Rarefaction waves modify the initial shock particle motions and ultimately set up a flow field that initiates and eventually completes the actual crater excavation (e.g., Croft 1980).

At the moment the shock-induced particle motion ceases, the total excavated and temporarily displaced target materials form the “transient cavity.” The transient cavity is significantly deeper than the final excavation cavity even if their diameters are similar (Fig. 1.13). Later, during the modification stage, the transient cavity is modified by rim collapse and floor rebound. Both collapse of the rim of the transient cavity with downward and inward slumping material and the unloading of the compressed materials leading to upward motion in the crater center are responsible for the shallower apparent crater compared to its transient cavity. A more detailed discussion of cratering mechanics can be found in Melosh (1989) and in Chapter 5.

2.1.4. Nature of ejecta. The nature of impact ejecta varies with radial distance from the crater (Fig. 1.13). Generally, ejecta deposits are highly centrosymmetric; non-centrosymmetric ejecta deposits and elongated crater cavities are observed only for craters formed by oblique impacts (e.g., Gault and Wedekind 1978; Melosh 1989; Schultz and Gault 1990). Although individual ejecta fragments follow ballistic trajectories, they cumulatively form a so-called ejecta curtain that gradually extends outward and thins. Continuous ejecta deposits are located closest to the crater, discontinuous ejecta deposits are farther away, and ejecta rays form the most distal parts of the ejecta deposits. Continuous ejecta deposits completely cover or disrupt the preexist-

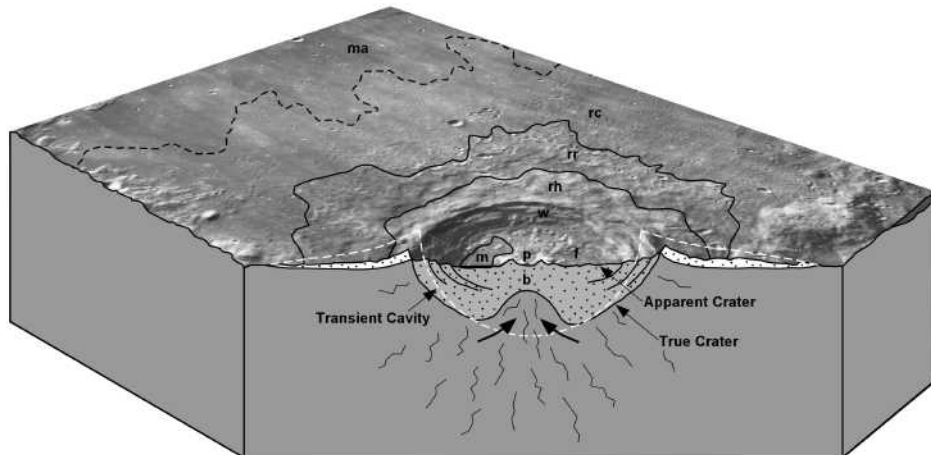


Figure 1.13. Block diagram of an idealized typical large impact crater. Crater subunits are the rim (rh), floor (f), central peak (p), wall (w), and impact melt pond (m). Ejecta deposits consist of hummocky deposits (rh), radial deposits (rr), and deposits cratered by secondary craters (rc); mare regions which are not influenced by the crater ejecta (ma). Dashed white line shows the transient cavity and its relationship to the apparent crater and the true crater. Collapsed wall material and brecciated material (b) filled the true crater to form the apparent crater.

ing surface in contrast to discontinuous ejecta deposits, which are patchy and characterized by localized deposits and shallow elongated secondary craters that frequently occur in clusters. Ejecta deposits form by ballistic sedimentation and thus incorporate local substrate, with the proportion of local material increasing with distance from the crater (e.g., Oberbeck et al. 1974; Oberbeck 1975; Haskin et al. 2003; Li and Mustard 2003). Ejecta rays occurring beyond the discontinuous ejecta deposits are relatively thin, long streaks that are oriented radially to the crater.

Recent experiments using two and three-dimensional particle image velocimetry (PIV) techniques (e.g., Cintala et al. 1999; Anderson et al. 2000, 2001, 2003) allow the study of individual particle motions within the ejecta curtain (Fig. 1.14a,b). These studies indicate that the angle of ejection of particles is not constant throughout an impact but decreases gradually with increasing radial distance from the impact point. Within an ejecta curtain, finer material that has been ejected at higher velocities and higher ejection angles during the early phases of the cratering process is found high in the ejecta curtain and deposits farthest away from the crater. Coarser material that originates from deeper target levels is ejected with lower velocities and at lower angles, and is deposited closer to the crater. This sequence produces an inverted stratigraphy of the target in the ejecta deposits with deepest target strata close to the crater and shallow target strata deposited farthest away from the crater.

The Moon is easily observed and thus allows detailed investigation of craters as products of impact-cratering processes in the inner solar system. By understanding the lunar cratering processes, we have been able to infer processes on the other terrestrial planets and their moons (e.g., Sharpton 1994; Pike 1980, 1988; Ivanov 1992) (Fig. 1.15). On Mars, for example, Mariner and Viking images showed numerous craters with multiple lobate ejecta deposits and pedestal craters. These craters have been interpreted as having formed by incorporation of ground water or ground ice into the ejecta (e.g., Carr et al. 1977; Kuzmin et al. 1988) or by atmospheric effects, that is, the entrainment and interaction of the atmosphere with the ejecta curtain (e.g., Schultz and Gault 1979; Barnouin-Jah and Schultz 1996, 1998). Similarly, flow lobes of craters on Venus have been interpreted to form by entrainment of thick atmosphere into the ejecta curtain (e.g., Barnouin-Jah and Schultz 1996). Modeling and extrapolating lunar cratering processes to conditions on Mercury revealed that the impact rate there

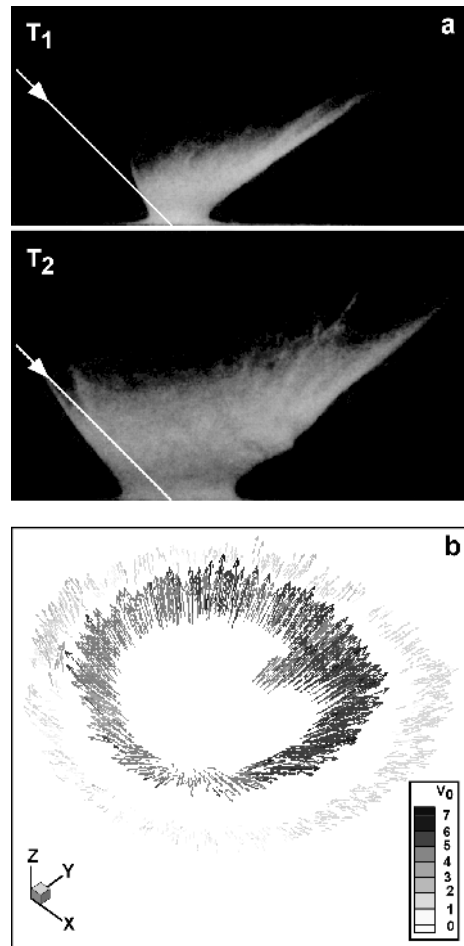


Figure 1.14. Two time steps (a) of an oblique impact experiment at 45° impact angle (Schultz and Anderson 1996) and 3D PIV velocity vectors (b) for a 30° oblique impact (Anderson et al. 2000).

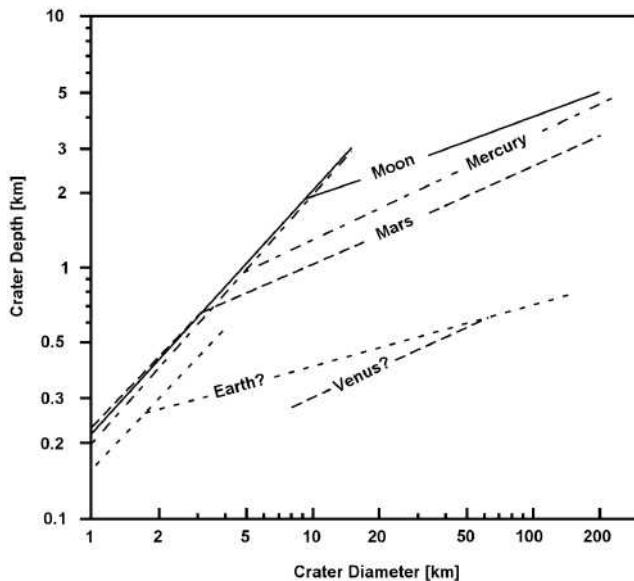


Figure 1.15. Depth/Diameter ratios of impact craters of the terrestrial planets and the Moon. (Used by permission of The Geological Society of America, after Sharpton 1994, *Large Meteorite Impacts and Planetary Evolution*, Fig. 1, p. 20).

is 5.5× higher than on the Moon, impact velocities are 60% higher, impact-melt production is 14× greater, and vapor production is 20× greater than on the Moon (Cintala 1992). Apparent crater morphologies on the icy satellites of Jupiter, especially Europa, can vary significantly from those on the Moon. Shallow depressions seen along the terminator zone have irregular shapes characteristic of endogenic origin (Chapman et al. 1997), others have slightly raised rims suggesting an impact origin (Greeley et al. 1998).

2.1.5. Shock metamorphism. In addition to ejection from the crater, target materials are also highly modified by the shock wave of the impact with pressures that exceed pressures known from internally-driven processes, especially within planetary crusts (Fig. 1.16). In addition, temperatures and strain rates associated with impacts can be orders of magnitude higher than those of internal processes and can lead to shock-metamorphism (see Chapter 5). At high shock pressures large amounts of energy are deposited in the target material, raising the temperature above the melting or vaporization points. The degree of shock metamorphism is heavily dependent on the material behavior at ultrahigh temperatures and pressures. At pressures of 5–12 GPa, minerals and rocks behave plastically instead of elastically. Between 40 and 100 GPa thermal effects become more important and melting begins. Vaporization occurs at pressures in excess of about 150 GPa, and finally ionization occurs at pressures of a few hundred GPa (e.g., Hötz et al. 1991). Table 1.3 summarizes shock effects in rocks and minerals calibrated for the shock pressure by recovery experiments.

All types of lunar rocks returned to Earth have, to some degree, been affected by impact processes. The last shock event, which may have only displaced the rock fragment at very low shock pressure or may have strongly shock metamorphosed it in this “last” impact event, can be diagnosed by specific shock effects in the constituent minerals (Chao 1968, Stöffler 1972, 1974, 1984; Bischoff and Stöffler 1992; see also compilation by French 1998). Progressive stages of shock metamorphism are defined by an increasing intensity of shock, which is inversely proportional to the original distance of the shocked rock unit from the impact center. The

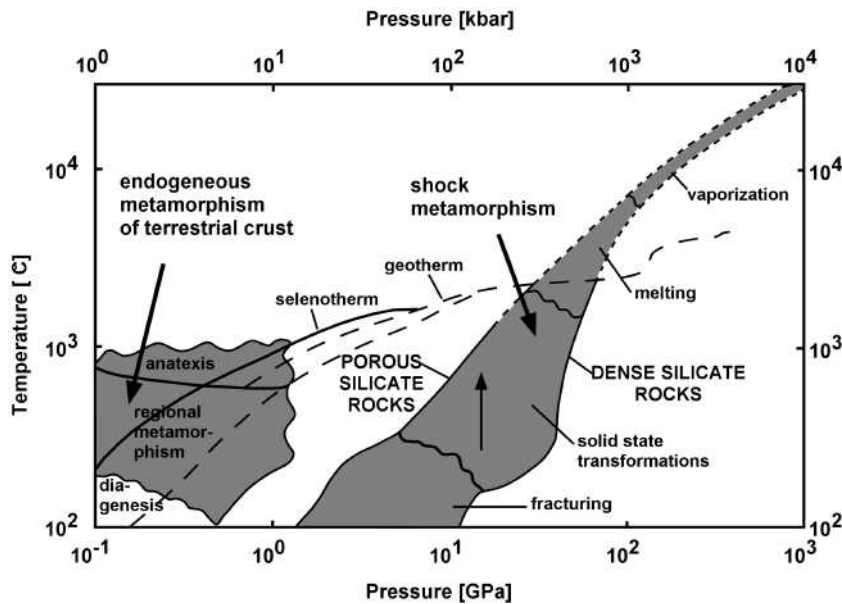


Figure 1.16. Pressure temperature fields for progressive shock metamorphism of lunar rocks in comparison to terrestrial endogenic metamorphism; upper curve of P-T-field of shock metamorphism holds for porous regolith and regolith breccias (data sources see Tables 1.3 and 1.4) and lower curve holds for dense, non porous mafic rocks of basaltic to peridotitic to anorthositic composition (data sources see Tables 1.3 and 1.4); dashed parts of boundaries of shock metamorphism is based on Davies (1972); geotherms from Anderson (1981) (upper curve = oceanic, lower curve = continental).

complete system of progressive shock metamorphism is given in Table 1.4 for the main types of lunar rocks (see also Chapter 5).

2.1.6. Thermal metamorphism. The collections of returned lunar samples and of meteorites contain a group of rocks called “feldspathic granulitic impactites.” Previously, some of these rocks were interpreted to be products of igneous plutons or thermal metamorphism (Heiken et al. 1991). Compositionally, these samples are exclusively derived from the lunar highlands (70–80% modal plagioclase; Cushing et al. 1999) and appear to represent an essential fraction of the lunar crust (Warner et al. 1977). They occur in all sample suites that sampled lunar highlands materials (Ap 14, 15, 16, 17; Luna 20) and are ubiquitous in lunar meteorites of highland provenance (Korotev et al. 2003b). Recently, three different textural types of granulitic breccias were identified: poikilitic, granoblastic, and poikilitic-granoblastic breccias (Cushing et al. 1999). The equilibrium temperatures of granulitic breccias are near 1000–1100 °C as deduced from pyroxene thermometry and other observations (Warner et al. 1977; Ostertag et al. 1987; Cushing et al. 1999). Cushing et al. (1999) suggested that some granulitic breccias cooled relatively rapidly (0.5–50 °C/year) at shallow depths of <200 m, and argued that they were formed in craters of 30–90 km in diameter, physically associated with impact-melt breccias or fine-grained fragmental precursor lithologies. Others (see, for example, Korotev and Jolliff 2001) think it more likely that granulitic rocks were assembled by very large impacts (basins) that penetrated to mid-crustal levels, and that later impacts re-excavated these rocks and brought them to the surface. Gibson et al. (2001) proposed that granulites do not need to have formed from contact metamorphism of older breccias in or close to impact-melt sheets, because brecciation, melting, and high-temperature metamorphism can occur at a variety of crustal depths in the core of a central uplift during an impact. Granulitic lithologies have radiometric

Table 1.3. Shock wave barometry for lunar rock-forming minerals and for whole rock melting.

Mineral/Rock	Shock Effects	Shock Pressure (GPa)
Olivine	undulatory extinction	4–5 to 10–15
	mosaicism	10–15 to 60–65
	planar fractures	15–20 to 60–65
	planar deformation features	35–40 to 60–65
Plagioclase	melting and recrystallization	> 60–65
	undulatory extinction	5–10 to 10–12
	mosaicism	10–12 to 28/34*
	diaplectic glass	28/34* to 45
Pyroxene	melting	> 45
	undulatory extinction	5–10 to 20–30
	mechanical twinning	> 5
	mosaicism	20–30 to 75–80
Quartz (minor phase in lunar rocks)	planar deform. features	30–35 to 75–80
	incipient melting	> 75–80
	planar fractures (0001) and {1011}	> 5–10
	planar deformation features {1013}	> 10
Basalt/gabbro	planar deformation features {1012}	> 20
	diaplectic quartz glass	34 to 50
	stishovite	12 to 45
	melting	> 50
Dunite	whole rock melting	> 75–80
Anorthosite	whole rock melting	> 60–70
Regolith	whole rock melting	> 45–50
whole rock melting		> 40

* noritic anorthositic composition

Compilation by Stöffler 2003, unpublished; data from Müller and Hornemann 1969; Hornemann and Müller 1971; Stöffler and Hornemann 1972; Stöffler 1972, 1974; Snee and Ahrens 1975; Kieffer et al. 1976; Schaal and Hörz 1977; Stöffler and Reimold 1978; Schaal et al. 1979; Bauer 1979; Ostertag 1983; Stöffler et al. 1986, 1991; Bischoff and Stöffler 1992; Stöffler and Langenhorst 1994; Schmitt 2000).

ages ranging from 3.75 to >4.2 b.y. (Bickel 1977; Ostertag et al. 1987; Stadermann et al. 1991) and therefore mostly predate the postulated “terminal cataclysm,” if it existed. The source of heat and setting of ancient thermal metamorphism on the Moon remains enigmatic.

2.1.7. Impact melts. In the Apollo collection, impact-melt rocks, breccias, and glasses constitute some 30–50% of all hand-sized samples returned from the highland landing sites and about 50% of all soil materials, including the mare soils. Figure 1.17a,b shows a numerical model of impact-melt generation and an example of a lunar impact-melt pond associated with King crater. Impact melts are a homogenized mixture of the target lithologies and several compositional and textural characteristics distinguish them from conventional igneous rocks. One is the occurrence of clasts of target materials and schlieren within melted matrices. Lunar impact-melts can be identified by remnants of the projectile itself, particularly by the detection of high concentrations in Ni, Co, Ir, Au, and other highly siderophile elements (e.g., Korotev 1987, 1990; Warren 1993; Warren et al. 1997).

Identification and proper assignment of impact melts to specific basin-forming events is crucial for dating these events in order to derive a coherent, absolute lunar stratigraphy (e.g., Stöffler and Ryder 2001). Cintala (1992) compared the impact-melt production of lunar and

Table 1.4. Progressive shock metamorphism of most common lunar non-porous crystalline rocks and of lunar regolith (Stöffler 2003, unpublished); Shock pressure corresponds to the final equilibration peak shock pressure for polycrystalline rocks (in GPa); post-shock temperature is the temperature increase (in °C) after pressure release relative to any ambient pre-shock temperature; PDF's = planar deformations features = isotropic lamellae of distinct crystallographic orientation (low Miller indices planes); Table based on data as referenced in Stöffler (1972, 1974, 1984), Stöffler et al. (1980, 1986, 1988), Bischoff and Stöffler (1992), and Schmitt (2000).

Anorthosite (< 10 vol. % of mafics)			Basalt, gabbro, norite, granulitic rocks and breccias*			Regolith (impactoclastic detritus)		
Shock stage	Shock P	Post-shock T	Shock effects	Shock stage	Post-shock T	Shock effects	Shock stage	Post-shock T
0			sharp opt. extinct. of minerals; fract.	0		fractures, sharp optical extinction of minerals	0	
1a	< 5	50	plag with undulat. extinct., px with mechanic. twinn.	1a	< 5	50 fractured minerals with undulatory optical extinction	1	
1b	26	220	plag partially isotropic and PDF's; mosaic. in px	1b	20-22	200 plag with PDF's and und. ext., mechan. twinn. px and ilm	2	
2	28	300	diaplectic plag glass; mosaicism and PDF's in px	2	28	300 diaplectic plag glass; px with mosaicism	3	10
3	40-45	800-900	plag with flow struct. and vesicul.; strong mosaic and PDF's in px; mixed melt of plag and px	3	40-45	~ 900 plag with incipient flow structure, mafics as in stage 1/2 but strong mosaic.	4	20
4	60	1850	complete whole rock melting and fine-grained crystallization of quenched melt	4	~ 60	~ 1400 normal plag glass with flow structures and residues; px with strong mosaic; and PDF's; incipient edge melting of mafics	5	> 40
5	> 100	> 3000	whole rock vaporization	5	~ 80	~ 1600 vesicul. plag glass increasingly mixed with melt products of coexisting minerals		> 2000
				6	> 100	> 1800 complete whole rock melting and incr. vaporization		

Abbreviations: ol = olivine; plag = plagioclase; px = pyroxene; ilm = ilmenite; mosaic = mosaicism; ext. or extinct. = extinction, incr. = increased; fract. or fr. = fractures; mechan. = mechanical; twinn. twinning; pl. or plan. = planar; opt. = optical; undulat. or und. = undulatory; struct. = structure; vesicul. = vesiculation; submicr. = submicroscopic; intergr. = intergranular; interg. = intergranular; melt = melt; glass = glass; note that pressure calibration is adjusted to plag of An>90 for anorthosite and related rocks and for plag of An>80 for basaltic/gabbro rocks (Osterrieth 1983; Stöffler et al. 1986).

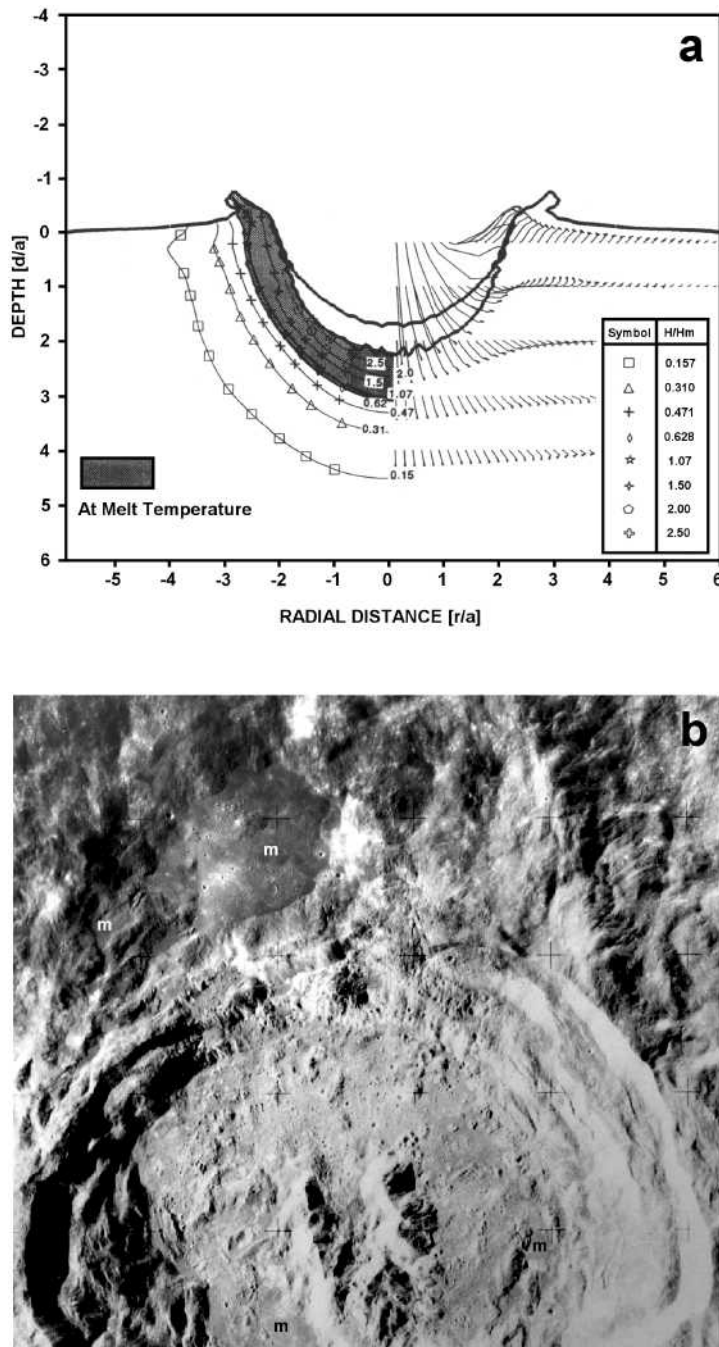


Figure 1.17. Simulation of impact-melt generation (O'Keefe and Ahrens 1994) and example of impact-melt ponds associated with King crater (Ap 16 frame H-19580). (Used by permission of The Geological Society of America, after O'Keefe and Ahrens 1994, *Large Meteorite Impacts and Planetary Evolution*, Fig. 3, p. 107).

mercurian craters. From his model, Cintala (1992) concluded that the surface temperature is important but that the impact velocity is the dominant factor controlling the amount of impact-melt produced by an impact. Cintala and Grieve (1994) pointed out that craters on the Moon should contain proportionately less impact melt than terrestrial craters and that the clast content in lunar impact melt should be higher.

2.1.8. Crater frequency and bombardment history. Statistical investigations of impact-crater populations are providing key data for understanding the history and evolution of the Moon and the solar system. Because the distribution of impact-crater diameters reflects the number and mass distribution of the incoming projectiles, it provides fundamental information about the collision dynamics in the solar system, such as the mass frequency and the time-integrated flux of impacting objects.

The exact shape of the size frequency distribution of craters created on a fresh surface has long been debated (e.g., Shoemaker 1970; Hartmann 1971; Baldwin 1971; Hartmann et al. 1981; Neukum 1983; Neukum et al. 2001). Part of the problem is the difficulty of finding large enough contiguous units that are much younger than the mare areas. Since the publication of the Lunar Source Book (Heiken et al. 1991), Galileo and Clementine data allowed McEwen et al. (1993, 1997) to estimate the size frequency distribution of rayed (Copernican) craters. Neukum et al. (2001) showed that a non-power-law shape of the production function gives a good fit to the new data (Fig. 1.18). With this production function at hand, crater statistics can be used to date planetary surfaces because older surfaces accumulate more craters than younger ones. The density of craters in any given region therefore yields the relative age of a geologic unit. Correlating crater statistics of a region with radiometric ages from returned samples not only allows calculation of absolute crater production rates and absolute projectile fluxes, but also provides absolute model ages for unsampled lunar regions (Fig. 1.19a,b). Neukum et al. (2001) concluded that for the last 4 b.y., the shape of the production function did not change within the limits of observational accuracy. The size-frequency distribution of the crater-forming bodies on the Moon is similar to the size-frequency distribution of asteroids in the Main Belt; from this, it appears that asteroids from the Main Belt and Near Earth Asteroids (NEAs) are the main source for lunar impact craters, and comets play only a minor role.

Most non-volcanic rocks in the Apollo sample collection have ages rang-

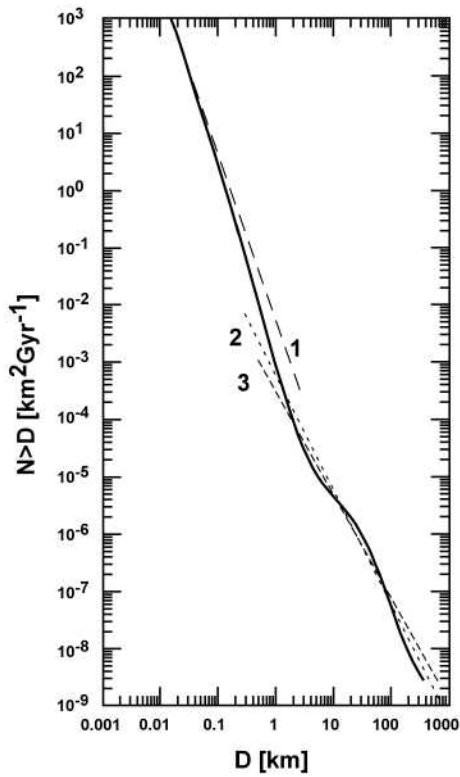


Figure 1.18. Comparison of the lunar production function (Neukum et al. 2001) with power-law distributions from (1) Shoemaker (1970), (2) Hartmann (1971), and (3) Baldwin (1971), and Hartmann et al. (1981). (Used by permission of Kluwer Academic Publishers, after Neukum et al. 2001, *Chronology and Evolution of Mars*, Fig. 2, p. 61).

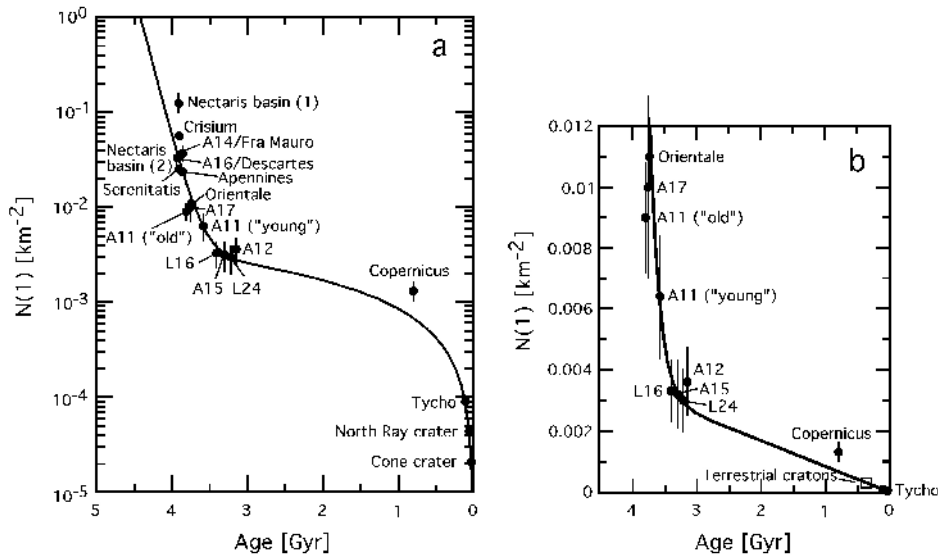


Figure 1.19. Lunar cratering chronology in (a) log form and (b) linear form (after Neukum et al. 2001; see also Stöffler and Ryder 2001, discussion in chapter 5, Fig. 5.33).

ing from 4.5 to 3.8 b.y. and are thus only 10–30% older than most mare basalts, yet the highlands surfaces display 10–50× more craters >15 km than do the mare-basalt surfaces. Thus, it has been concluded that the crater production was significantly higher between 4.5 and 3.8 b.y. compared to the last 3.8 b.y. Interpretations differ on this finding. One group of workers sees this difference as the tail of the original planetary accretion process (e.g., Hartmann 1975; Neukum and Wise 1976; Neukum et al. 2001), whereas others propose that a cataclysmic increase in the infalling projectiles occurred 3.8–4.0 b.y. ago (e.g., Tera et al. 1974; Ryder 1990; Cohen et al. 2000; Ryder 2002; Kring and Cohen 2002), as evidenced by the narrow range of ages of the sampled impact-melt breccias (mostly 3.8–4.0 b.y.). The issue of a terminal lunar cataclysm is not resolved and remains one of the key objectives in crater-chronology research.

2.1.9. Impact erosion. Meteorite impacts are a major process in transporting material vertically and laterally, and they are the major erosional process on the Moon. Very small impacts have an abrasive effect similar to sandblasting, whereas larger projectiles up to centimeters in size can completely shatter a target by “collisional fragmentation” (Gault and Wedekind 1969). Erosion rates by abrasion have been estimated to be about 1 mm/10⁶ years for kilogram-sized lunar rocks, with faster erosion rates for larger rocks (Ashworth 1977). Collisional fragmentation is a faster and more effective process than abrasion and it is estimated that on average, a rock of 1 kg survives at the lunar surface for about 10 Ma before becoming involved in another impact event. Craddock and Howard (2000) recently compared the topography of simulated craters with the topography of degraded craters on the Moon and estimated that the average erosion rate since the Imbrian Period has been $\sim 2.0 \pm 0.1 \times 10^{-1}$ mm/million years.

2.1.10. Regolith formation. Impacts are the most important metamorphic process on the Moon, altering the textures of rocks and generating new ones, such as glasses, impact melts and fragmental rocks (breccias). Repetitive and frequent impacts cause shattering, burial, exhumation, and transportation of individual particles in a random fashion. The numerous large impacts that occurred during the period of heavy bombardment shattered and fragmented the lunar crust down to several kilometers and produced a global layer of chaotically mixed

impact debris, termed “megaregolith” (Fig. 1.20). Seismic evidence and estimates on the effects of large-scale bombardment of the highlands during the epoch of intense bombardment suggested that the cumulative ejecta thickness on the lunar highlands is 2.5–10 km, possibly tens of kilometers (e.g., Short and Foreman 1972; Toksöz et al. 1973; Hörz et al. 1977; Cashore and Woronow 1985). The average depth to which the lunar crust is mechanically disturbed by impacts is not well known but conservative estimates indicate a thickness of the ejecta blankets of at least 2–3 km (megaregolith), a structural disturbance to depths of more than 10 km, and fracturing of the *in-situ* crust reaching down to about 25 km (Fig. 1.20).

In terms of moving large masses of material and reshaping the Moon’s crust, basin-forming impacts are by far the dominant force. Large basin-forming events can distribute pervasive ejecta deposits to about 6 final crater radii, and can make significant contributions to the megaregolith at any location on the lunar surface (Haskin 2000). For example, at the Apollo 16 landing site ejecta deposits of Nectaris, Serenitatis, and Imbrium each are expected to be, on average, in excess of 500 m thick (Haskin 2000) with younger basin deposits eroding into older, underlying deposits.

Over lunar geologic time, bombardment by large impactors decreased and smaller impacts became relatively more important. The result of these smaller impacts is an accumulated fine-grained powdery layer on the lunar surface above the megaregolith. This uppermost part of the megaregolith layer is called “regolith” and is continuously “gardened” or turned over by

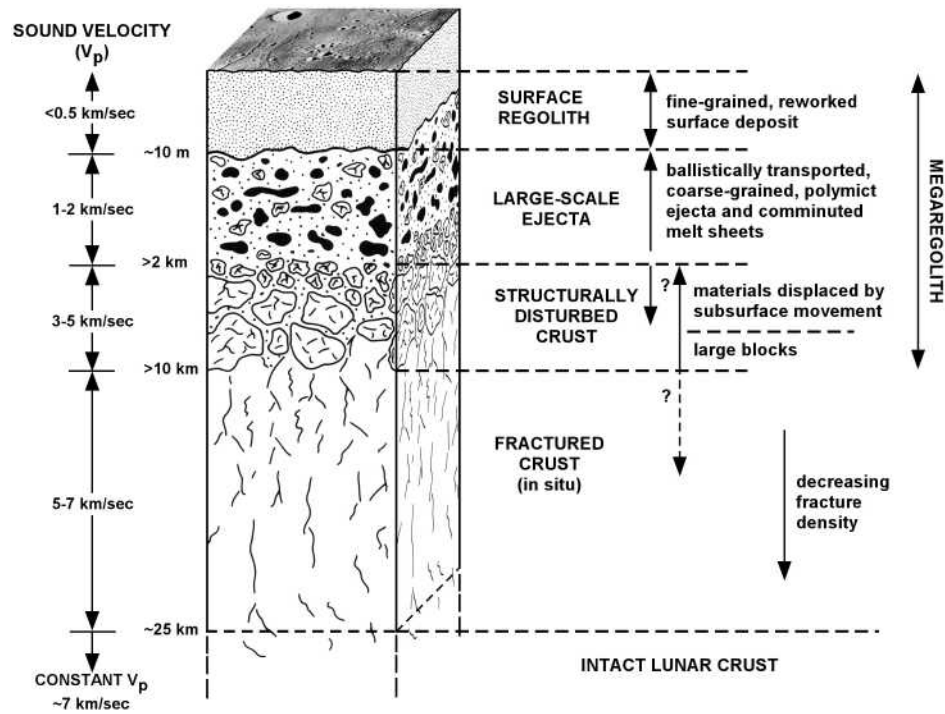


Figure 1.20. Highly idealized cross-section through the internal structure of the megaregolith illustrating the effects of large-scale cratering on the structure of the upper crust. The depth scale of this figure is highly uncertain because regional variations are expected depending on the degree to which a region has been influenced by basin-sized impacts. (Used by permission of Cambridge University Press, after Hörz et al. 1991, *Lunar Sourcebook*, Fig. 4.22, p. 93).

impacts (Fig. 1.20). In the development and evolution of the regolith, rare large craters play an important role because they can create a layered regolith column despite the tendency of the smaller craters to homogenize the upper parts of the regolith. In general, the composition of the regolith is largely controlled by the underlying local “bedrock,” which may itself be megaregolith, and regolith samples from any given Apollo site usually show a relatively narrow compositional variation (see Chapter 2).

Although much of the regolith derives from local sources (e.g., Rhodes 1977; Hörz 1978), remotely sensed data of highland/mare boundary regions indicate clear evidence that lateral transport of material owing to meteorite impacts occurred on the Moon (e.g., Mustard and Head 1996; Li and Mustard 2000). Projectiles that are responsible for the macroscopic evolution of the regolith are typically 10–1000 cm in diameter. Based on the number of such impact events, the regolith thicknesses are typically only a few meters for mare areas and >10 m for the highlands. Shkuratov et al. (2001), on the basis of new radar data, estimated that the average thickness of the regolith is ~5–12 m. Thin regoliths (~4 m) were derived for Mare Serenitatis, Mare Tranquillitatis, and Mare Humorum, and a thick regolith was derived for Mare Nectaris (~9 m). Shkuratov et al. (2001) argued that the regolith thickness correlates with age and that a higher regolith production rate existed prior to ~3.5 b.y. ago. The overall growth rate of regolith decreases with time because the regolith itself acts as a shield that protects the bedrock from incorporation into the regolith. Only rare large craters can penetrate the regolith to incorporate “fresh” bedrock; smaller impacts only redistribute the existing regolith.

2.1.11. Bright ray craters. Bright rays and topographic freshness were used as the main criteria to assign a Copernican age to craters (e.g., Wilhelms 1987). However, using recent Clementine data, Hawke et al. (1999) found that bright rays of fresh craters can be due to differences in maturity (e.g., Messier), composition (e.g., Lichtenberg), or a combination of both (e.g., Tycho, Olbers A). Grier et al. (1999) used bright ray craters to study the cratering rate in the last few hundred million years. On the basis of maturity maps derived from Clementine images, Grier et al. (1999) determined relative ages of rayed craters and concluded that there is no evidence for a change in the cratering rate since Tycho (~109 Ma; Grier et al. 1999) compared to the cratering rate since Copernicus (~810 Ma; Grier et al. 1999).

2.1.12. Lunar swirls. The origin of light and dark colored “swirl-like” markings, up to hundreds of kilometers across, (e.g., Reiner Gamma) is still under debate and a variety of models including cometary impacts, magnetic storms, volcanism, or alteration by gases from the lunar interior have been suggested for their origin (e.g., El-Baz 1972; Schultz and Srnka 1980). However, recent magnetic data suggest a link to impact-related magnetism because the swirls in Mare Ingenii and near Gerasimovich crater are associated with relatively strong magnetic anomalies antipodal to some of the young impact basins such as Imbrium and Crisium (Hood 1987; Lin et al. 1988; Hood and Williams 1989; Halekas et al. 2001; Hood et al. 2001; Richmond et al. 2005). Because the Reiner Gamma and Rima Sirialis magnetic anomalies are oriented radially to the Imbrium basin, Hood et al. (2001) proposed that the most likely sources are Imbrium ejecta beneath a thin veneer of mare basalts. If so, the albedo markings associated with Reiner Gamma may be consistent with a model involving magnetic shielding of freshly exposed mare materials from the solar wind ion bombardment, resulting in a reduced rate of surface darkening relative to the surrounding basalts (Hood et al. 2001). In an independent study, Halekas et al. (2001) argued that a cometary origin of the swirls appears to be unlikely because some of them are found in locations antipodal to large farside impact basins. They favor an origin as buried, magnetized Imbrium ejecta similar to Hood et al. (2001).

2.2. Volcanic processes

2.2.1. Nature of lunar volcanism. The presence, timing and evolution of volcanic activity on the surface of a planet are indicative of its thermal evolution. On the Moon, a one-plate

planetary body, volcanism apparently resulted from melting of mantle rocks that was unlikely to be contaminated by recycled crust. Such melting was caused by the decay of naturally radioactive elements and resulted in the production of partial melts, most commonly of basaltic composition (45–55% SiO₂ and relatively high MgO and FeO contents). In order to produce basaltic melts on the Moon, temperatures of >1100 °C and depths of >150–200 km would have been required. Radiometric ages of returned lunar samples indicate that most volcanism on the Moon ceased approximately 3 b.y. ago, implying that the mantle long ago cooled below the temperature necessary to produce partial melts. However, crater counts on mare basalt surfaces suggest that some basalts erupted as late as ~1–2 b.y. ago (Hiesinger et al. 2003). Recent two- and three-dimensional modeling of the thermal evolution of the Moon suggests the growth of a 700–800 km thick lithosphere while the lower mantle and core only cooled 100–200 °C (Spohn et al. 2001). According to such models, the zone of partial melting necessary for the production of basaltic magmas would migrate to depths too great for melts to reach the surface at ~3.4–2.2 b.y. ago. However, a non-uniform distribution of heat-producing elements in the mantle as indicated by Lunar Prospector data could extend the potential for melting to more recent times.

Basaltic lavas cover about 17% or 7×10^6 km² of the lunar surface and make up ~1% of the volume of the lunar crust (Head 1976) (Fig. 1.21). These basalts are almost exclusively exposed within the nearside basins, are rare on the lunar farside, and form the relatively smooth dark areas visible on the lunar surface. They appear to be correlated with the distribution of KREEP (especially Oceanus Procellarum) suggesting a possible genetic relationship between the two phenomena (Haskin et al. 2000a,b; Wieczorek and Phillips 2000; see also Chapters 3 and 4). Besides these lava flows, other products of basaltic volcanism occur on the Moon. Fire fountaining, driven by gas exsolution from erupting lava, dispersed melt as fine droplets in the form of pyroclastic deposits or volcanic ash (Chou et al. 1975; Delano and Livi 1981; Delano 1986). On the basis of either their glass-rich nature or their abundant titanium-rich black spheres, pyroclastic deposits can be clearly distinguished from lava flow products with

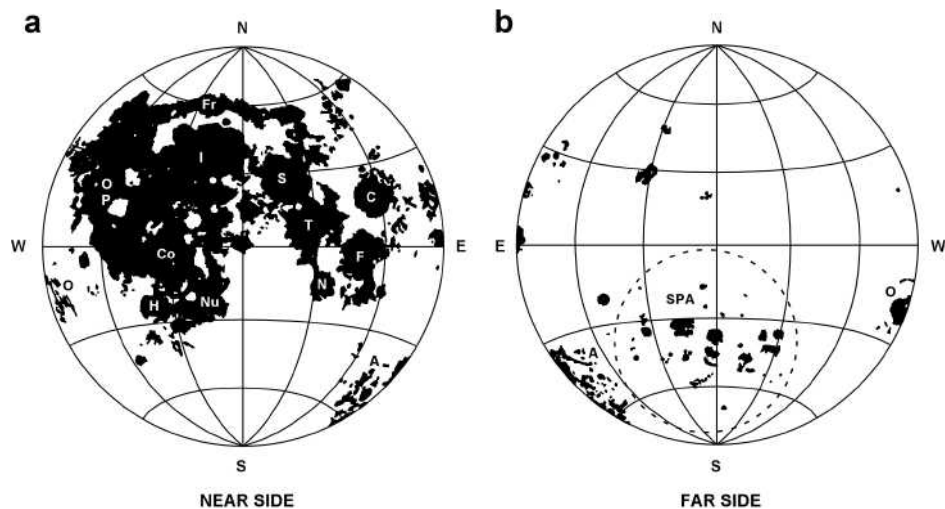


Figure 1.21. Map of the distribution of mare basalts on the lunar nearside (a) and the farside (b) (Head 1976). Note the highly asymmetric distribution of mare basalts on the nearside and the farside. Australe (A), Crisium (C), Cognitum (Co), Fecunditatis (F), Frigoris (Fr), Humorum (H), Imbrium (I), Nectaris (N), Nubium (Nu), Orientale (O), Oceanus Procellarum (OP), Serenitatis (S), South Pole-Aitken (SPA), Tranquillitatis (T).

multispectral remote-sensing techniques. However, identifying pyroclastic deposits of low-Ti content with current remote sensing techniques is problematic.

2.2.2. Lava flows. Very early, Galileo Galilei interpreted the smooth dark mare plains as oceans, thus the Latin name “mare,” and other interpretations included emplacement as pyroclastic flows (Mackin 1964) and deep dust mass-wasted from the highlands (Gold 1966). However, samples returned from the Apollo and Luna missions provided firm evidence that the mare areas formed by large-volume eruptions of low-viscosity basaltic lavas, similar in style to the Columbia River flood basalts on Earth. Additional support for such an origin comes from telescopic and spacecraft images, which show lava flows several tens of meters thick that extend for hundreds to thousands of kilometers across the surface. In Mare Imbrium, the youngest lavas flowed in three successive events for 1200, 600, and 400 km across slopes of 1:1000 (Fig. 1.22a) (Schaber 1973; Schaber et al. 1976). Lobate flow fronts bounding these flows were found to be 10–63 m high, averaging ~35 m (Gifford and El Baz 1978).

Measurements of molten lunar basalts revealed that their viscosity is unusually low, only a few tens of poise at 1200 °C, allowing them to flow for long distances across the surface before solidifying (Hörz et al. 1991). Thin lava flows such as the ones in Mare Imbrium are not unusual and have been observed elsewhere on the Moon, for example, within the Hadley Rille at the Apollo 15 landing site (Fig. 1.22b). In Hadley Rille at least three flows are exposed in the upper 60 m below the surface (Howard et al. 1973). Further support for thin lunar lava flows stems from investigations of the chemical/kinetic aspects of lava emplacement and cooling. Basalt samples of the Apollo 11, 12, and 15 sites indicate that individual flow units are no thicker than 8–10 m (Brett 1975). Many lunar lava flows lack distinctive scarps and this has been interpreted as indicating even lower viscosities, high eruption rates, ponding of lava in shallow depressions, subsequent destruction by impact processes, or burial by younger flows.

Distinctive kinks in the cumulative distributions of crater size-frequencies derived from Lunar Orbiter images have been used to estimate the thickness of lava flows (e.g., Hiesinger et al. 2002). This technique expands considerably the ability to assess lava flow unit thicknesses and allows one to obtain thicknesses and volumes for additional flow units that have not been detected in low-sun angle images. Using this method, Hiesinger et al. (2002) found lava flow units to average 30–60 m in thickness. These thicknesses are commonly greater than those typical of terrestrial basaltic lava flows and more comparable to those of terrestrial flood basalts; a correlation consistent with evidence for high effusion rates and volumes for basalt eruptions in the lunar environment (Head and Wilson 1992). An alternative technique to estimate the thickness of lava flows is to look at distinctive compositions of the ejecta deposits of small-scale craters in high-resolution Clementine color data. Using the depth/diameter relationship of lunar craters, one can derive the depth to the compositionally distinctive underlying material, which is equivalent to the thickness of the uppermost layer (e.g., Hawke et al. 1998; Antonenko et al. 1995).

2.2.3. Sinuous rilles. Besides the prominent lava flows of the lunar maria, other volcanic landforms have been observed on the Moon, such as sinuous rilles, domes, lava terraces, cinder cones, and pyroclastic deposits. Sinuous rilles are meandering channels that commonly start at a crater-like depression and end by fading downslope into the smooth mare surface (Greeley 1971) (Fig. 1.23a). Most sinuous rilles appear to originate along the margins of the basins and to flow towards the basin center. Schubert et al. (1970) reported that sinuous rilles vary from a few tens of meters to 3 km in width and from a few kilometers to 300 km in length. The mean depth of these rilles is ~100 m. The Apollo 15 landing site was specifically selected to study the formation process of sinuous rilles. No evidence for water or pyroclastic flows was found and it was concluded that sinuous rilles formed by widening and deepening of channelized lava flows due to melting the underlying rock by very hot lavas (Hulme 1973; Coombs et al. 1987). On the basis of geochemical studies of a lava tube in the Cave Basalt flows, Mount St. Helens, Williams et al. (2001) concluded that mechanical and thermal erosion operated simultaneously

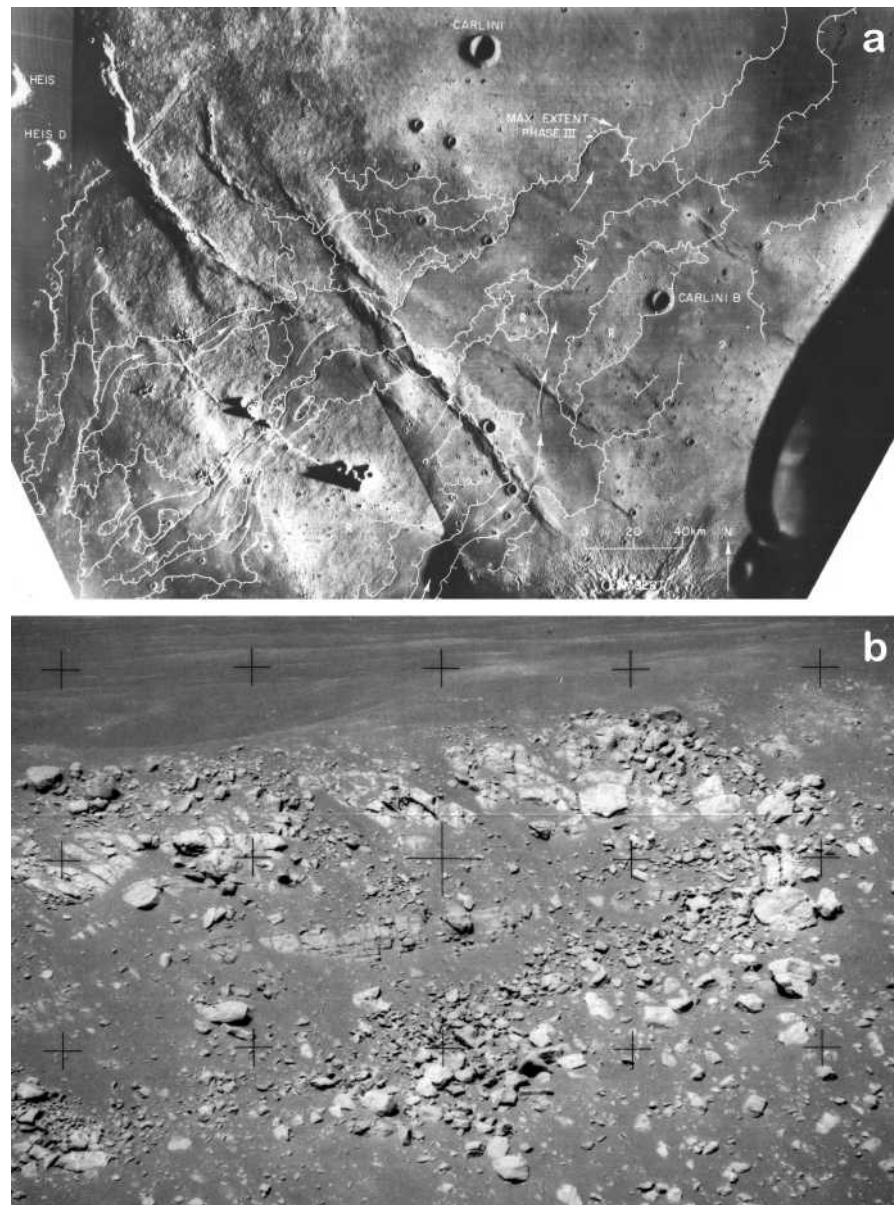


Figure 1.22. Examples of volcanic landforms; (a) mare flows in Mare Imbrium (Ap 15 frame M-1556) (Schaber 1973; Schaber et al. 1976) and (b) flows exposed within the wall of Hadley Rille (Ap 15 frame H-12115).

to form the lava tube. The much larger sizes of lunar sinuous rilles compared to terrestrial lava tubes are thought to result from lower gravity, high melt temperatures, low viscosities, and high extrusion rates. Since the publication of the Lunar Source Book (1991), new work by Bussey et al. (1997) showed that the process of thermal erosion is very sensitive to the physical conditions in the boundary layer between lava and solid substrate. They found that thermal erosion rates

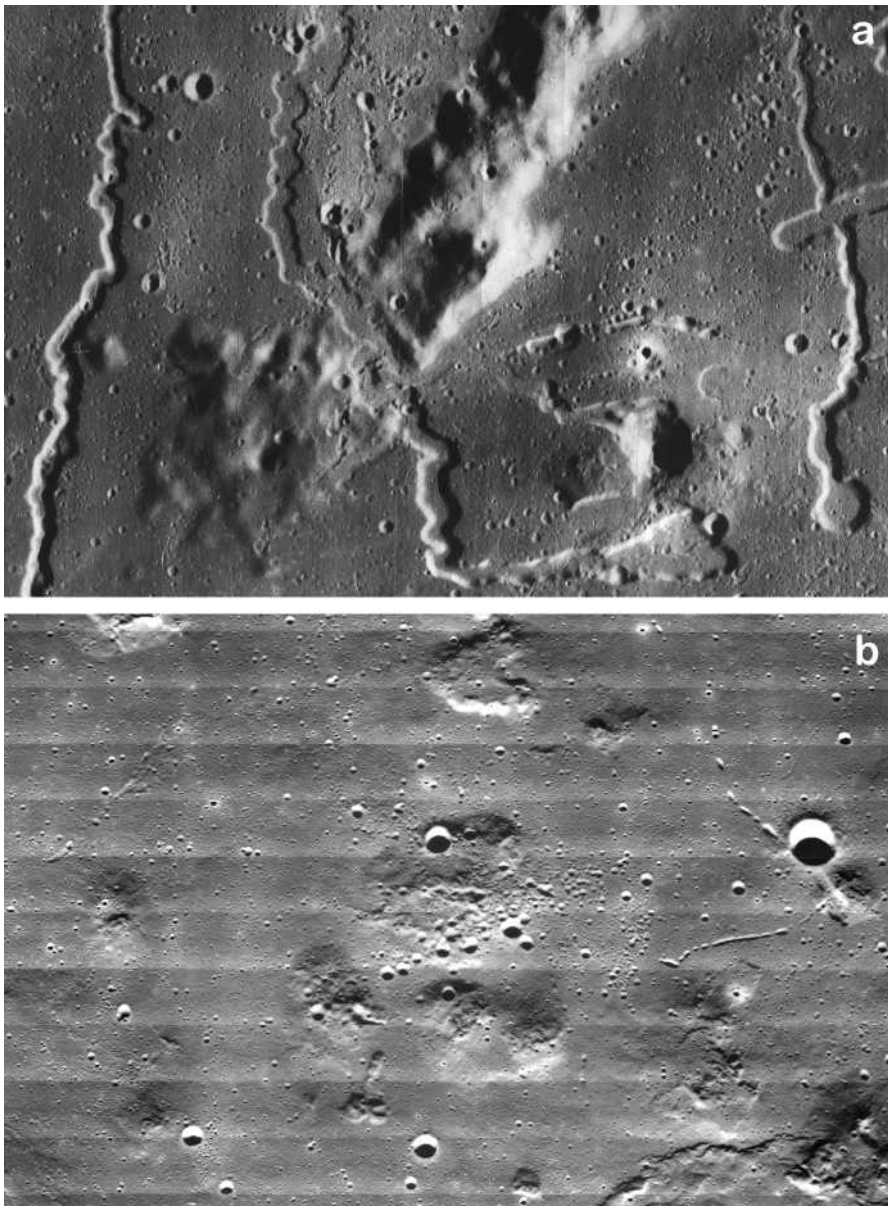


Figure 1.23. Examples of volcanic landforms; (a) sinuous rilles of Rimae Prinz (LO V 191H1) and (b) mare domes of the Marius Hills (LO V M-210).

depend on the slopes, effusion rates, and thermal conductivities of the liquid substrate boundary layer. In their model, the highest thermal erosion rates occur when thermal conductivities are high for the liquid substrate and low for the solid substrate.

2.2.4. Cryptomaria. Cryptomaria are defined as mare-like volcanic deposits that have been obscured from view by subsequent emplacement of lighter material, commonly ejecta

from craters and basins (Head and Wilson 1992). These deposits have been studied through investigation of dark halo craters (e.g., Schultz and Spudis 1979, 1983; Hawke and Bell 1981), through multispectral images (e.g., Head et al. 1993; Greeley et al. 1993; Blewett et al. 1995; Mustard and Head 1996), and Apollo orbital geochemistry (e.g., Hawke and Spudis 1980; Hawke et al. 1985). Significant progress has been made in the last ten years and the new data show that if cryptomaria are included, the total area covered by mare deposits exceeds 20% of the lunar surface, compared to ~17% of typical mare deposits alone (Head 1976; Antonenko et al. 1995). Recent studies using Clementine color data further expand the extent of cryptomare, especially in the Schickard region (e.g., Hawke et al. 1998; Antonenko and Yingst 2002). Similarly, Clark and Hawke (1991), on the basis of Apollo X-ray fluorescence data, found a mafic enrichment of areas south of crater Pasteur apparently associated with buried basalts. The data not only show a wider spatial distribution of products of early volcanism, but also indicate that mare volcanism was already active prior to the emplacement of Orientale ejecta. Even older cryptomare may exist but evidence for such ancient cryptomare is likely to be even more obscured by superposed ejecta deposits. Using Clementine multispectral images and Lunar Prospector gamma-ray spectrometer data, Giguere et al. (2003) and Hawke et al. (2005) report that the buried basalts in the Lomonosov-Fleming and the Balmer-Kapteyn regions are very low to intermediate titanium basalts. Sampling and subsequent analysis of such deposits is required to understand the true nature of cryptomaria. Until then, careful study of crater ejecta using, for example, high-resolution reflectance spectra, should lead to a better understanding of the extent and importance of the very earliest volcanism on the Moon.

2.2.5. Volcanic centers. Several areas of the Moon are characterized by an anomalously high concentration of volcanic features. Examples include the Marius Hills (Fig. 1.23b) and the Aristarchus Plateau/Rima Prinz region in Oceanus Procellarum. The Marius Hills (~35,000 km²) consist of more than 100 domes and cones and 20 sinuous rilles (Weitz and Head 1998), and the Aristarchus Plateau/Rima Prinz region (~40,000 km²) shows at least 36 sinuous rilles (Guest and Murray 1976; Whitford-Stark and Head 1977). The large number of sinuous rilles suggests that these two regions are loci of multiple high-effusion-rate, high-volume eruptions, which may be the source for much of the lavas exposed within Oceanus Procellarum (Whitford-Stark and Head 1980). Work by McEwen et al. (1994), using Clementine color data, indicates the presence of mare basalts that underlie a 10–30 m thick layer of pyroclastic material and anorthosite within the Aristarchus crater. Clementine altimetry profiles show the Aristarchus Plateau sloping ~1° to the north-northwest and rising about 2 km above the lavas of the surrounding Oceanus Procellarum (McEwen et al. 1994).

2.2.6. Domes, sills, and shields. Lunar mare domes are generally broad, convex, semi-circular landforms with relatively low topographic relief (Fig. 1.23b). Guest and Murray (1976) mapped 80 low domes with diameters of 2.5–24 km, 100–250 m heights, and 2–3° slopes with a high concentration in the Marius Hills complex. Some of the domes of the Marius Hills have steeper slopes (7–20°) and some domes have summit craters or fissures. The formation of mare domes is thought to be related to eruptions of more viscous (more silicic) lavas, intrusions of shallow laccoliths, or mantling of large blocks of older rocks with younger lavas (e.g., Heather et al. 2003; Lawrence et al. 2005). Importantly, no shield volcanoes larger than ~20 km have been identified on the Moon (Guest and Murray 1976).

Large shield volcanoes (>50 km) are the most prominent volcanic features on Earth, Venus, and Mars. They are built by a large number of small flows derived from a shallow magma reservoir where the magma reaches a neutral buoyancy zone (e.g. Ryan 1987; Wilson and Head 1990). The presence of shield volcanoes and calderas indicates shallow buoyancy zones, stalling and evolution of magma there, production of numerous eruptions of small volumes and durations, and shallow magma migration to cause caldera collapse. The general absence of such shield volcanoes implies that shallow buoyancy zones do not occur on the Moon, and that lavas

did not extrude in continuing sequences of short-duration, low-volume eruptions from shallow reservoirs. This is a fundamental observation and it makes the Moon an unique endmember compared to other terrestrial planets. However, in a few cases magma may have stalled near the surface and formed shallow sills or laccoliths, as possibly indicated by the formation of floor-fractured craters (Schultz 1976). This interpretation is supported by studies of Wichman and Schultz (1995, 1996) and by modeling of floor-fractured craters, which led Dombard, and Gillis (2001) to conclude that, compared to topographic relaxation, laccolith emplacement is the more viable formation process. Wichman and Schultz (1996) presented a model that allowed them to estimate the minimum depth of a 30 km wide and 1900 m thick intrusion beneath crater Tauruntius to be on the order of 1–5 km. The magma excess pressure was modeled to be on the order of 9 MPa.

2.2.7. Cones. Cinder cones, the most common terrestrial subaerial volcanic landform, are frequently associated with linear rilles on the Moon, for example in crater Alphonsus (Head and Wilson 1979). Lunar cones are less than 100 m high, are 2–3 km wide, have summit craters of less than 1 km, and have very low albedos (Guest and Murray 1976).

2.2.8. Lava terraces. In some craters small lava terraces have been observed and interpreted as remnants of lava that drained back into a vent or by flow into a lower basin (Spudis and Ryder 1986). As for all other small-scale, low-relief features (e.g., cones, flow fronts), lava terraces are difficult to recognize and require special image qualities such as high spatial image resolution combined with favorable low-sun angle illumination to enhance their morphology.

2.2.9. Pyroclastic deposits. Regional pyroclastic deposits are extensive ($>2500 \text{ km}^2$) and are located on the uplands adjacent to younger maria (e.g., Gaddis et al. 1985; Weitz et al. 1998). In contrast, localized pyroclastic deposits are smaller in extent and are more widely dispersed across the lunar surface (Head 1976; Hawke et al. 1989; Coombs et al. 1990). Pyroclastic glass beads and fragments are especially abundant at the Apollo 17 site (e.g., Figure 1.24a). The Apollo 17 orange glasses and black vitrophyric beads formed during lava fountaining of gas-rich, low-viscosity, Fe-Ti-rich basaltic magmas (Heiken et al. 1974). Experiments by Arndt and von Engelhardt (1987) indicated that crystallized black beads from the Apollo 17 landing site had cooling rates of $100 \text{ }^\circ\text{C/s}$, which is much slower than expected from blackbody cooling in a vacuum. Apollo 15 green glasses are also volcanic in origin as are other pyroclastic glasses found in the regolith of other landing sites (Delano 1986). Although trivial in volume, these glasses are important because they indicate that lava fountaining occurred on the Moon and because, as melts generally unmodified by crystal fractionation, they may represent the best samples for studying the lunar mantle. Regional dark-mantle deposits, which cover significant areas of the lunar surface, can be detected in remotely sensed data (e.g., Hawke et al. 1979, 1989; Head and Wilson 1980; Gaddis et al. 1985; Coombs et al. 1990; Greeley et al. 1993; Weitz et al. 1998; Weitz and Head 1999; Head et al. 2002). These deposits tend to occur along the margins of impact basins and in association with large vents and sinuous rilles, implying that they were formed by large-volume sustained eruptions.

Regional dark-mantle deposits are interpreted to result from eruptions in which continuous gas exsolution in the lunar environment caused Hawaiian-style fountaining that distributed pyroclastic material over tens to hundreds of kilometers (Wilson and Head 1981, 1983). Figure 1.24b is an example for near-surface propagation of a dike, which resulted in an extensional surface stress field forming a graben (i.e., Hyginus Rille). Gas exsolution from the dike formed numerous pit craters along the graben floor (e.g., Head et al. 1998). Significant progress in understanding the ascent and eruption conditions of pyroclastic deposits has been made over the last decade and we point the reader, for example, to Head et al. (2002), references therein, and to Chapter 4 of this volume. There is also strong evidence that at least some of the observed dark-halo craters are volcanic (i.e., pyroclastic) in origin, whereas others are impact craters

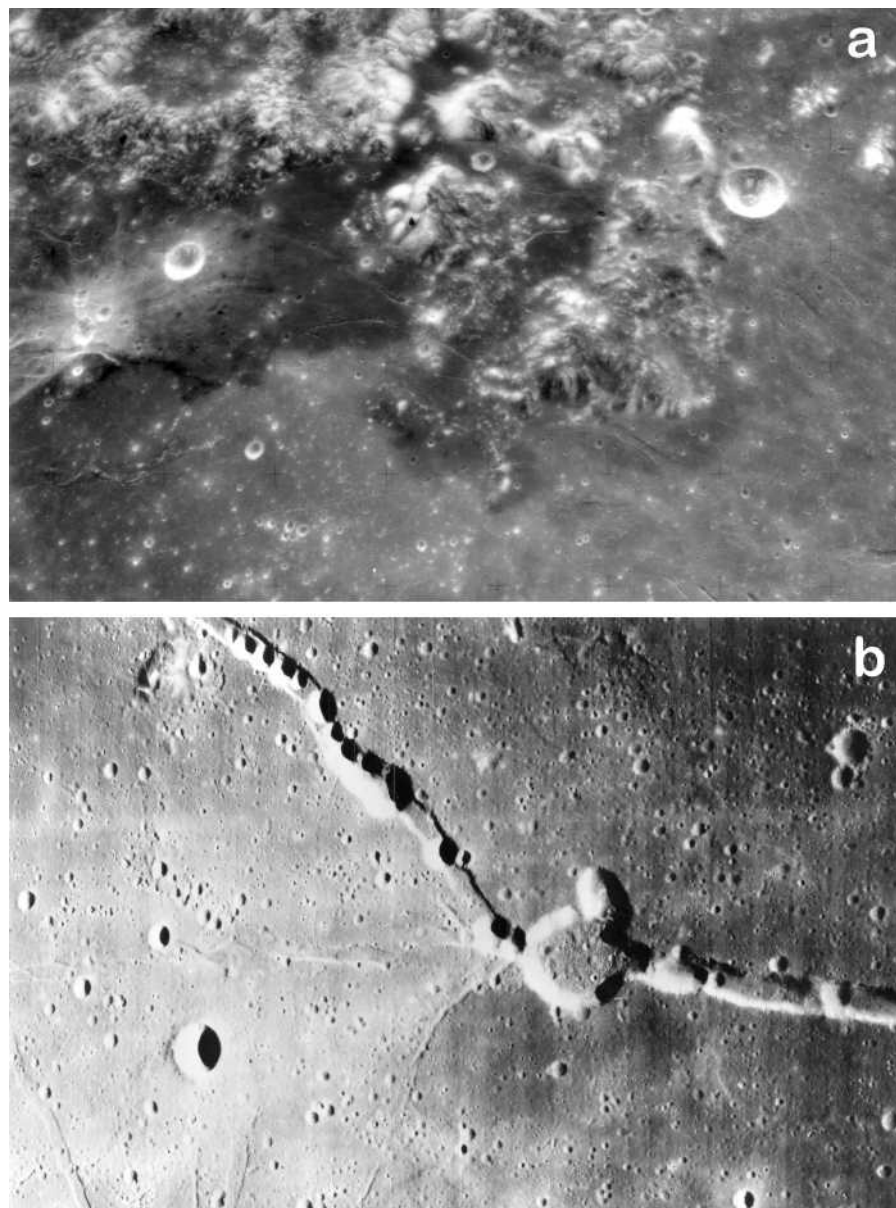


Figure 1.24. Examples of volcanic landforms; (a) pyroclastic deposits close to the Apollo 17 landing site (Ap 15 frame M-1404) and (b) pit craters of Rima Hyginus (LO V M-97).

that excavated darker material from subsurface levels. Dark-halo craters that are volcanic in origin are commonly located along fractures and on the floors of larger craters and do not have the same morphologies as impact craters. From studies of dark-halo craters within crater Alphonsus, it appears likely that they formed from vulcanian-style eruptions (Head and Wilson 1979; Coombs et al. 1990).

2.2.10. Filling of the basins. Studies of impact-basin formation indicate that immediately after the impact excavation, the transient cavity collapses, leading to large-scale fracturing of the crust and providing structures along which magma could ascend to the surface (also see the discussion in Chapter 4 and in section 1.2.2.13 of this chapter). It appears that physical uplift of mantle material during basin formation occurred in association with a decrease of lithostatic pressure caused by sudden removal of overburden (Brett 1976). If uplifted mantle materials were already near their melting temperatures, decreasing confining pressure might have led to melting and magma generation below the basin. However, from the absolute age dating of specific rock samples, it would appear that significant periods of time elapsed between basin formation and extrusion of mare basalts into the basin. For example, the Imbrium basin is thought to be 3.85 b.y. old, but the lavas sampled at the Apollo 15 site are about 3.3 b.y. old. Nonetheless, deeper, buried basalts at the Apollo 15 site and elsewhere in Mare Imbrium could be much older. Volcanism in some of the lunar nearside basins lasted several billion years after the basin impact events (Hiesinger et al. 2000, 2003), and it appears unlikely that magma would ascent along impact-induced fractures for such extended periods of time. Also, recent thermal modeling suggests that craters of 300–350 km in diameter likely did not raise uplifted mantle material above its solidus in order to produce mare basalts (Ivanov and Melosh 2003).

Differences also exist in the distribution and amount of lava filling lunar basins. Nearside basins were flooded with basalts to a significantly greater degree than farside basins, seemingly corresponding to differences in crustal thickness. However, Wieczorek et al. (2001) have argued that crustal thickness plays only a minor role in the eruption of basalt. The ascent and eruption of basalt remains a complex issue and is discussed in more detail in Chapters 3 and 4.

2.2.11. Volumes of basalts. The total volume of volcanic products can be used to estimate the amount of partial melting and how much of the lunar mantle was involved in the production of the mare basalts. Establishing the volume of mare basalts emplaced on the surface as a function of time (the flux) sets an important constraint on the petrogenesis of mare basalts and their relation to the thermal evolution of the Moon (Head and Wilson 1992). A variety of techniques have been used to estimate the thicknesses of basalts within the large lunar impact basins (summarized by Head 1982). Crater-geometry techniques using pristine crater morphometric relationships and the diameter of partially to almost entirely flooded craters yield values of basalt thickness up to 2 km, ranging 200–400 m on average (DeHon and Waskom 1976). Hörz (1978) reviewed the assumptions underlying the thickness estimates of DeHon and Waskom (1976) and concluded these values were overestimates.

More recently, thickness estimates have been updated using new Clementine spectral data by Budney and Lucey (1998), who investigated craters that penetrated the maria and excavated underlying nonmare material to derive the thickness of basalts in Mare Humorum. Their results agree better with results from Hörz (1978) than with results from DeHon (1975, 1977, 1979) and Head (1982). Figure 1.25 is a map of the DeHon and Waskom (1976) data; insets compare thickness estimates of (a) Budney and Lucey (1998) with those of (b) DeHon and Waskom (1976). Studies of mascons, that is, positive gravity anomalies observed for many of the mare basins, indicate basalt thicknesses of 1–2 km and volumes of $6 \times 10^6 \text{ km}^3$ (e.g., Head 1975a, Thurber and Solomon 1978). Because even the largest estimates are still <1 % of the volume of the lunar mantle, it appears that high degrees of partial melting involving large regions of the mantle did not occur within the Moon.

Equally important to estimates of the total erupted basalt volumes are estimates of volumes for individual basalt flow units. Since the publication of the Lunar Source Book (1991), several studies on this aspect of lunar volcanism have been conducted (e.g., Yingst and Head 1997, 1998; Hiesinger et al. 2002). Yingst and Head (1998) investigated individual isolated lava ponds in Mare Smythii and Mare Marginis and, from morphologic evidence, concluded that these lavas were emplaced during a single eruptive phase. They found that pond volumes in both

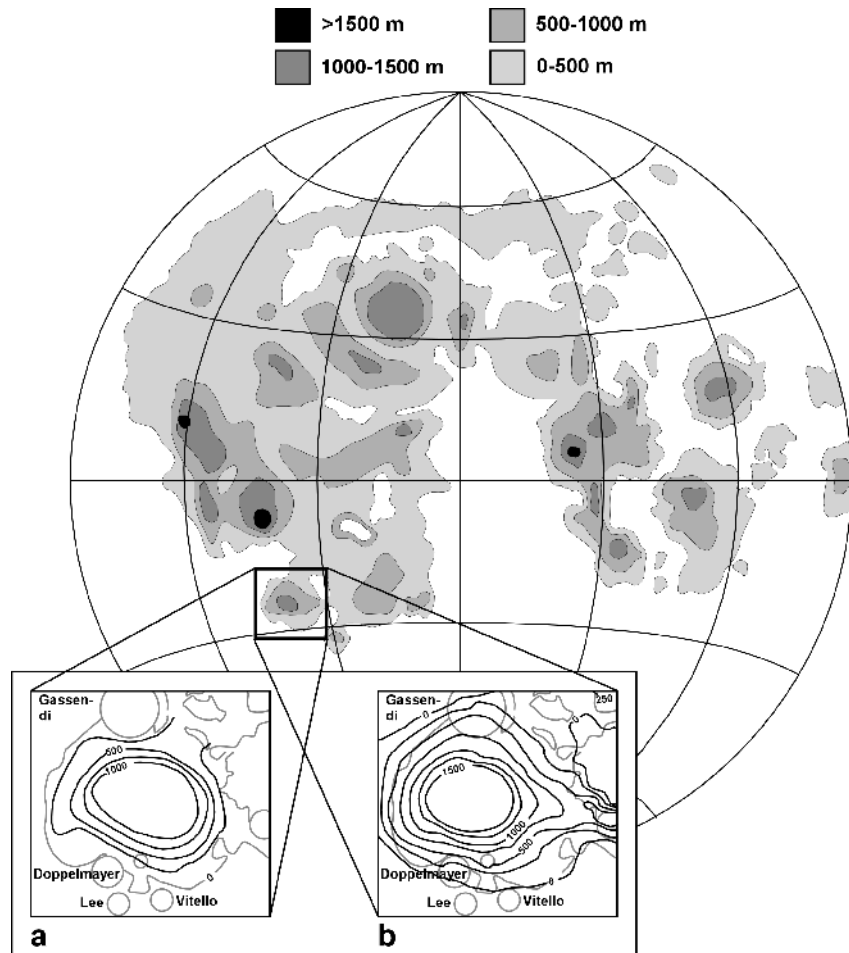


Figure 1.25. Thickness of basalts on the lunar nearside (DeHon and Waskom 1976). Inserts compare estimates for Mare Humorum of (a) Budney and Lucey (1998) and (b) DeHon and Waskom (1976).

maria range from 15 km^3 to 1045 km^3 . The mean pond volume in Mare Smythii is $\sim 190 \text{ km}^3$ and about $\sim 270 \text{ km}^3$ in Mare Marginis. Ponds in the South Pole-Aitken basin that were also interpreted to be single eruptive phases have volumes ranging from 35 to 8745 km^3 and average 860 km^3 (Yingst and Head 1997). Flow units in the Mare Orientale/Mendel-Rydberg basins have volumes of 10 to 1280 km^3 and a mean volume of 240 km^3 (Yingst and Head 1997). From a study of 58 mare flow units in the major nearside basins, Hiesinger et al. (2002) found that the range of volumes is $30\text{--}7700 \text{ km}^3$. The minimum average volume of all investigated flow units was estimated to be $\sim 590 \text{ km}^3$ and the maximum average volume, $\sim 940 \text{ km}^3$.

2.2.12. Ages of lunar mare basalts. The onset and extent of mare volcanism are not very well understood (summarized by Nyquist et al. 2001). The returned samples revealed that mare volcanism was active at least between ~ 3.9 and 3.1 Ga (Head 1976; Nyquist and Shih 1992). Ages of some basaltic clasts in older breccias point to an onset of mare volcanism prior to 3.9 b.y. (Ryder and Spudis 1980), perhaps as early as $4.2\text{--}4.3 \text{ b.y.}$ in the Apollo 14 region (Taylor et al. 1983; Dasch et al. 1987; Nyquist et al. 2001). Early volcanism is also supported by remote-

sensing data. For example, Schultz and Spudis (1979), Hawke and Bell (1981), and Antonenko et al. (1995) interpreted dark halo craters as impacts into basaltic deposits that are now buried underneath a veneer of basin ejecta. These underlying basalts might be among the oldest basalts on the Moon, implying that volcanism was active prior to ~ 3.9 b.y. ago.

Remote-sensing data suggest that the returned samples represent only a small number of basalt types from a few limited locations and that the majority has still not been sampled (Pieters 1978; Giguere et al. 2000). On the basis of crater degradation stages, Boyce (1976) and Boyce and Johnson (1978) derived absolute model ages that indicate volcanism might have lasted from 3.85 ± 0.05 b.y. until 2.5 ± 0.5 b.y. ago. Support for such young basalt ages comes from a recently collected lunar meteorite, Northwest Africa 032, which shows a Ar-Ar whole rock age of ~ 2.8 b.y. (Fagan et al. 2002). Schultz and Spudis (1983) made crater size-frequency distribution measurements for basalts embaying the Copernican crater Lichtenberg and concluded that these basalts might be less than 1 b.y. old.

Over the last five years, a large effort has been made to systematically determine model ages of all basalts on the lunar surface using crater counts (e.g., Hiesinger et al. 2000, 2001, 2003). At the time of writing ~ 220 basalt units have been dated (Fig. 1.26). Hiesinger et al. (2000, 2001, 2003) applied a new approach based on color-ratio composites to ensure the definition of spectrally homogeneous lithologic units for which they performed crater counts. The model ages so derived indicate that mare volcanism lasted from ~ 4.0 to 1.2 b.y. Their results also indicate that lunar volcanism was not evenly distributed throughout time but peaked in the Late Imbrian and drastically declined during the Eratosthenian Period. The ages of lunar mare basalts are discussed in more detail in Chapter 4.

2.2.13. Magma generation and eruption. Petrologic models are discussed in Chapter 4; here we convey only some basic concepts about the ascent and eruption styles of lunar magmas.

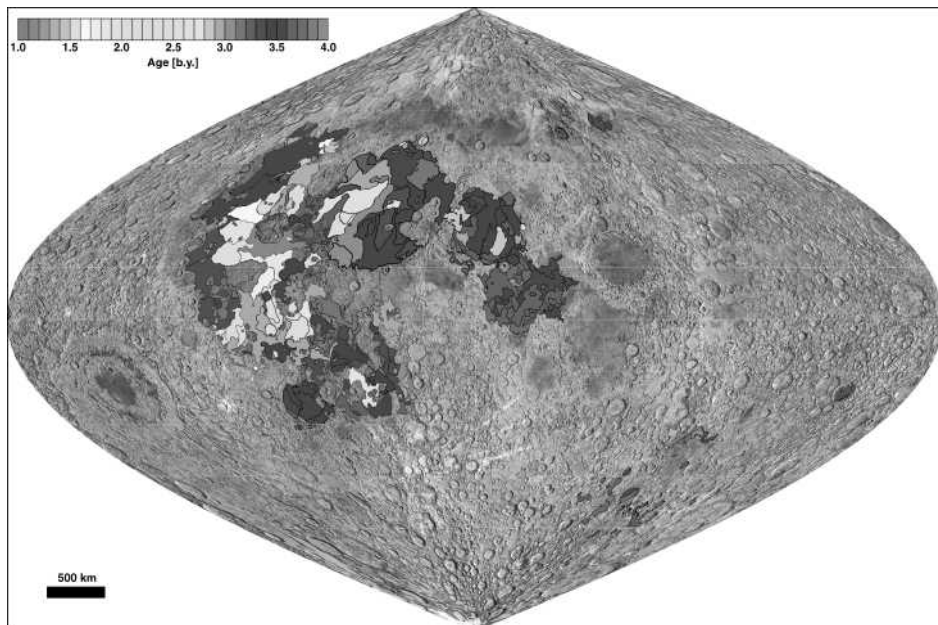


Figure 1.26. Absolute model ages of mare basalts based on crater counts on spectrally and morphologically defined mare units (Hiesinger et al. 2000, 2001, 2003). Base map is a shaded relief in sinusoidal projection. See Plate 1.1 for a color version of this figure.

Most petrologic models of lunar basaltic magmas suggest an origin by partial melting at 200–400 km depth (e.g., Ringwood and Essene 1970; Hubbard and Minear 1975; Ringwood and Kesson 1976; BVSP 1981; Taylor 1982). Interestingly, experimental data suggest the volcanic (pyroclastic) glasses were derived from greater depths within the lunar mantle (360–520 km) than the crystalline mare basalts (e.g., Green et al. 1975; Longhi 1992a,b, 1993). It was thought early on that magma ascent was related to impact-induced fracture and fault zones, with the location of conduits having been affected by impact structures (Solomon and Head 1980). However, it is unlikely that basin-induced fractures would have remained open for the extended periods of time (several hundred million years) that are indicated for extrusion of lavas by radiometrically dated samples and crater counts (Hiesinger et al. 1999; Melosh 2001). Dike propagation models further suggest that fractures played little to no role in controlling the paths of dikes. In addition, petrologic and geochemical evidence suggest that the basaltic melts are less dense than the lunar mantle but denser than the overlying crust. Hence, basaltic diapirs would rise buoyantly through the lunar mantle, but would stall at the base of the crust and would not erupt onto the surface if they simply followed fracture zones in the crust (Head and Wilson 1992).

Head and Wilson (1992) suggested instead that overpressurization of basaltic diapirs was the key to upward dike propagation into overlying rocks (Fig. 1.27). The excess pressure required to propagate a dike to the surface is on the order of ~15 MPa for a ~64 km thick

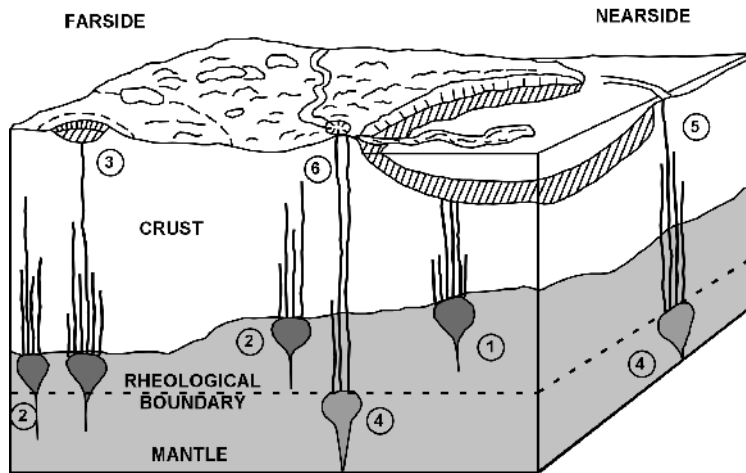


Figure 1.27. Magma transport from neutral buoyancy zones (Head and Wilson 1992). Diagrammatic representation of the emplacement of secondary crust on the Moon. At (1), early basaltic magmas rise diapirically to the density trap at the base of the crust. Those below topographic lows (thin crust) associated with lunar impact basins are in a favorable environment for dike propagation and extrusion of lavas to fill the basin interior. Diapirs reaching the base of the thicker crust on the farside and parts of the nearside (2) at the same time stall and propagate dikes into the crust, most of which solidify in the crust and do not reach the surface. Variations in regional and local compensation produce a favorable setting for emplacement of some lavas in craters and the largest basins on the farside (3). With time, the lithosphere thickens and ascending diapirs stall at a rheological boundary, (4) build up of excess pressure to propagate dikes toward the surface. At the same time, loading and flexure of the earlier mare deposits creates a stress environment that favors extrusion at the basin edge (5); lavas preferentially emerge at the basin edge, flowing into the subsiding basin interior. The latest eruptions are deepest and require high stress buildups and large volumes in order to reach the surface; thus, these tend to be characterized by high-volume flows and sinuous rilles (6). Deepening of source regions over time and cooling of the Moon causes activity to diminish and eventually cease.

nearside crust and about ~20 MPa for a ~86 km thick farside crust (Head and Wilson 1992). To erupt magma onto the surface, slightly higher pressures of ~21 and ~28 MPa, respectively, are required. These conditions correspond to dike widths of a few to several hundred meters (Head and Wilson 1992). This model predicts that volcanic material should preferentially occur on the lunar nearside where the crust is thinner and more dikes can reach the surface. On the farside more dikes would stall within the crust, extruding only in the deepest basins. This argument, however, does not explain the paucity of basalts in the South Pole-Aitken basin. From recent crustal thickness models and the presumption of a mafic lower crust, Wieczorek et al. (2001) concluded that all basaltic magmas would be less dense than the lower crust; thus, when a basin-forming impact excavated the upper portion of the crust, any basaltic magma could reach the surface. A more comprehensive knowledge of crustal thickness, crustal composition with depth, and basalt compositions around the globe are needed to improve our understanding of eruption of basalts on the Moon.

The common occurrence of volcanic glasses among the lunar samples and as observed with remote sensing indicates that some lavas rose through the crust rapidly in order to reach the surface with little or no crystallization. Head and Wilson (1979) calculated that the rising velocity of magma would have to be >0.5–1.0 m/s to maintain lava fountains even if no explosive lava fountaining occurred. Vesicles indicate that volatile phases, most likely CO, were present when the rocks were molten and only 250–750 ppm of CO are required to disrupt magmas at depths of 15–40 km, causing explosive eruptions. In a study of a 180 km wide dark pyroclastic ring south of the Orientale basin, Weitz et al. (1998) estimated that the plume height was on the order of 20 km and that ejection velocities were ~320 m/s. In a recent study, Head et al. (2002) derived similar velocities of ~350–420 m/s.

By coupling the estimated eruptive volumes (discussed above) with basalt ages (absolute and relative), estimates of the flux of mare volcanism on the Moon are possible (e.g., Hartmann et al. 1981; Wilhelms 1987; Head and Wilson 1992). Head and Wilson (1992) pointed out that during the Upper Imbrian $\sim 9.3 \times 10^6 \text{ km}^3$ of mare basalts were emplaced. Assuming steady emplacement throughout the Upper Imbrian yields an average eruption rate of $\sim 0.015 \text{ km}^3/\text{yr}$. Applying the same approach to the Eratosthenian and Copernican Period indicates an average eruption rate of $\sim 1.3 \times 10^{-4} \text{ km}^3/\text{yr}$ and $\sim 2.4 \times 10^{-6} \text{ km}^3/\text{yr}$ respectively. Head and Wilson (1992) reported that at its peak average flux, lunar global eruption rates are $\sim 10^{-2} \text{ km}^3/\text{yr}$, an amount comparable to eruption rates of a single terrestrial volcano such as Vesuvius or Kilauea, Hawaii. However, some lunar sinuous rilles have been estimated to emplace $\sim 1000 \text{ km}^3/\text{yr}$ (Hulme 1973), hence representing about 70,000 years of the average flux. On the basis of their investigation of the dark Orientale ring deposit, Head et al. (2002) estimated the total erupted mass to be on the order of $7\text{--}17 \times 10^{13} \text{ kg}$, an eruption rate of $\sim 2 \times 10^8 \text{ kgs}^{-1}$, and a total duration of the eruption of $\sim 4\text{--}11$ days.

2.2.14. Non-mare domes. Several presumably volcanic features on the Moon have albedos, spectral characteristics, and morphologies that differ from typical mare volcanic features. Examples of such non-mare volcanism are the Gruithuisen domes ($\sim 36^\circ\text{N}$, $\sim 40^\circ\text{W}$; Fig. 1.28), the Mairan domes and cones ($\sim 40^\circ\text{N}$, $\sim 46^\circ\text{W}$), as well as Hansteen Alpha ($\sim 12^\circ\text{S}$, $\sim 50^\circ\text{W}$) and Helmet ($\sim 17^\circ\text{S}$, $\sim 32^\circ\text{W}$) (see Hawke et al. 2003). These domes are up to 20 km in diameter with a topographic relief of more than 1000 m and their shapes are consistent with extrusion of viscous lava (Gruithuisen domes) and explosive volcanism (Mairan cones) (Head and McCord 1978; Chevrel et al. 1998; Wilson and Head 2003b). Spectrally they are characterized by a downturn in the ultraviolet, similar to the “red spots” mapped elsewhere (Wood and Head 1975; Bruno et al. 1991; Hawke et al. 2002a). No samples collected and returned from the landing sites match their spectral characteristics. Due to the relatively small size and steep slopes of these features their age is difficult to determine. From recent crater counts, the Gruithuisen domes appear to be contemporaneous with the emplacement of the surrounding mare basalts but postdate the

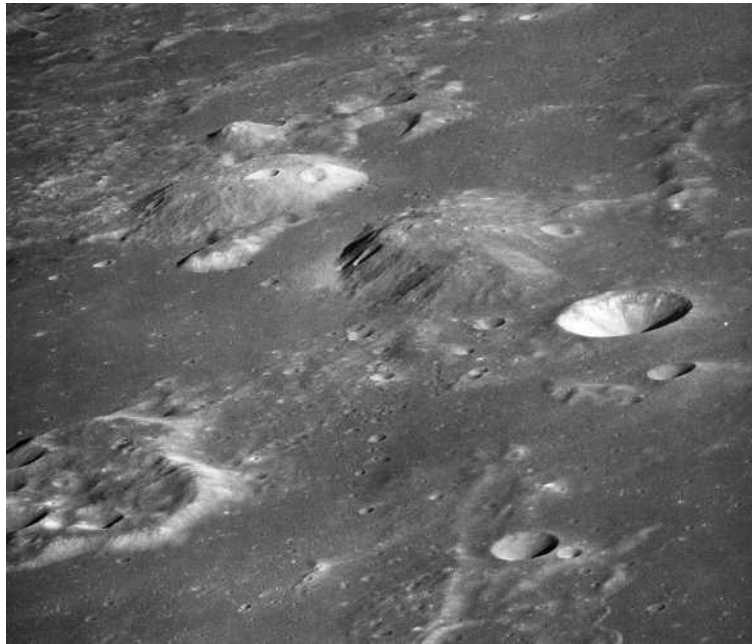


Figure 1.28. Oblique view of the non-mare Gruithuisen domes.

formation of post-Imbrium crater Iridum (Wagner et al. 1996, 2002). Contemporaneity with the maria has been interpreted to indicate petrogenetic linkages; one possibility is that mare diapirs stalled at the base of the crust and partially remelted the crust, which produced more silicic viscous magmas (e.g., Head et al. 2000). Malin (1974) argued that lunar “red spots” are the surface manifestation of more radioactive pre-mare basalts such as occur among the Apollo 12 and 14 KREEP-rich material). Hawke et al. (2003), however, showed that one of these, Hansteen Alpha, although occurring in an area of elevated Th concentrations, is not enriched in Th relative to surrounding mare basalts. However, more recent work by Lawrence et al. (2005), who re-modeled Lunar Prospector Th data for this area, showed Hansteen Alpha contains up to 25 ppm Th. Head and Wilson (1999) reported that the yield strength ($\sim 10^5$ Pa), plastic viscosity ($\sim 10^9$ Pa s), and effusion rates (~ 50 m³/s) of the Gruithuisen domes are similar to those of terrestrial rhyolites, dacites, and basaltic andesites. The viscosity of lava that formed the Gruithuisen Domes is orders of magnitudes larger than for typical mare basalts (0.45–1 Pa s; Murase and McBirney 1970; Wilson and Head 2003). On the basis of near-IR spectra, Hawke et al. (2002a) concluded that Helmet is noritic in composition, implying on average slightly higher SiO₂ compared to mare basalts. For the most recent discussion of the composition of non-mare domes, we defer to Hawke et al. (2001, 2002a,b, 2003) and Lawrence et al. (2005).

2.2.15. Light plains. The origin of lunar “light plains” is still not well understood and is a controversial topic. Prior to the Apollo 16 mission, light plains (in this case, the Cayley Formation) were thought to be products of some sort of highland volcanism because of their smooth texture and their filling of highland craters. Crater counts suggested that these plains formed between the latest basin-scale impact event and the emplacement of the maria. Thus it was thought that significant amounts of highland volcanism occurred during the Early Imbrian. However, samples from the Apollo 16 site showed that light plains mainly consist of impact breccias and not volcanic material. Fieldwork and laboratory studies indicate that light plains can form by

ballistic erosion and sedimentation processes (Oberbeck et al. 1974; Oberbeck 1975). Light plains appear not to represent a single ejecta blanket (e.g., from Orientale or Imbrium), but consist of deposits mixed dynamically from primary ejecta and local sources. New crater counts of light plains deposits, however, show a wide variety of ages that cannot be exclusively attributed to either the Orientale or Imbrium events, suggesting that at least some of the light plains might be of volcanic origin (Neukum 1977; Köhler et al. 1999, 2000). Spudis (1978) and Hawke and Head (1978) suggested that some light plains might be related to KREEP volcanism. Hawke and Bell (1981), Antonenko et al. (1995), and Robinson and Jolliff (2002) presented evidence that ancient lava plains (cryptomare) might be present beneath some light plains. In summary, these studies suggest that light plains may have formed by a variety of processes and that the interpretation of their origin should be addressed on a case-by-case basis.

2.3. Tectonic processes

2.3.1. A one-plate planetary body. Tectonic features suggest that the Moon underwent global expansion before about 3.6 b.y. ago, followed by net global contraction from that point until today (e.g., Solomon and Head 1980). However, compared to Earth, there is no evidence for plate tectonics on the Moon. This raises several questions. Why are these planetary bodies so different and how do they compare to other planets? What is the driving force in their evolution? How do tectonic styles and heat-loss dynamics change with time?

Crystallization of a globally continuous, low-density crust from a magma ocean may have precluded the development of plate tectonics early in lunar history. Following the establishment of such a nearly continuous low-density crust or stagnant lid, conductive cooling dominated the heat transfer on the Moon, which resulted in the production of a globally continuous lithosphere rather than multiple, moving, and subducting plates as on Earth. Heat flow experiments carried out during the Apollo missions revealed values much less than those on Earth (e.g., Langseth et al. 1976) and are consistent with heat loss predominantly by conduction. Furthermore, nearside seismic data indicate the presence of an outer relative rigid, 800–1000 km thick lithosphere. The large ratio of surface area to volume of the Moon is very effective in cooling the planet by conduction, i.e. radiating heat into space. Thus the lithosphere of the Moon thickened rapidly and the Moon quickly became a one-plate planet, which lost most of its heat through conduction (Solomon 1978). In this respect the Moon is more similar in its lithospheric heat transfer mechanism, that is conduction, to Mercury and Mars, and even Venus, than it is to Earth (Solomon and Head 1982). Venus is presently characterized by conductive heat loss, but there is evidence that the heat loss on Venus may have been episodic. On the other hand, Earth is dominated by plate recycling and radioactive decay of elements sequestered in the continental crust, while yet another heat loss mechanism, advective cooling through constant volcanic eruptions, characterizes the innermost Galilean satellite, Io.

2.3.2. Moonquakes. Most information about lunar tectonic processes has been gathered from the interpretation of surface images, the Apollo seismometers, and from modeling of the thermal state of the crust and the mantle. Compared to Earth, the internal tectonic activity on the Moon, i.e., moonquakes, is a minor process, probably releasing less than 10^{-12} of the energy of terrestrial seismic activity (e.g., Goins et al. 1981). The crust of the Moon appears to be thick, rigid, immobile, and cool, inhibiting large-scale motion. The lack of crustal deformation is consistent with the returned samples that show virtually no textures typical of plastic deformation. There are two types of moonquakes, which differ in the location of their source region. Based on a re-evaluation of Apollo seismic data, the source depths of moonquakes have recently been re-investigated (e.g., Khan et al. 2000; Nakamura 2003, 2005). Shallow moonquakes are now thought to originate at depths of ~50–220 km and deep moonquakes, at depths of ~850–1100 km (Khan et al. 2000). Deep-seated moonquakes, which are correlated with the Earth's tides, originate from so-called nests that repeatedly release seismic energy (e.g., Nakamura 1983). All but one of these nests are located on the lunar nearside, a phenomenon not well understood

(e.g., Oberst et al. 2002). One explanation could be that if the lunar mantle is partially molten at depths of ~1000 km below the surface, one would not be able to measure farside S-waves, which is necessary for the location of moonquakes on the lunar farside (Nakamura et al. 1973). However, in a re-evaluation of the Apollo seismic data, Nakamura (2005) identified ~30 nests of deep moonquakes that are likely to be on the lunar farside, although he noted that only a few of them are locatable with the currently available Apollo seismic data.

2.3.3. Impact-induced tectonism. Impacts extensively shatter the subsurface and cause lateral and vertical movements of the crust. Ahrens and Rubin (1993) pointed out that damage caused by impact-induced rock failure decreases as a function of $\sim r^{-1.5}$ from the crater, indicating a dependence on the magnitude and duration of the tensile pulse. In order to adjust to the post-impact stress field, subsequent movements likely occurred along impact-induced faults, which may be kept active for long periods of time or may be reactivated by seismic energy from subsequent impacts (e.g., Schultz and Gault 1975). Post-impact isostatic adjustments of large impact structures might have occurred; however, the rigidity of the lunar crust inhibits this process, resulting in numerous basins that remain in isostatic disequilibrium even several billion years after the impact. Although the existence of the Procellarum basin is still debated (e.g., Wilhelms 1987; Spudis 1993; Neumann et al. 1996; Schmitt 2000a, 2001), Cooper et al. (1994) proposed that the Procellarum basin is the result of faulting associated with the Imbrium event. A similar argument has been made for Frigoris (see review in Spudis 1993).

2.3.4. Loading-induced tectonism. Loading of large basin structures by infilling with basalts produced extensional stress fields that may have led to the formation of concentric graben at the edges of the basins (Fig. 1.29a). The loading also produced down-warping of the basin center accompanied by compressional stresses that caused the formation of wrinkle ridges (Fig. 1.29b). Graben in the Humorum area that are concentric to the basin structure are a few hundred kilometers long and are filled with basaltic lavas, indicating that they were relatively early extensional features. These graben extend virtually unobstructed from the mare into the adjacent highlands and cut across preexisting craters, which suggests that they were formed by a substantial, possibly deep-seated, basin-wide stress field. Schultz and Zuber (1994) investigated faulting caused by axisymmetric surface loading and pointed out that geophysical models of flexural stresses in an elastic lithosphere due to loading typically predict a transition with increased distance from the center from radial thrust faults to strike-slip faults to concentric normal faults. These models (e.g., Melosh 1978; Golombek 1985) are inconsistent with the absence of annular zones of strike-slip faults around the lunar maria. Schultz and Zuber (1994) suggested that this paradox is caused by difficulties in relating failure criteria for brittle rocks to stress models. Their findings apply not only to basin loading with lunar maria but also to loading of the venusian and martian lithospheres with large volcanoes or, for example, the Tharsis rise. Freed et al. (2001) showed that lunar curvature, certain initial stress distributions, and certain failure criteria reduce and perhaps eliminate the zone of strike-slip faulting.

2.3.5. Tidal forces. Dynamical considerations indicate that during its early history the Moon was closer to Earth than it is today (e.g., Thompson and Stevenson 1983; Kokubo et al. 2000; Touma 2000). If this is true or if the Moon underwent any reorientation (e.g., Melosh 1975), tidal and synchronous rotational stresses could have built up to 100 kbar (at Earth-Moon distances of $< 8 R_e$) within the early lunar lithosphere, an amount large enough to produce major tectonic deformation. However, this deformation would have occurred during the times of intense impact bombardment, which would have destroyed the evidence for such deformation. Today, tidal forces deform the Moon into a triaxial ellipsoid and tidal stresses of ~0.2 bar at depths of 700–1100 km appear sufficiently large to trigger deep moonquakes. Recently, detailed maps of lunar lineaments have been compared to predicted stress patterns caused by tidal forces. Chabot et al. (2000) found that patterns on the near and farside are similar. However, because patterns of the sub-Earth and anti-Earth regions are indistinguishable from patterns in

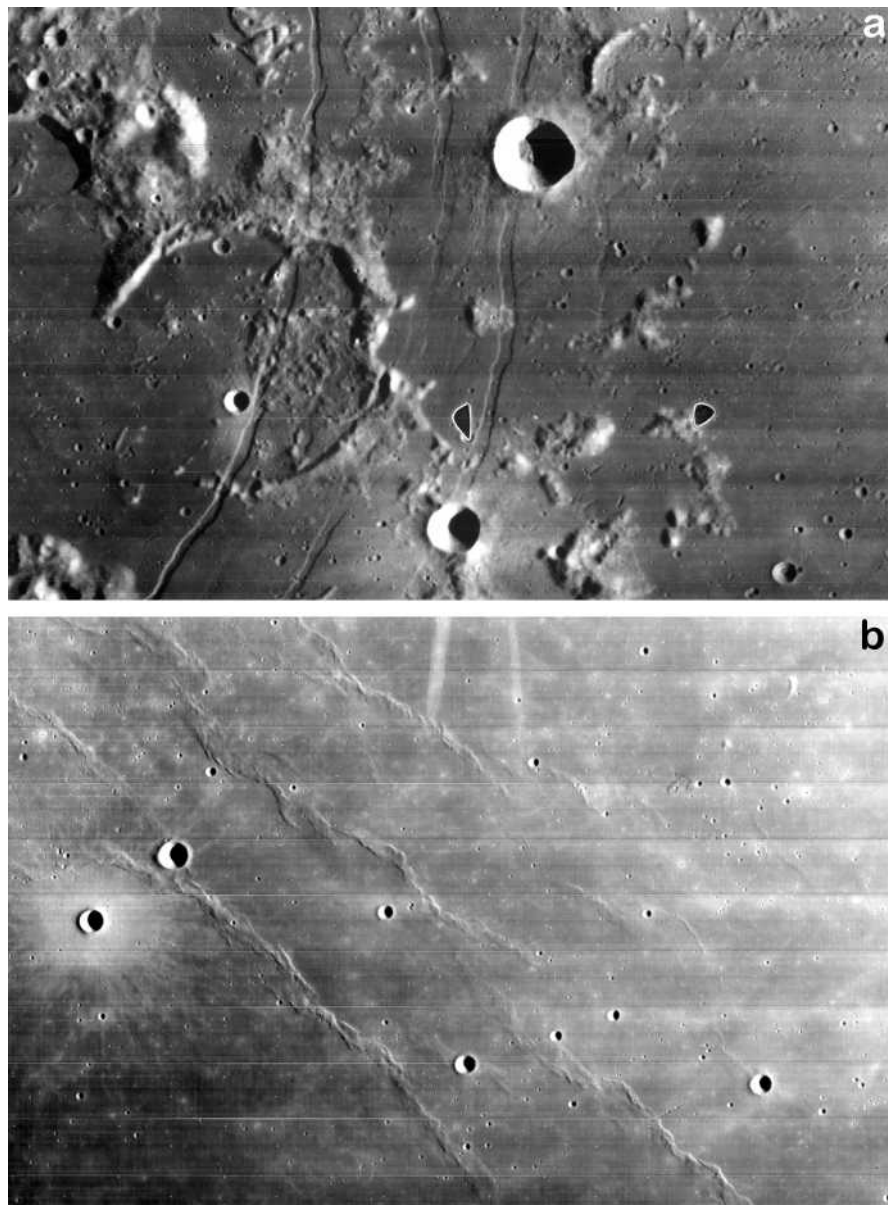


Figure 1.29. Examples of tectonic landforms; (a) linear rilles (LO IV 123H1) and (b) wrinkle ridges (LO IV 163H1).

other areas, they concluded that the lunar lineament patterns do not support the predictions of a global tectonic pattern due to the collapse of a once larger tidal bulge on the Moon.

2.3.6. Thermal effects. Models of the thermal evolution of the Moon indicate that during the first billion years, thermal expansion produced extensional stresses in the lunar crust and that during the next 3.5 b.y. until the present, cooling and contraction have caused compressional

stresses (e.g., Solomon and Chaiken 1976). Pritchard and Stevenson (2000) point out that the thermal models have many adjustable and unconstrained parameters that influence the evolution of the planetary radius and the resulting stress field. The amount of these stresses are still not well understood, but early lunar tectonic activity may have been dominated by tidal stresses and internally generated stresses may have been insignificant. However, graben that are most likely related to loading of basin centers with basalts could not have formed without the presence of global, mildly tensile stresses (e.g., Solomon and Head 1979). After about 3.6 b.y., the lunar stress field became compressional and internally driven tectonic activity may have ceased for 2.5–3 b.y. until sufficient stress (>1 kbar) had accumulated to produce small-scale thrust faults. Pritchard and Stevenson (2000) argued that a cessation of graben formation at 3.6 b.y. is a nonunique constraint because local effects including flexure and magmatic pressures could mask the signal from global stress.

2.3.7. Formation of ridges. The en-echelon offsets of wrinkle ridges in Mare Serenitatis indicate a formation due to compressional stresses. The ridges in Mare Serenitatis are concentric to the basin, and Muehlberger (1974) and Maxwell (1978) estimated a centrosymmetric foreshortening of ~0.5–0.8% in order to produce the ridges. Ground-penetrating radar data from the Apollo Lunar Sounding Experiment (ALSE) revealed significant upwarping and possibly folding and faulting of the basaltic surface down to ~2 km below the wrinkle ridges. Lucchitta (1976) suggested that wrinkle ridges are associated with thrust faulting and folding, a concept recently supported by Golombek et al. (1999, 2000) on the basis of new MOLA topographic data of martian wrinkle ridges.

Although most ridges on the Moon are interpreted to have formed by compressive stresses, some may result from subsurface magma emplacement (Strom 1964). Similarly, Schultz (1976) suggested that some floor-fractured craters formed by uplift and expansion due to the emplacement of sills below the crater floor.

3. GEOLOGIC SETTING AND SIGNIFICANCE OF THE APOLLO AND LUNA LANDING SITES

3.1. Overview

Six manned American Apollo missions (1969–1972) and three automated soviet Luna missions (1970–1976) returned samples from the nearside lunar surface. Each of these landing sites is, in its unique way, useful for understanding and interpreting the new global data sets from Clementine and Lunar Prospector because each provides ground truth for numerous geologic investigations and experiments, the calibration of data, and the development of new techniques of data reduction. Here we briefly review the geologic setting of each landing site in order to provide a framework for the following chapters. In addition, geologic cross-sections and the traverses of extravehicular activities (EVA) are intended to put the returned samples into geologic context and to familiarize the reader with the local topography, morphology, geology, and the sites where scientific experiments were carried out.

3.2. Apollo 11 (July 1969)

The Apollo 11 mission returned samples of basalt from Mare Tranquillitatis, confirming the hypothesis that the dark, circular basins contained extruded lavas formed by partial melting of the lunar mantle (e.g., Smith et al. 1970). Unlike terrestrial basalt, however, these were marked by extraordinarily high TiO_2 concentrations, and the high proportions of ilmenite were found to be consistent with their spectrally “blue” character. Their ages were determined to be 3.57–3.88 b.y. old (BVSP 1981 and references therein), which, coupled with crater densities, provided an early calibration point in the lunar chronology and showed that volcanism on the Moon was indeed ancient by terrestrial standards. Also found among

the samples were pieces of non-volcanic material, including fragments of plagioclase-rich anorthosites, which were interpreted to be from the adjacent light-colored highlands. From these pieces of rock, the general feldspathic character of the lunar crust and the first concepts of lunar differentiation were correctly inferred (e.g., Wood et al. 1970; Smith et al. 1970). The Apollo 11 landing site, which is about 40–50 km from the nearest mare/highland boundary within Mare Tranquillitatis (0.7°N , 24.3°E), was chosen primarily for safety reasons (Fig. 1.30a,b). During their 2.5 hours EVA, the astronauts collected 21.6 kg of lunar samples. Samples were collected about 400 m west of West crater, a sharp-rimmed, rayed crater \sim 180 m in diameter and \sim 30 m deep. The regolith there is about 3–6 m thick, and Beaty and Albee (1978) suggested that most of the collected samples were ejected from West crater. Among

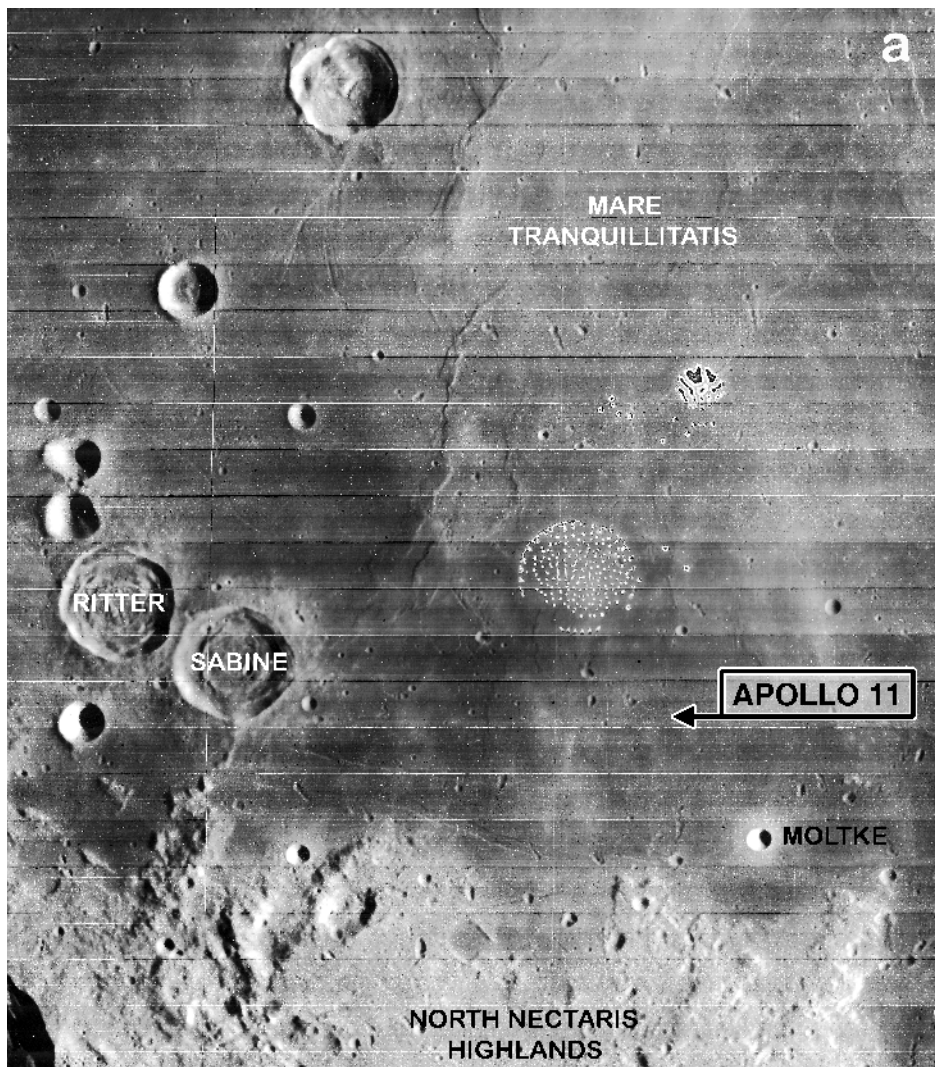


Figure 1.30. The geologic setting of the Apollo 11 landing site;
(a) LO IV 85H1 context image. (b) is on facing page.

these samples, five geochemically distinctive groups of mare basalts have been identified (see Neal and Taylor 1992, for a summary). In addition, some of the returned regolith samples consist of feldspathic lithic and mineral fragments that were derived from highland regions (Wood et al. 1970; Smith et al. 1970). Despite its location in a mare region, Apollo 11 regolith contains up to ~28% of nonmare material, which is similar in composition to the regolith of the Cayley Plains at the Apollo 16 landing site (Korotev and Gillis 2001). Korotev and Gillis (2001) suggested that the nonmare material is most likely Imbrium ejecta deposits excavated from beneath the basalt flows by impact craters. For further information about the geology of the Apollo 11 landing site see Chapter 2 and, for example, Shoemaker et al. (1970a) and Beatty and Albee (1978, 1980).

3.3. Apollo 12 (November, 1969)

In order to demonstrate the capability of pinpoint landings, Apollo 12 was sent to the Surveyor 3 site, a flat mare site with only a few large boulders. Apollo 12 touched down within 200 m of the Surveyor 3 landing site in southeastern Oceanus Procellarum (3.2°N , 23.4°W), and was the first spacecraft to demonstrate the capability of pinpoint landings on another planetary body (Fig. 1.31a,b). Compared to the Apollo 11 site, this site is less cratered, hence younger, and sampled mare basalts differ in their spectral characteristics and composition from the Apollo 11 basalts. Differences in age and chemistry between basalts of the Apollo 11 and Apollo 12 landing sites demonstrated variability in mantle sources and basalt production processes on the Moon. Exposures of non-mare materials near the landing site, mostly part of the Fra Mauro Formation, indicate that the basalts are relatively thin (Head 1975b). Exposures of non-basaltic formations and mare basalts form a complex topography and crater counts and D_L values (defined as the diameter of craters with wall slopes of 1°) reveal that the landing site basalts are older than basalts 1 km away to the east and west (Wilhelms 1987). Despite the fact that the landing site is dominated by the ejecta of several craters larger than ~100 m, the regolith is only half the thickness of the Apollo 11 regolith and craters only 3 m deep penetrate into basaltic bedrock. Non-volcanic materials are abundant, as anticipated because of the crossing of the site by a prominent ray from crater Copernicus. Although there are probably multiple sources of

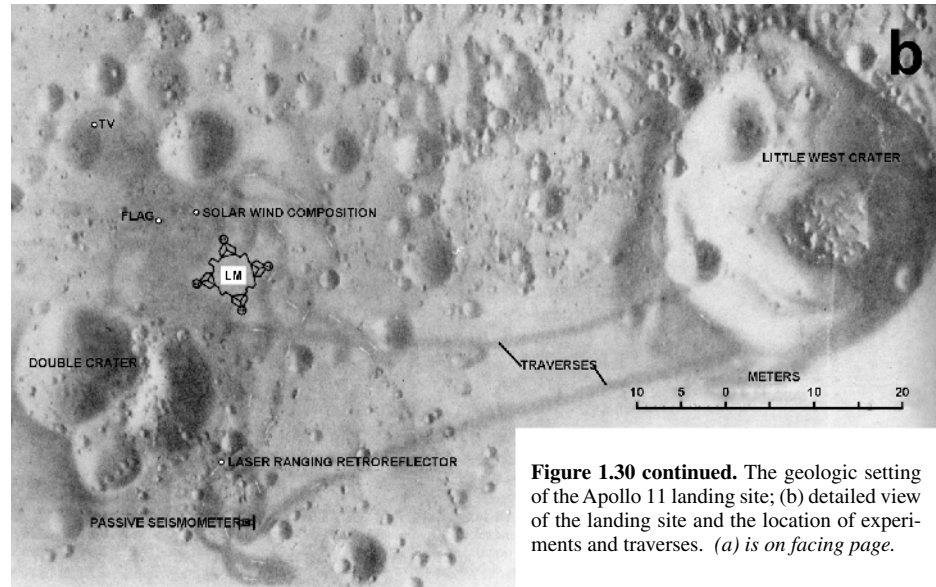


Figure 1.30 continued. The geologic setting of the Apollo 11 landing site; (b) detailed view of the landing site and the location of experiments and traverses. (a) is on facing page.

the non-volcanic materials at the Apollo 12 site, including material mixed into the surface from impact-melt formations that underlie the basalts, analyses of non-volcanic materials record a major disturbance at about 800–900 m.y. ago, and this has been inferred to be the age of crater Copernicus, although no sample has been unambiguously related to this crater.

The astronauts performed two EVAs and collected 34.3 kg of samples, mostly basalts. Radiometric dating showed the basalts to range in age between 3.29 and 3.08 b.y. Based on the large rock samples, at least three chemically distinctive groups of mare basalts were identified (e.g., James and Wright 1972; Neal et al. 1994 a,b). The mare basalt flows (20–21% FeO) cover the older Fra Mauro Formation, which contains about 10% FeO (Wilhelms 1987; Jolliff et al. 1991, 2000). Apollo 12 was the first mission to bring back KREEP material with a very specific and unique geochemical signature (enriched in potassium, rare-earth elements, phosphorus, and other incompatible elements) that requires substantial magmatic differentiation, consistent with

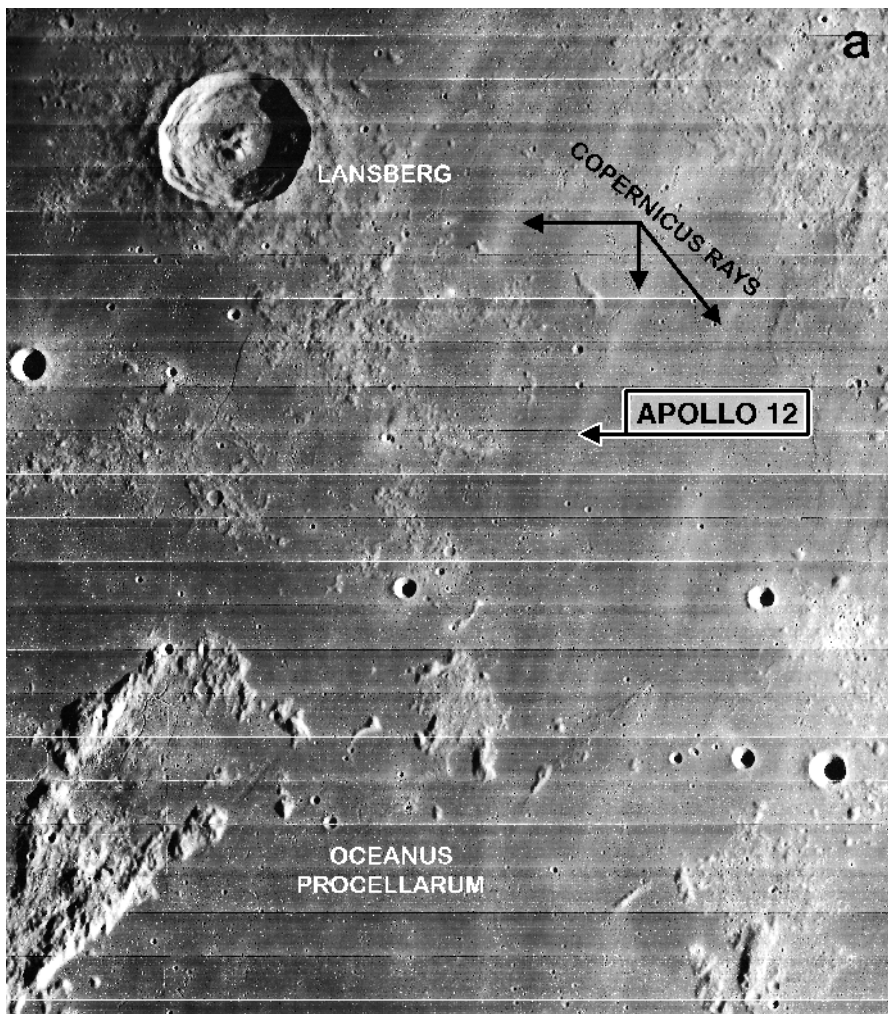


Figure 1.31. The geologic setting of the Apollo 12 landing site;
(a) LO IV 125H3 context image, (b) is on facing page.

a strongly differentiated Moon that differs significantly from all known classes of meteorites. This KREEP material occurs in form of dark, ropy glasses similar in composition to Apollo 14 soils and a subset of Apollo 14 impact glasses (Wentworth et al. 1994). Because these glasses contain lithic fragments including anorthosite, KREEP basalt and felsite (Wentworth et al. 1994), they appear to represent impacted surface material similar to that exposed in the Fra Mauro Formation (Jolliff et al. 2000). The KREEP material is derived mostly from the Procellarum KREEP Terrane and was probably incorporated into the regolith of the landing site by a combination of lateral transport and vertical mixing (Jolliff et al. 2000). For additional discussions of the Apollo 12 landing site, the reader is referred to Shoemaker et al. (1970b), Warner (1970), Rhodes et al. (1977), and Wilhelms (1984).

3.4. Apollo 14 (January–February, 1971)

Apollo 14 landed on a hilly terrain north of Fra Mauro crater (3.7° S, 17.5° W) and became the first mission to sample the lunar “highlands” (Fig. 1.32a,b). The landing site is ~550 km south of the Imbrium basin and was chosen primarily to collect samples from this basin in order to characterize its ejecta, which was thought to be derived from deep crustal levels, and to date the Imbrium event, which serves as a major stratigraphic division of the lunar history. During two EVAs 42.3 kg of samples were collected, including complex fragmental breccias, impact-melt breccias, and clast-poor impact melts with generally basaltic and KREEP-rich compositions. These breccias were formed about 3.9–3.8 b.y ago but whether they formed in the Imbrium event itself, or through later, smaller impacts into Imbrium ejecta is still contended,

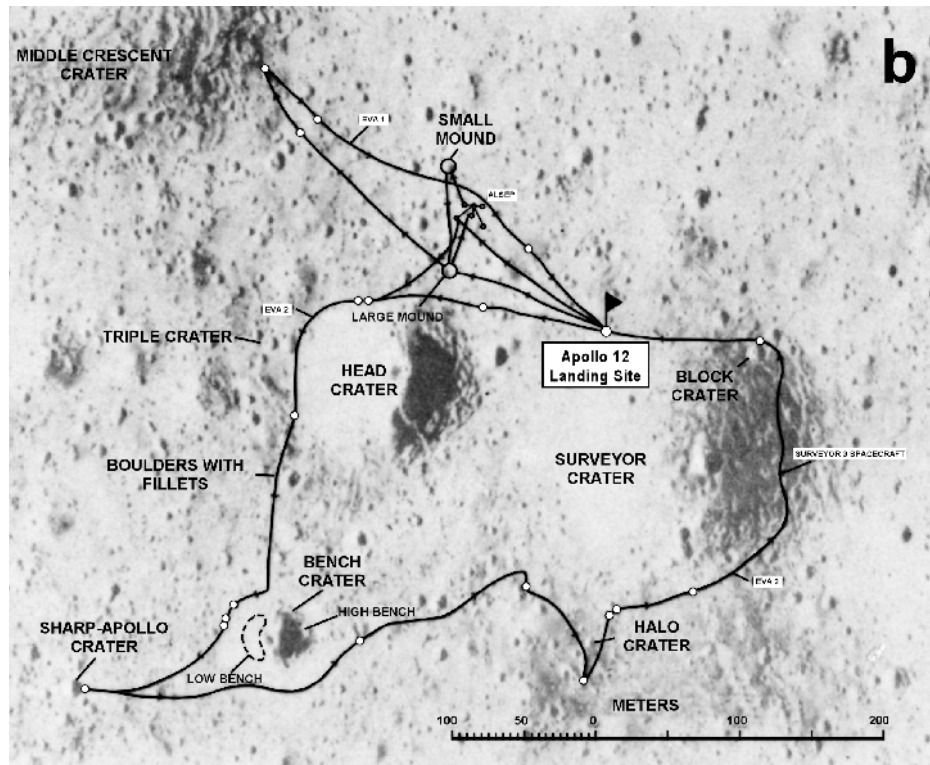


Figure 1.31 continued. The geologic setting of the Apollo 12 landing site; (b) detailed view of the landing site and the location of experiments and traverses. (a) is on facing page.

and it is still unclear which Apollo 14 samples represent true Imbrium ejecta or locally derived materials. The Fra Mauro Formation has been interpreted as primary Imbrium ejecta (Wilhelms 1987). Haskin et al. (2002) argued that it consists of about 58% Imbrium ejecta and Morrison and Oberbeck (1975) proposed that the Fra Mauro Formation is mostly dominated by local material with intermixed 15–20% Imbrium ejecta.

The Apollo 14 landing site is usually considered as a “highland” landing site, but from a geochemical point of view it is neither mare nor feldspathic highlands. Rather, the Apollo 14 site is located within the Procellarum KREEP terrane, which recent Lunar Prospector gamma-ray data indicated it contained exceptionally high thorium concentrations. However, this anomaly was not known at the time of the site selection. The Apollo 14 landing site is also characterized by relatively aluminous basalts, a subset of which are also enriched in K. These

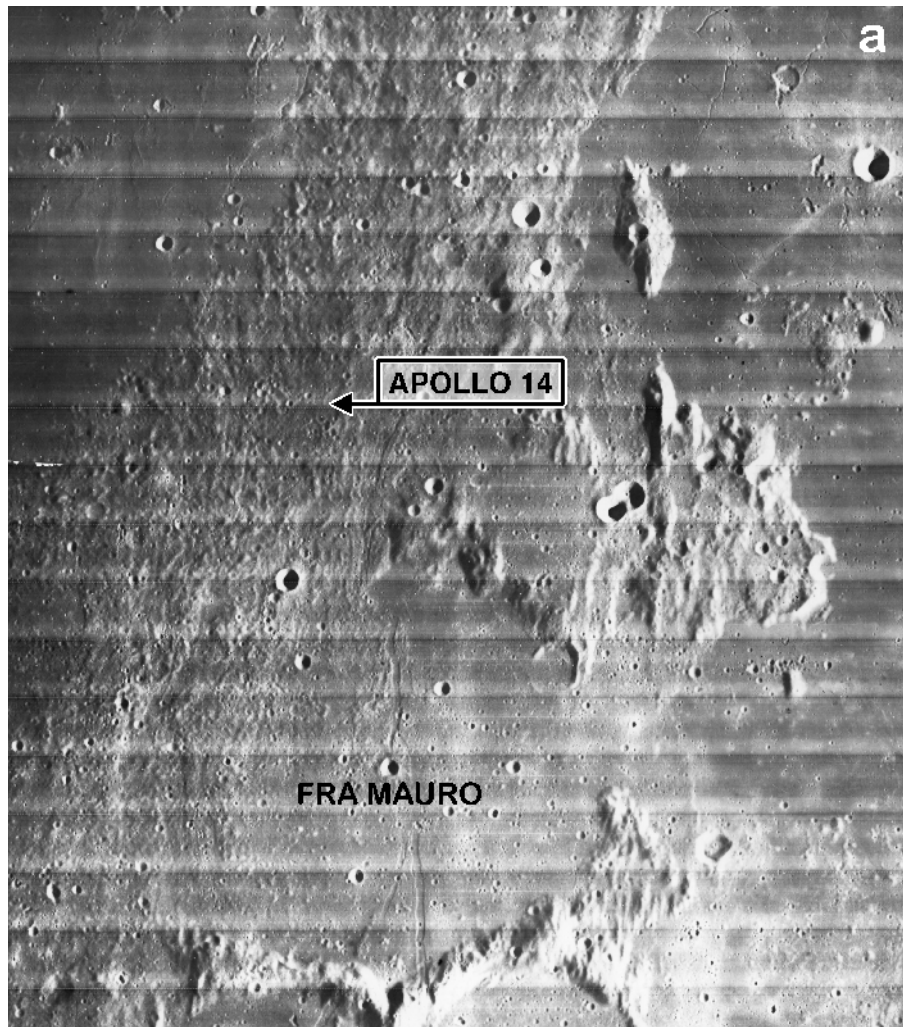
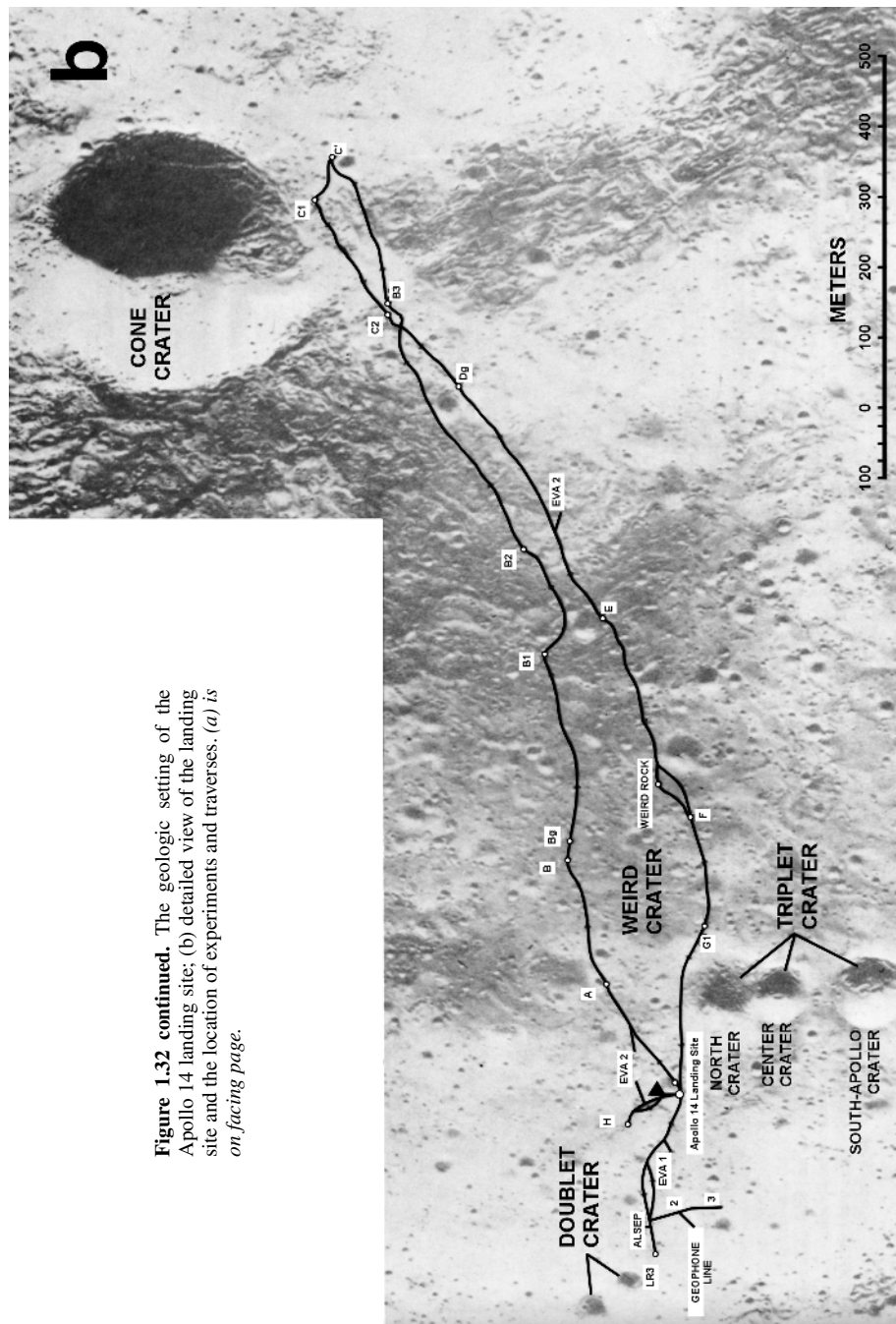


Figure 1.32. The geologic setting of the Apollo 14 landing site;
(a) LO IV 120H3 context image, (b) is on facing page.



aluminous and high-K basalts are unknown from other Apollo mare landing sites (e.g., Shervais et al. 1985a,b), although aluminous basalts were returned by the Soviet Luna missions (see below). A “model” mixture of the regolith at the Apollo 14 site consists of ~60% impact-melt breccias, ~20–30% noritic lithologies, ~5–10% each mare basalts and troctolitic anorthosites, and minor amounts of meteoritic components (Jolliff et al. 1991). Compared to the regolith of the Apollo 11 landing site, the Apollo 14 regolith shows little variation in composition, both vertically (tens of centimeters) and laterally (kilometers around the landing site). The landing site is located ~1100 m west of Cone crater, a crater ~340 m in diameter and 75 m deep that ejected blocks of up to ~15 m across. The landing site shows numerous subdued craters up to several hundreds of meters across and the regolith was estimated to be 10–20 m thick (Swann et al. 1971). The geology of the Fra Mauro area is discussed in detail in Chapter 2 and by Chao (1973), Swann et al. (1977), Hawke and Head (1977), and Simonds et al. (1977).

3.5. Apollo 15 (July-August, 1971)

The Apollo 15 mission was the first advanced (“J”) mission that carried the Lunar Roving Vehicle (LRV) and was sent to a complex multi-objective landing site in the Hadley-Apeninne

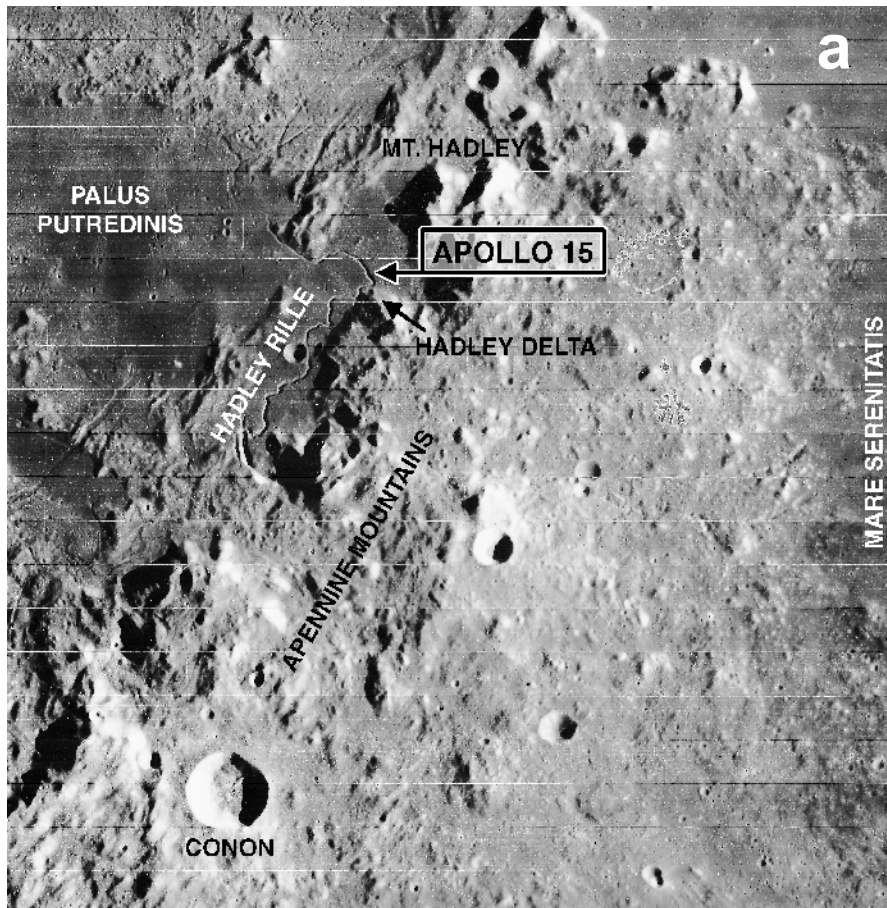


Figure 1.33. The geologic setting of the Apollo 15 landing site;
(a) LO IV 102H3 context image, (b) is on facing page.

region (26.1°N , 3.7°E) (Fig. 1.33a,b). The purpose of this mission was to sample and study the massifs and highlands of the Imbrium rim, and the mare lavas and landforms of Palus Putredinis (e.g., Hadley Rille). Extensive lava plains are exposed west of the landing site and the main Imbrium ring rises ~ 3.5 km above the plains at Hadley Delta, only 4 km south of the Apollo 15 landing site. Exposed inside the Imbrium ring and within a few kilometers from the landing site is the Apennine Bench Formation, a light plains unit that probably underlies the Upper Imbrian basalts at the Apollo 15 landing site. Rays from crater Autolycus and Aristillus cross the landing site and the regolith thickness varies widely depending on the local terrain. The regolith, which is only ~ 5 m thick at the landing site, is absent at the Hadley Rille. Photographs show the wall of Hadley Rille to be a layered basalt-flow sequence. In total, the astronauts performed three

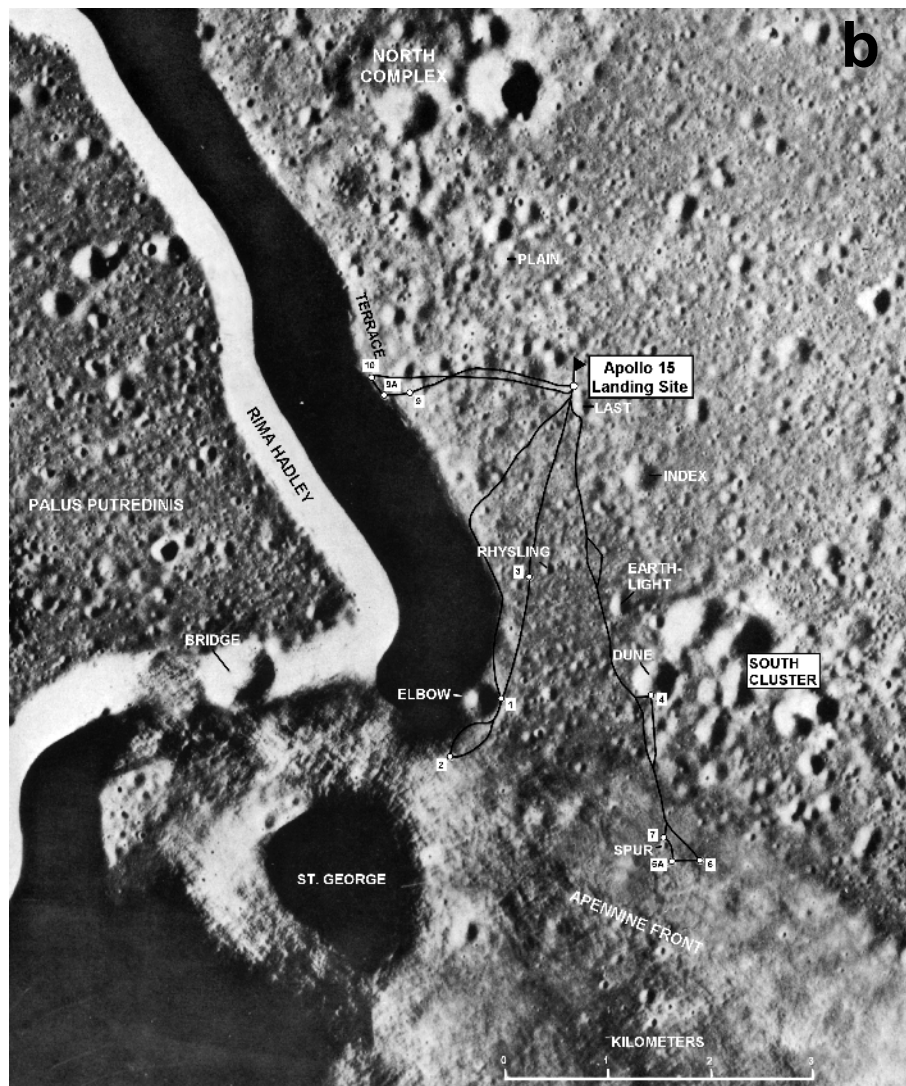


Figure 1.33 continued. The geologic setting of the Apollo 15 landing site; (b) detailed view of the landing site and the location of experiments and traverses. (a) is on facing page.

EVAs with the LRV collecting 77.3 kg of samples, both mare and nonmare rocks. Two types of lavas were collected at this landing site (quartz normative and olivine normative; e.g., Rhodes and Hubbard 1973; Chappell and Green 1973; Dowty et al. 1973), both basically identical in age (3.3 b.y.). Non-volcanic samples consist of anorthosites, magnesian-suite plutonic rocks, impact melts, and granulites, many of which occur as individual clasts in regolith breccias. In addition, KREEP-rich non-mare basalts and green ultramafic volcanic glasses were collected at this site. Based on evidence from the Apollo 14 and Apollo 15 sites, the Imbrium basin is interpreted to be 3.85 b.y. old. Swann et al. (1972), Spudis and Ryder (1985, 1986), Spudis et al. (1988), and Spudis and Pieters (1991) provide a further discussion of the geology of the Apollo 15 landing site.

3.6. Apollo 16 (May, 1972)

This mission was to explore the lunar highlands, especially the smooth Cayley Formation and the hilly and furrowed Descartes Formation, both of which were thought to be volcanic in origin (e.g., Hiners 1972) (Fig. 1.34a,b). Other goals were to sample highland material far from any mare region and to investigate two nearby, fresh 1–2 km craters. Apollo 16 landed at 9°S latitude and 15.5°E longitude near Descartes crater. Three long EVAs were performed with the

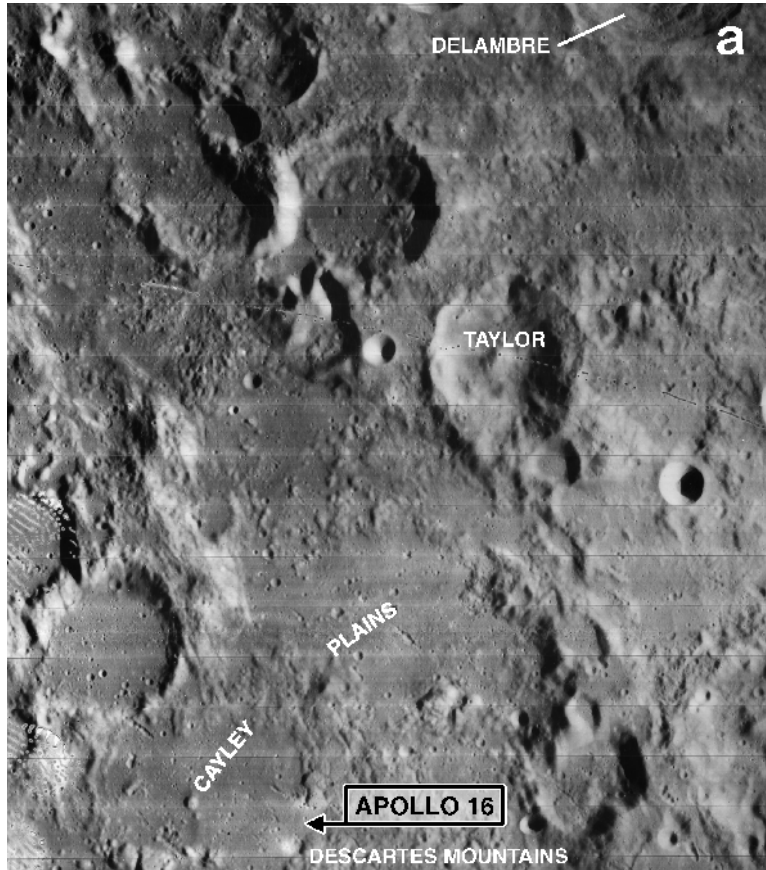


Figure 1.34. The geologic setting of the Apollo 16 landing site;
(a) LO IV 89H3 context image, (b) is on facing page.

LRV, and 95.7 kg of samples were returned. The Apollo 16 landing site is considered the only true highland landing site of the Apollo program and is sometimes taken to be representative of typical lunar highlands. However, surface morphology, vicinity to the Imbrium basin distributing material of the Procellarum KREEP terrane across the site, composition of the regolith, and lithologic components of the regolith argue against Apollo 16 having landed on “typical” highlands. The landing site is characterized by numerous overlapping subdued craters of ~500 m size, two young fresh craters, North Ray (1 km wide, 230 m deep) and South Ray (680 m wide, 135 m deep), as well as Stone Mountain (Fig. 1.34b). Freeman (1981) reported that the regolith thickness on both the Cayley and the Descartes Formations ranges from 3–15 m and averages about 6–10 m. Contrary to pre-mission expectations, the returned samples are

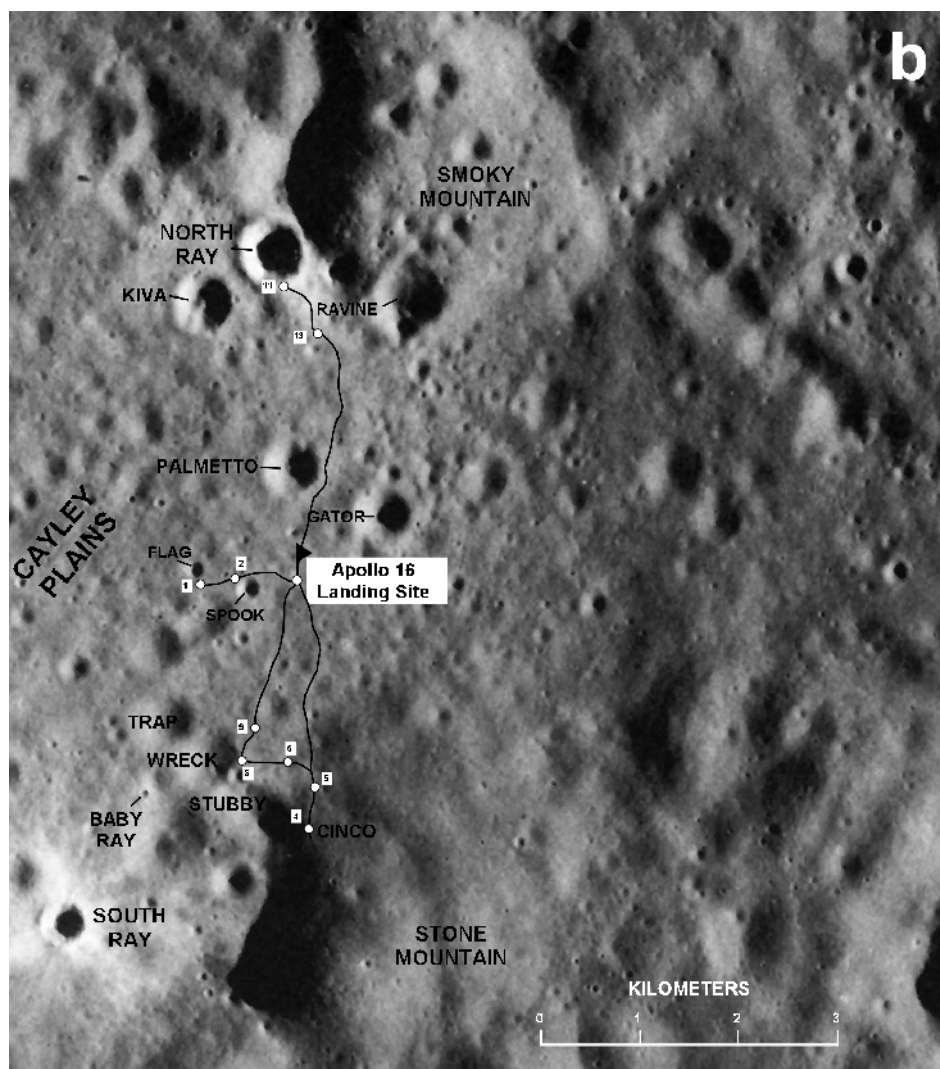


Figure 1.34 continued. The geologic setting of the Apollo 16 landing site; ((b) detailed view of the landing site and the location of experiments and traverses. (a) is on facing page.

all impact products, most of them impact melt or fragmental breccias, and some anorthositic rocks. On the basis of the returned samples, neither the Cayley Formation nor the Descartes Formation are volcanic in origin but instead are related to ejecta deposition of the Imbrium, Serenitatis, and Nectaris basins, and the relative amounts of ejecta contributed to the landing site by each are still open questions (e.g., Head 1974; Muehlberger et al. 1980; Spudis 1984; Haskin et al. 2002). Some impact melts of the Apollo 16 site have been interpreted as products of the Nectaris event, indicating a formation of the Nectaris basin 3.92 b.y. ago (e.g., Wilhelms 1987; Stöffler and Ryder 2001). For more information about the geology of the Apollo 16 landing site see Muehlberger et al. (1980), Ulrich et al. (1981), James and Hötz (1981), James (1981), Spudis (1984), Stöffler et al. (1985), and Spudis et al. (1989).

3.7. Apollo 17 (December, 1972)

Apollo 17 marked the end of the Apollo program and was sent to the highland/mare boundary near the southeastern rim of the Serenitatis basin, the Taurus-Littrow Valley (20.2°N , 30.8°E) (Fig. 1.35a,b). This site was selected in order to examine two highland massifs where rocks from deep crustal levels could be collected, to investigate the presumably basaltic valley floor, and to study the low-albedo deposit that mantles both highlands and mare at the site. Thus, the Apollo 17 and 15 sites are the most geologically complex of the landing sites. Using the

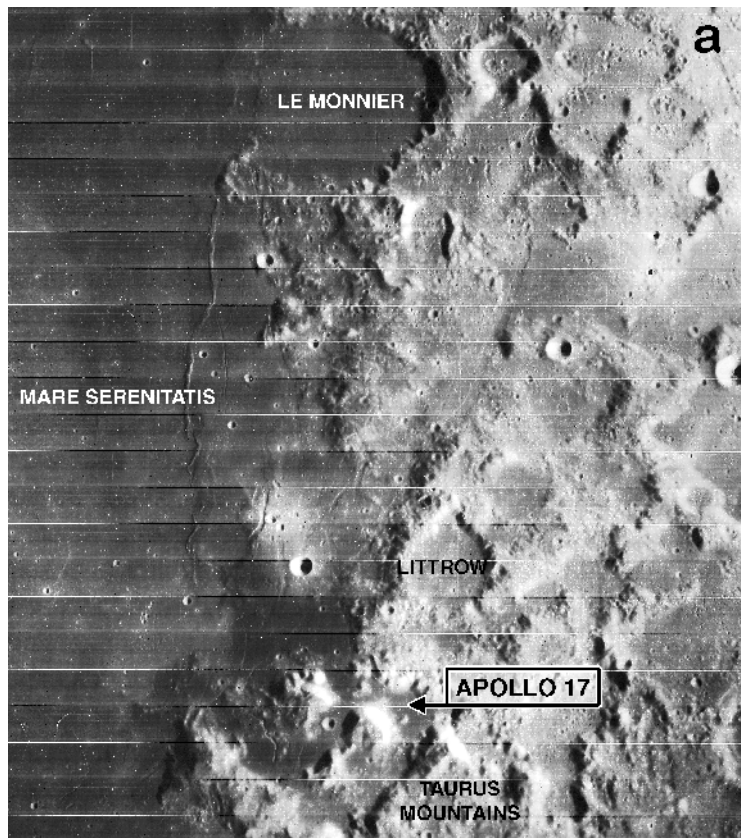


Figure 1.35. The geologic setting of the Apollo 17 landing site;
(a) LO IV 78H3 context image, (b) is on facing page.

LRV the astronauts performed three EVAs and collected 110.5 kg of samples, bringing the total amount of returned samples to 381.7 kg. Samples from this site confirmed a Ti-rich basaltic composition of the valley floor and several chemical subgroups of basalts were identified, ranging in age from 3.8 to 3.7 b.y.

The Apollo 17 impact melts were collected from thick impact ejecta deposits on the rim of the Serenitatis basin and are likely of Serenitatis origin. A small subset of the impact-melt breccias have trace element signatures similar to some groups from Apollo 15 and Apollo 14, suggesting a minor component from the later Imbrium basin. Deep-seated magnesian-suite rocks and granulitic breccias are also found in the highland massif regolith (e.g., Warner et al. 1977; Warner et al. 1978; Lindstrom and Lindstrom 1986).

The regolith at the Apollo 17 landing site was found to be on the order of 15 m thick. The highland regions along this part of the Serenitatis rim are relatively FeO-rich because of

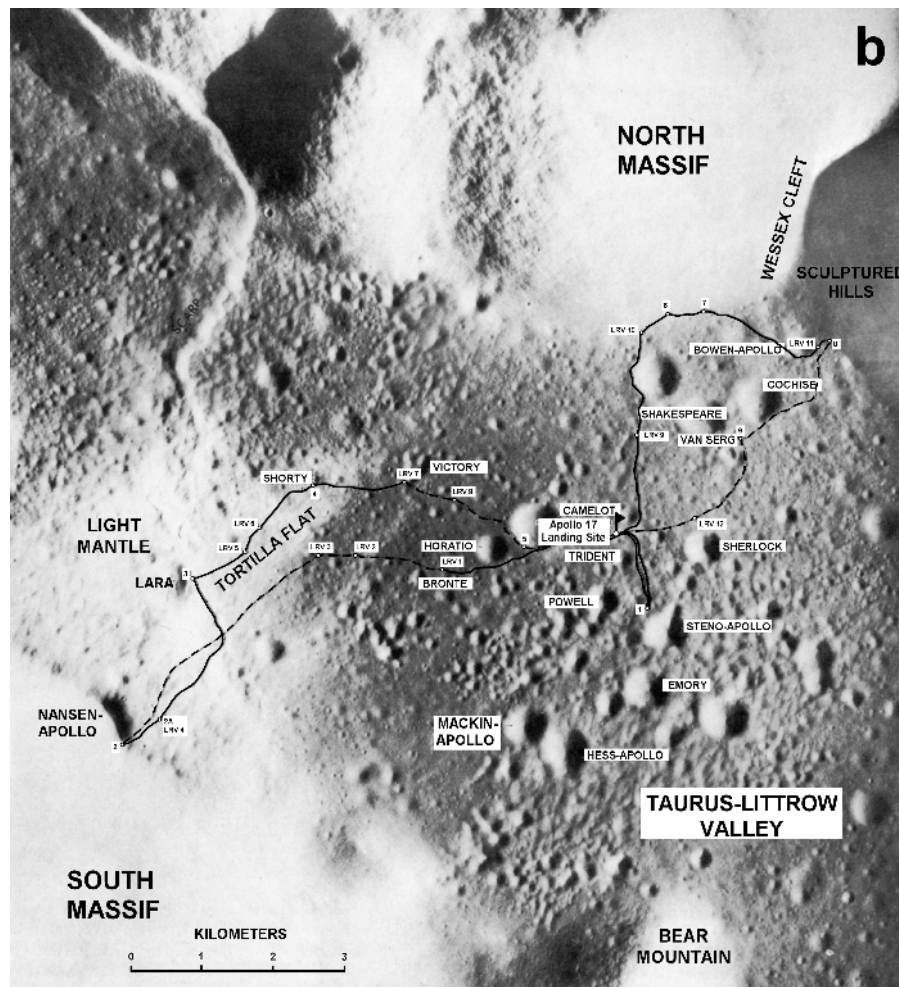


Figure 1.35 continued. The geologic setting of the Apollo 17 landing site; (b) detailed view of the landing site and the location of experiments and traverses. (a) is on facing page.

abundant mafic impact melt breccias and additions of basaltic material as impact debris and pyroclastic deposits. Recent work coupling Clementine data to landing site and sample data include Weitz et al. (1998) and Jolliff (1999). On the basis of topographic-photometrically corrected Clementine data, massif compositions are consistent with mixtures of noritic impact melt and feldspathic granulitic material, plus variable amounts of high-Ti basalts on the flanks at low elevations and pyroclastic deposits at high elevations (Robinson and Jolliff 2002). Hence, the highlands at this site consist of complex impact-melt breccias and plutonic rocks of the Mg-suite. Impact-melt breccias have been dated to be 3.87 b.y. old and have been interpreted to reflect the formation of the Serenitatis basin. The dark mantling deposits consist of orange and black volcanic glass beads of high-Ti basaltic composition, approximately 3.64 b.y. old. Photogeology suggests that a light colored mantle unit results from an avalanche triggered by secondary impacts from Tycho crater (e.g., Lucchitta 1977). Cosmic-ray exposure ages were used to derive an age of ~100 m.y. for the avalanche materials, and it has been argued that this age represents the age of the Tycho event. A detailed discussion of the geology of the Taurus-Littrow Valley and the Apollo 17 landing site may be found in Schmitt (1973), Wolfe et al. (1981), Spudis and Ryder (1981), Spudis and Pieters (1991), and Ryder et al. (1992).

3.8. Luna 16 (September, 1970)

Luna 16 was the first successful automated Soviet sample return mission and landed in northern Mare Fecunditatis at 0.7°S and 56.3°E (Fig. 1.36). Work by DeHon and Waskom (1976) indicated that Luna 16 landed on a sequence of relatively thin basalt flows ~300 m in thickness. The landing site is influenced by ejecta and ray material from Eratosthenian crater Langrenus (132 km), Copernican crater Tauruntius (56 km), as well as the more distant craters Theophilus and Tycho (McCauley and Scott 1972). Like all Luna samples, the Luna 16 samples are derived from shallow regolith drill cores. The drill core reached a depth of 35 cm and provided 101 g of dark gray regolith with preserved stratigraphy (Vinogradov 1971). No visible layering was observed within the core but 5 zones of increasing grain sizes with depth were recognized. Luna 16 samples are from a mare basalt regolith, which consists of moderately-high-Ti, high-Al basalt fragments, approximately 3.41 b.y. old. Mare basalts from this landing site are among the most Fe- and Mg-poor basalt samples returned from the Moon and, with ~13.5% Al_2O_3 , are the most Al-rich basalts yet sampled (e.g., Ma et al. 1979). More information about the Luna 16 site can be found in McCauley and Scott (1972).

3.9. Luna 20 (February, 1972)

This mission landed in the highlands south of Mare Crisium (3.5°N, 56.5°E) and returned samples from an anorthositic highland regolith that contains lithic fragments of granulites, anorthosites, impact melts, and polymict breccias (Fig. 1.36). The Luna 20 landing site sampled the rim of the Nectarian Crisium basin and the landing site is characterized by smooth rounded hills and shallow linear valleys that give the region a hummocky appearance. The landing site is topographically ~1 km above the basaltic surface of Mare Fecunditatis and is influenced by Apollonius C, a 10 k.y. fresh Copernican crater located only a few kilometers to the east. Luna 20 returned a drill core that contained ~50 g of fine-grained light-gray regolith. No stratification has been observed within the core but mixing during transport might have occurred. The majority of lithic regolith fragments are breccias of anorthositic-noritic-troctolitic composition and impact-melt rocks of noritic-basaltic composition. Compared to the regolith of the Apollo 16 landing site, the Luna 20 regolith contains less K and P, fragments of anorthosites are rare, and MgO-rich spinel troctolites are common (e.g., Brett et al. 1973; Taylor et al. 1973; Papike et al. 1998). The higher concentrations of MgO in the Luna 20 samples are important to note because they may reflect the addition of an unknown mafic highland rock material, that is present at the Luna 20 site itself but is absent at the Apollo 16 landing site (Papike et al. 1998). Because K and P concentrations are low it has been argued that the samples of the Luna 20 landing site have not been contaminated with KREEP-rich Imbrium ejecta but instead represent

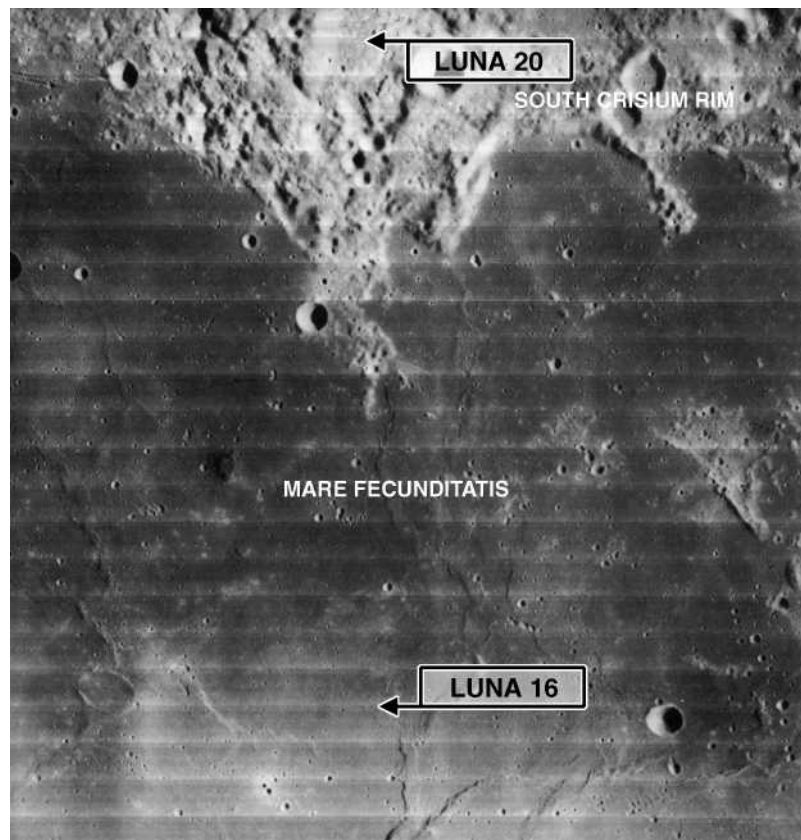


Figure 1.36. The geologic settings of the Luna 16 and Luna 20 landing sites (LO I M-33).

middle to lower crustal material ejected by the Crisium impact. Heiken and McEwen (1972) and Vinogradov (1973) discuss the Luna 20 landing site in more detail.

3.10. Luna 24 (August, 1976)

The last and most successful Luna mission was Luna 24, which landed in southern Mare Crisium (12.7°N , 62.2°E) (Fig. 1.37). The landing site is located within the inner ring of Crisium, which is marked by wrinkle ridges, and about 40 km north of the main basin ring, which is $\sim 3.5\text{--}4.0$ km higher than the landing site (Florenskiy et al. 1977; Butler and Morrison 1977). Head et al. (1978a,b), using remote-sensing techniques, identified several distinctive basalt types in Mare Crisium, the thickness of which was estimated to be $\sim 1\text{--}2$ km. Several bright patches and rays indicate that nonmare material has been dispersed across the basin by impacts such as Giordano Bruno and Proclus (e.g., Maxwell and El-Baz 1978; Florenskiy et al. 1977). Luna 24 returned 170 g of mostly fine-grained mare regolith in a 1.6 m long drill core. Stratification was well preserved in the core sample and, on the basis of color and grain size differences, four layers were identified (Florenskiy et al. 1977; Barsukov 1977). Basaltic fragments from this core are very low in TiO_2 , low in MgO , high in Al_2O_3 and FeO , and are 3.6–3.4 b.y. old. Concentrations of FeO in the mare basalts and soils of Luna 24 are very similar, suggesting that only minor amounts of nonmare material are present at the landing site. The local and regional geology of the Luna 24 landing site is further discussed by Head et al.

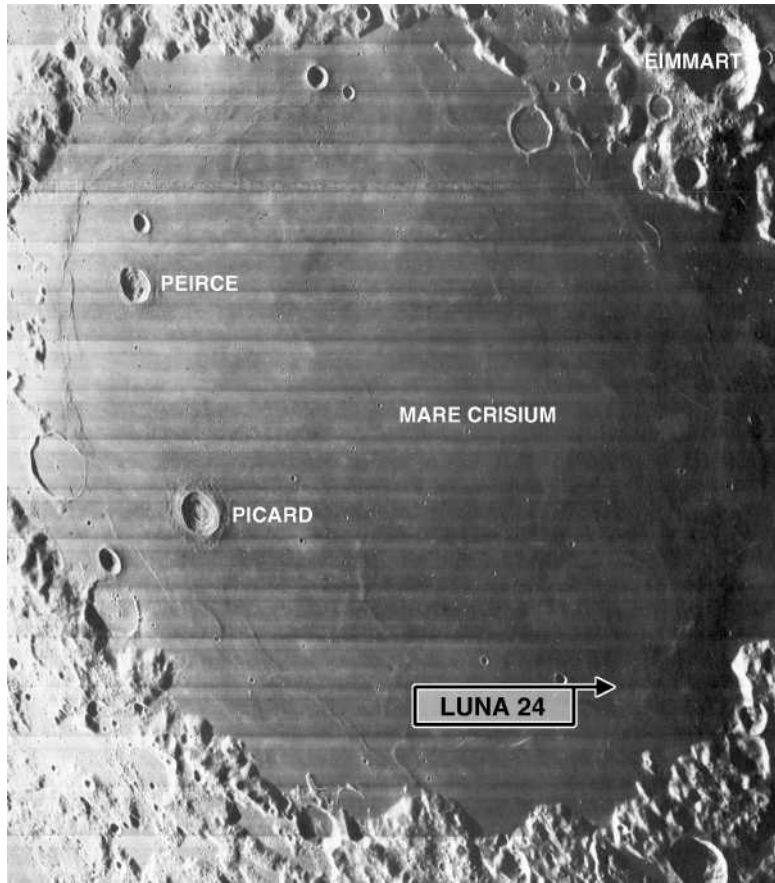


Figure 1.37. The geologic setting of the Luna 24 landing site (LO IV 191H3).

(1978a,b). A comprehensive summary of numerous contributions about the Luna 24 landing site and Mare Crisium can be found in Merrill and Papike (1978).

3.11. Significance of landing sites for the interpretation of global data sets

Our geologic understanding of the Moon relies heavily on the information derived from the lunar landing sites. A key advantage of landing-site exploration and sample return is the strength and synergy of having samples with known geologic context. Samples returned from these sites can be analyzed in great detail in laboratories with sophisticated, state-of-the-art techniques. Portions of samples set aside for future analysis with new methods offer many advantages over *in-situ* robotic measurements, which are restricted to techniques available at the time of the mission. Equally important, numerous geophysical experiments done by astronauts while on the surface improved our knowledge of the physical properties and the internal structure of the Moon. Again, these data can be used in new investigations, and on the basis of these data, new models have been and will be developed and tested long after the end of the Apollo missions. The landing sites also provide important ground-truth for all remote-sensing experiments. Calibration of remotely-sensed data to the landing sites and the lunar samples allows derivation of information about areas not yet sampled.

We consider briefly examples of how each individual landing site contributes to a comprehensive understanding of impact-basin structures and materials, because the impact-basin process is largely responsible for shaping the first-order features of the lunar surface. Figure 1.38a provides a schematic cross-section that illustrates the geologic setting of the Apollo landing sites relative to a multi-ringed impact structure. Figure 1.38b shows the Apollo landing sites in relation to morphologic features of the youngest lunar impact basin, Orientale. As shown in the figure, each landing site sampled very specific terrain types associated with large lunar impact basins. Apollo 16 sampled old pre-basin highland terrain, Apollo 14 landed on radially textured ejecta.

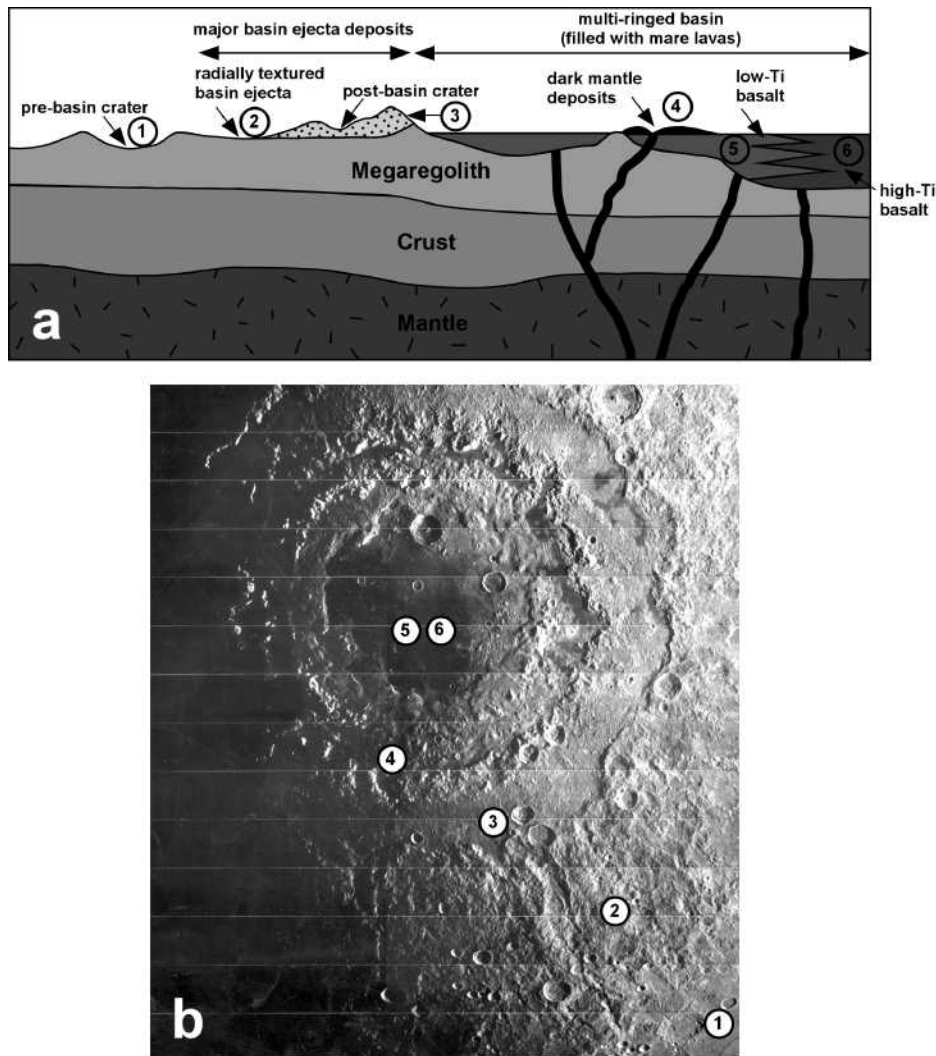


Figure 1.38. The Apollo and Luna landing sites; (a) schematic cross-section showing the Apollo and Luna landing sites in the context of a multi-ringed impact basin, (b) plan-view of the Orientale basin with superposed locations similar to the Apollo and Luna landing sites; (1) similar to Apollo 16 and Luna 20, (2) similar to Apollo 14, (3) similar to Apollo 15, (4) similar to Apollo 17, (5) similar to Apollo 12 and Luna 24, (6) similar to Apollo 11 and Luna 16.

basin-ejecta deposits, and Apollo 15 samples contain polymict breccias, which were formed by a post-basin crater. Besides other investigations, Apollo 17 examined dark mantle deposits in detail, and Apollo 11 and 12 investigated different types of basalts. All sample return sites, except Apollo 16 and Luna 20, returned basaltic samples that have provided our best window into the lunar mantle as no mantle xenoliths have been found in the returned basalt samples.

One of the major findings of Lunar Prospector was the identification of a large area with elevated thorium concentrations on the lunar nearside (e.g., Lawrence et al. 1998, 2000; Elphic et al. 2000). The origin of this anomaly is still debated and is discussed elsewhere in this volume. Several models have been put forward such as accumulation of KREEP-rich magma beneath a region of thinned crust presently corresponding to the region of Oceanus Procellarum or accumulation above a degree-1 downwelling of dense ilmenite cumulates (e.g., Warren 2001; Parmentier et al. 2000). The precise carrier of the Th-rich compositional signature in broad areas of the Procellarum region is not clearly known from remote sensing alone. Yet the question of what carries the Th enrichment is of great importance for the magmatic and thermal evolution of the Moon due to radiogenic heat production (e.g., Wieczorek and Phillips 2000). As it turned out, several Apollo landing sites, i.e., Apollo 12, Apollo 14, and Apollo 15, were located within the Procellarum KREEP terrane and thus allow study of the KREEP signature from returned samples. Investigation of samples from the Apollo 12 and 14 landing sites indicate that impact-melt breccias and derivative breccias, such as regolith breccias and agglutinates, are the main carriers of KREEP. However, at the Apollo 15 landing site, internally generated basalt is an important carrier of KREEP. Haskin (1998) and Haskin et al. (1998) proposed that the Imbrium basin impacted into the Procellarum KREEP terrane and distributed KREEP-rich material across the lunar surface globally. This proposition is consistent with the observation that abundant KREEP-rich material occurs in impact-melt breccias of landing sites located outside the Procellarum KREEP terrane, such as Apollo 11, 16, 17, but less KREEP-rich material in soils from the Luna 16, 20, and 24 landing sites, which are located at greater distances from the Procellarum KREEP terrane (see subsequent chapters).

Clementine was the first spacecraft in orbit around the Moon that provided high-resolution multispectral reflectance data. The Clementine mission permitted, for the first time, location of individual sampling stations at the Apollo 15, 16, and 17 landing sites (Blewett et al. 1997; Lucey et al. 1998) because these missions included rovers that allowed the astronauts to travel distances that can be resolved in the high-resolution Clementine data. Comparing spectra from 39 sampling stations with their average soil composition, Blewett et al. (1997) found a strong correlation between spectral variations and compositions. On the basis of this correlation, Lucey et al. (1998) developed an algorithm that estimates the FeO and TiO₂ concentrations on the lunar surface globally to about 1–2 wt% accuracy. Knowledge of the variability and spatial distribution of basalts relative to these two compositional parameters is important for understanding the petrogenesis of mare basalts and the history and evolution of magmatic processes on the Moon.

The lunar landing sites and their returned samples are extremely important for understanding the absolute chronology in order to anchor the Moon's geologic record. One of the major geologic goals of the Apollo and Luna missions was to return lunar samples. These returned samples could be dated radiometrically (e.g., U-Pb, Rb-Sr, Sm-Nd, and ⁴⁰Ar-³⁹Ar), but this provides highly accurate absolute ages for only a few small areas on the Moon (i.e., the landing sites). Obtaining ages for the vast unsampled regions relies on remote-sensing techniques such as crater counts. In order to derive absolute model ages from crater counts for any unsampled lunar region, we first have to correlate the radiometric ages from returned samples with the crater counts from the landing sites to establish the lunar cratering chronology. For this purpose, crater counts for the Apollo 11, 12, 14, 15, 16, and 17 and the Luna 16 and 24 landing sites were performed and correlated with the corresponding radiometric ages of these sites (e.g., BVSP 1981; Neukum 1983; Strom and Neukum 1988; Neukum and Ivanov

1994; Stöffler and Ryder 2001). A variety of interpretations as to which radiometric sample ages are most representative for a given landing site has resulted in several empirically derived lunar impact chronologies. These are discussed in Chapter 5 of this volume. We can use the lunar chronology to derive ages for any area for which crater counts have been conducted. It is important to note here that for the accurate derivation of the lunar chronology it is important to have data points over the entire period of time from lunar formation to present. Rocks from the sample collection yield ages from about 4.5 b.y. (ferroan anorthosite) to 2 m.y. (exposure age of Cone crater), allowing accurate modeling of the impact flux on the Moon.

Although this section highlights the importance of samples and surface exploration as ground-truth for remote sensing, information derived from orbital data feeds back into our understanding of the planet and as context for the landing sites. As an example, global compositional data, as recorded by both the Clementine and Lunar Prospector missions, show that a vast area of the Moon is not particularly well represented by the returned samples (Feldspathic Highlands terrane) or not at all (South Pole-Aitken region). This statement is supported by the lunar meteorites, which now include enough specimens to approach a statistically significant and more-or-less random sampling of the Moon. These rocks are dominated by feldspathic breccias and by low- to intermediate-Ti basalts. The feldspathic breccias appear to represent the Feldspathic Highlands terrane better than Apollo 16. The distribution of basalt compositions also appears to be more like what is anticipated from remote sensing, unlike the Apollo basalts, which disproportionately sampled high-Ti regions (e.g., Giguere et al. 2000). An optimal understanding of the planet, however, comes from integration of all of these datasets. This theme is elaborated in subsequent chapters of this volume.

4. SUMMARY AND OUTSTANDING QUESTIONS

The exploration of the Moon has revealed a geologically complex planetary body. Although at the beginning of modern lunar exploration most scientists would have agreed on the Moon being a rather simple object, exploration readily showed that the Moon is in fact more complicated than initially thought. Crew observations, lunar samples, geophysical measurements made on the lunar surface, the wealth of Galileo and Clementine multispectral reflectance data, and the Lunar Prospector gamma-ray and neutron spectrometer data, as well as magnetic and gravity data, all painted a picture vastly different from the one we had when we began the journey more than 35 years ago. The Moon is differentiated, has a complex history of volcanic and tectonic events, has weak crustal magnetic anomalies, shows crustal gravity anomalies, and is covered with craters of all sizes that were formed by impact rather than volcanic processes. In the planetary context the Moon is especially important because it provides an excellent record of primordial crust formation and complete records of the cratering history and the formation and evolution of its secondary crust.

As a result of many detailed investigations we now have a much better concept of the origin and evolution of the Moon, its structure, composition, stratigraphy, and physical properties, to name only a few fields in which enormous progress has been made over the past few decades. However, we are far from adequately “understanding” the Moon. Numerous questions remain unanswered and below is by no means an exhaustive list of such questions.

- What is the cause of the global asymmetry of the Moon? Is it related to convection and density inversion dynamics, early giant impacts, asymmetric crystallization of the magma ocean, or Earth-Moon tidal effects?
- How does a magma ocean work? Did this stage involve whole or partial melting of the Moon?
- What was the early thermal evolution of the Moon?

- What is the vertical and lateral structure of the lunar crust and how did it develop?
- What is the composition and structure of the lunar mantle?
- What is the size and composition of the postulated lunar core?
- What role did early (i.e., >4 Ga) volcanism play?
- What were the timing and the effects of major basin-forming events on the lunar stratigraphy?
- What is the nature of the South Pole-Aitken basin? Did it penetrate into the mantle, and how did it affect early crustal evolution?
- What was the impactor flux in the inner Solar System and how has this varied over time? Was there a terminal cataclysm at ~3.9 Ga?
- How and why is the Moon different from other planets and how do planets work in terms of, for example, surface processes, heat transfer, and geologic evolution?
- Are the Apollo geophysical measurements representative of the Moon, or are they only valid for the small regions encompassed by the Apollo landing sites?
- How does the formation and evolution of this small body and its well preserved record of impact modification and solar activity relate to Earth's ancient history and its development of habitability?

With new global data, e.g., from Clementine and Lunar Prospector in hand, we can revisit the post-Apollo paradigms. By integrating old and new data sets, and sample and remotely sensed information collected in the past decades, we have been able to test old ideas, put forward new ones, and so build a solid foundation for future lunar exploration. As a result, some of the post-Apollo models and hypotheses persevered and will no doubt continue to do so, while others underwent or will undergo substantial changes, and yet others have been or will be dismissed entirely. This is only possible because the lunar science community realized that it is beneficial to foster interdisciplinary approaches to address the major scientific questions about the origin and evolution of the Moon. Even with this integrated approach, we might not be able to answer all questions, but it will greatly advance our geologic understanding, will enable us to ask better questions in exploring the other planets, and will put us in a position to develop much better future planetary missions.

To optimize the Moon as the foundation and cornerstone of our understanding of planetary processes and evolution, future exploration should concentrate on some or all of the following goals: deconvolution of the complex record of early lunar crustal formation and evolution; determination of the nature of basic processes and their role in the evolution of the Moon; investigation of the relationships of these processes to the thermal evolution of the Moon and other one-plate planets; establishment of planetary perspectives on the first half of solar-system history; and extrapolation to the nature and evolution of terrestrial planetary bodies including Earth.

As we stand on the edge of a new era of planetary exploration, including new missions to the Moon, Mars, Mercury, Saturn and some asteroids and comets, we have the opportunity and obligation not only to understand the Moon's origin and evolution but also to use the lessons learned from lunar exploration to define the best ways of exploring the rest of our Solar System. In this sense the Moon is a keystone to our understanding of the terrestrial planets and a stepping-stone for future exploration of our Solar System. How do we explore planets? What types of measurements do we need to make? What strategies are most useful? Orbiting spacecraft or sample return missions, or both? Human exploration? From the experience with lunar exploration we know that each exploration strategy has its own benefits, but that it is the integration and simultaneous interpretation of various data sets that are most powerful to

further our knowledge. This is a very important lesson that needs to be considered in plans for the exploration of other planets.

The Moon is a geologically complex planetary body. And it is an excellent natural, easy-to-reach laboratory to test equipment and ideas on our way to other planetary bodies. In this sense the Moon might well prove to be the Rosetta stone for planetary exploration.

5. REFERENCES

- Agnor CB, Canup RM, Levison HF (1999) On the character and consequences of large impacts in the late stage of terrestrial planet formation. *Icarus* 142:219-237
- Ahrens TJ, Rubin AM (1993) Impact-induced tensional failure in rock. *J Geophys Res* 98(E1):1185-1203
- Anderson OL (1981) A decade of progress in Earth's internal properties and processes. *Science* 213:76-82
- Anderson JLB, Schultz PH, Heineck JT (2000) A new view of ejecta curtains during oblique impacts using 3D particle imaging velocimetry. *Lunar Planet Sci XXXI*:#1749
- Anderson JLB, Schultz PH, Heineck JT (2001) Oblique impact ejecta flow fields: An application of Maxwell's Z model. *Lunar Planet Sci XXXII*:#1352
- Anderson JLB, Schultz PH, Heineck JT (2003) Asymmetry of ejecta flow during oblique impacts using three-dimensional particle image velocimetry. *J Geophys Res* 108, doi 10.1029/2003JE002075
- Antonenko I, Yingst RA (2002) Mare and cryptomare deposits in the Schickard region of the Moon: New measurements using Clementine FeO data. *Lunar Planet Sci XXXIII*:#1438
- Antonenko I, Head JW, Mustard JF, Hawke BR (1995) Criteria for the detection of lunar cryptomaria. *Earth, Moon and Planets* 69:141-172
- Arai T, Warren PH (1999) Lunar meteorite QUE 94281: Glass compositions and other evidence for launch pairing with Yamato-793274. *Meteorit Planet Sci* 34:209-234
- Arkani-Hamed J (1998) The lunar mascons revisited. *J Geophys Res* 103(E2):3709-3739
- Arkani-Hamed J, Konopliv AS, Sjogren WL (1999) On the equipotential surface hypothesis of lunar maria floors. *J Geophys Res* 104(E3):5921-5932
- Arndt J, von Engelhardt W (1987) Formation of Apollo 17 orange and black glass beads. *J Geophys Res* 92:372-376
- Arnold JR (1979) Ice in the lunar polar regions. *J Geophys Res* 84(B10):5659-5668
- Ashworth DG (1977) Lunar and planetary impact erosion. In: *Cosmic Dust*. McDonnell JAM (ed) Wiley, p 427-526
- Baldwin RB (1971) On the history of lunar impact cratering: The absolute time scale and the origin of planetesimals. *Icarus* 14:36-52
- Baldwin RB (1974) On the origin of mare basins. *Proc Lunar Sci Conf* 5:1-10
- Baldwin RB (1987) On the relative and absolute ages of seven lunar front face basins. II - From crater counts. *Icarus* 71:19-29
- Barnouin-Jha OS, Schultz PH (1996) Ejecta entrainment by impact-generated ring vortices: Theory and experiments. *J Geophys Res* 101(E9):21099-21116
- Barnouin-Jha OS, Schultz PH (1998) Lobateness of impact ejecta deposits from atmospheric interactions. *J Geophys Res* 103(E11):25739-25756
- Barsukov VL (1977) Preliminary data for the regolith core brought to Earth by automatic lunar station Luna 24. *Proc Lunar Sci Conf* 8:3303-3318
- BVSP (Basaltic Volcanism Study Project) (1981) Basaltic Volcanism on the Terrestrial Planets. Pergamon Press
- Bauer JF (1979) Experimental shock metamorphism of mono- and polycrystalline olivine - A comparative study. *Proc Lunar Planet Sci Conf* 10:2573-2596
- Beaty DW, Albee AL (1978) Comparative petrology and possible genetic relations among the Apollo 11 basalts. *Proc Lunar Planet Sci Conf* 9:359-463
- Beaty DW, Albee AL (1980) The geology and petrology of the Apollo 11 landing site. *Proc Lunar Planet Sci Conf* 11: 23-35
- Belton MJS, Head JW, Pieters CM, Greeley R, McEwen AS, Neukum G, Klaasen KP, Anger CD, Carr MH, Chapman CR (1992) Lunar impact basins and crustal heterogeneity - New western limb and far side data from Galileo. *Science* 255:570-576
- Belton MJS, Greeley R, Greenberg R, McEwen A, Klaasen KP, Head JW, Pieters C, Neukum G, Chapman CR, Geissler P, Heffernan C, Breneman H, Anger C, Carr MH, Davies ME, Fanale FP, Gerasch PJ, Ingersoll AP, Johnson TV, Pilcher CB, Thompson WR, Veverka J, Sagan C (1994) Galileo multispectral imaging of the north polar and eastern limb regions of the Moon. *Science* 264:1112-1115
- Benz W, Slattery WL, Cameron AGW (1986) The origin of the moon and the single-impact hypothesis I. *Icarus* 66: 515-535
- Benz W, Slattery WL, Cameron AGW (1987) The origin of the moon and the single-impact hypothesis II. *Icarus* 71: 30-45

- Bickel CE (1977) Petrology of 78155 - An early, thermally metamorphosed polymict breccia. Proc Lunar Sci Conf 8: 2007-2027
- Binder AB (1980) On the internal structure of a moon of fission origin. J Geophys Res 85:4872-4880
- Binder AB (1998) Lunar Prospector: Overview. Science 281:1475-1476
- Bischoff A, Stöffler D (1992) Shock metamorphism as a fundamental process in the evolution of planetary bodies: Information from meteorites. Europ J Mineral 4:707-755
- Blewett DT, Hawke BR, Lucey PG, Taylor GJ, Jaumann R, Spudis PD (1995) Remote sensing and geologic studies of the Schiller-Schickard region of the Moon. J Geophys Res 100:16959-16978
- Blewett DT, Lucey PG, Hawke BR, Jolliff BL (1997) Clementine images of the lunar sample-return stations: Refinement of FeO and TiO₂ mapping techniques. J Geophys Res 102:16319-16325
- Boyce JM (1976) Ages of flow units in the lunar nearside maria based on Lunar Orbiter IV photographs. Proc Lunar Sci Conf 7:2717-2728
- Boyce JM, Johnson DA (1978) Ages of flow units in the far eastern maria and implications for basin-filling history. Proc Lunar Planet Sci Conf 9:3275-3283
- Brett R (1975) Thicknesses of some lunar mare basalt flows and ejecta blankets based on chemical kinetic data. Geochim Cosmochim Acta 39:1135-1143
- Brett R (1976) Reduction of mare basalts by sulfur loss. Geochim Cosmochim Acta 40:997-1004
- Brett R, Gooley RC, Dowty E, Prinz M, Keil K (1973) Oxide minerals in lithic fragments from Luna 20 fines. Geochim Cosmochim Acta 37:761-773
- Bruno BC, Lucey PG, Hawke BR (1991) High-resolution UV-visible spectroscopy of lunar red spots. Proc Lunar Planet Sci Conf 21:405-415
- Budney CJ, Lucey PG (1998) Basalt thickness in Mare Humorum: The crater excavation method. J Geophys Res 103: 16855-16870
- Burchell and Mackay (1998) Crater ellipticity in hypervelocity impacts on metals, J Geophys Res 103:22761-22774
- Bussey DBJ, Guest JE, Sørensen S-A (1997) On the role of thermal conductivity on thermal erosion by lava. J Geophys Res 102:10905-1090
- Butler P, Morrison DA (1977) Geology of the Luna 24 landing site. Proc Lunar Sci Conf 8:3281-3301
- Cameron AGW (1997) The origin of the Moon and the single impact hypothesis V. Icarus 126:126-137
- Cameron AGW, Ward WR (1976) The origin of the Moon. Lunar Planet Sci XII:120
- Cameron AGW, Benz W (1991) The origin of the Moon and the single impact hypothesis IV. Icarus 92:204-216
- Cameron AGW, Canup RM (1998) The giant impact and the formation of the Moon. Proceedings of Origin of the Earth and Moon, LPI Contribution No. 957, Lunar and Planetary Institute
- Canup RM, (2004) Simulations of a late lunar-forming impact. Icarus 168:433-456
- Canup RM, Esposito LW (1996) Accretion of the Moon from an impact-generated disk. Icarus 119:427-446
- Canup RM, Ward WR, Cameron AGW (2001) A scaling relationship for satellite-forming impacts. Icarus 150:288-296
- Carr MH, Crumpler LS, Cutts JA, Greeley R, Guest JE, Masursky H (1977) Martian impact craters and emplacement of ejecta by surface flow. J Geophys Res 82:4055-4065
- Cashore J, Woronow A (1985) A new Monte Carlo model of lunar megaregolith development. J Geophys Res 90:811-816
- Chabot NL, Hoppa GV, Strom RG (2000) Analysis of lunar lineaments: Far side and polar mapping. Icarus 147:301-308
- Chao ECT (1968) Pressure and temperature histories of impact metamorphosed rocks – based on petrographic observations. In: Shock Metamorphism of Natural Materials. French BM, Short NM (eds) Mono Book Corp., 135-158
- Chao ECT (1973) Geologic implications of the Apollo 14 Fra Mauro breccias and comparison with ejecta from the Ries crater, Germany. J Res US Geol Surv 1:1-18
- Chapman CR, Merline WJ, Bierhaus B, Keller J, Brooks S, McEwen A, Tufts BR, Moore J, Carr M, Greeley R, Bender KC, Sullivan R, Head JW, Pappalardo RT, Belton MJS, Neukum G, Wagner R, Pilcher C, and the Galileo Imaging Team (1997) Populations of small craters on Europa, Ganymede, and Callisto: Initial Galileo imaging results. Lunar Planet Sci XXVIII:217-218
- Chappell BW, Green DH (1973) Chemical composition and petrogenetic relationships in Apollo 15 mare basalts. Earth Planet Sci Lett 18:237-246
- Charette MP, McCord TB, Pieters C, Adams JB (1974) Application of remote spectral reflectance measurements to lunar geology classification and determination of titanium content of lunar soils. J Geophys Res 79:1605-1613
- Chevrel SD, Rosenberg C, Pinet PC, Shevchenko VV, Daydou Y (1998) Lunar swirl-like terrains exploration: The case of Mare Ingenii. Lunar Planet Sci XXIX:1660
- Chou C-L, Boynton WV, Sundberg LL, Wasson JT (1975) Volatiles on the surface of Apollo 15 green glass and trace element distributions among Apollo 15 soils. Proc Lunar Sci Conf 6:1701-1727
- Chyba CF (1991) Terrestrial mantle siderophiles and the lunar impact record. Icarus 92:217-233
- Cintala MJ (1992) Impact-induced thermal effects in the lunar and mercurian regoliths. J Geophys Res 97:947-973

- Cintala MJ, Grieve RAF (1994) The effects of differential scaling of impact melt and crater dimensions on lunar and terrestrial craters: Some brief examples. In: Large Meteorite Impacts and Planetary Evolution. BO Dressler, RAF Grieve, VL Sharpton (eds), The Geological Society of America, Special Paper 293, p 51-59
- Cintala MJ, Berthoud L, Hörz F (1999) Ejection-velocity distributions from impacts into coarse-grained sand. *Meteorit Planet Sci* 34:605-623
- Clark PE, Hawke BR (1991) The lunar farside - The nature of highlands east of Mare Smythii. *Earth, Moon, and Planets* 53:93-107
- Cohen BA, Swindle TD, Kring DA (2000) Support for the lunar cataclysm hypothesis from lunar meteorite impact melt ages. *Science* 290:1754-1756
- Cohen BA, Swindle TD, Kring DA (2000a) Argon-40-Argon-39 geochronology of lunar meteorite impact melt clasts. *Meteorit Planet Sci* 35, Supplement:A43
- Coombs CR, Hawke BR, Gaddis LR (1987) Explosive volcanism on the Moon. *Lunar Planet Sci XVIII*:197-198
- Coombs CR, Hawke BR, Peterson CA, Zisk SH (1990) Regional pyroclastic deposits in the north-central portion of the lunar nearside. *Lunar Planet Sci XXI*:228-229
- Cooper BL, Carter JL, Sapp CA (1994) New evidence for graben origin of Oceanus Procellarum from lunar sounder optical imagery. *J Geophys Res* 99:3799-3812
- Craddock RA, Howard AD (2000) Simulated degradation of lunar impact craters and a new method for age dating farside mare deposits. *J Geophys Res* 105:20387-20401
- Croft SK (1980) Cratering flow fields: Implications for the excavation and transient expansion stages of crater formation. *Proc Lunar Planet Sci Conf* 11:2347-2378
- Cushing JA, Taylor GF, Norman MD, Keil K (1999) The granulitic impactite suite: Impact melts and metamorphic breccias of the early lunar crust. *Meteorit Planet Sci* 34:185-195
- Dana J. D. (1846) On the volcanoes of the Moon. *Am J Sci* 2:335-353
- Darwin G (1879) On the procession of a viscous spheroid and on the remote history of Earth. *Philos Trans R Soc London* 170:447-538
- Dasch EJ, Shih C-Y, Bansal BM, Wiesmann H, Nyquist LE (1987) Isotopic analysis of basaltic fragments from lunar breccia 14321: Chronology and petrogenesis of pre-Imbrium mare volcanism. *Geochim Cosmochim Acta* 51: 3241-3254
- Davies GF (1972) Equations of state and phase equilibria of stishovite and a coesite-like phase from shock-wave and other data. *J Geophys Res* 77:4920-4933
- DeHon RA (1975) Mare Spumans and Mare Undarum - Mare thickness and basin floor. *Proc Lunar Sci Conf* 6:2553-2561
- DeHon RA (1977) Mare Humorum and Mare Nubium - Basalt thickness and basin-forming history. *Lunar Planet Sci Conf* 8:633-641
- DeHon RA (1979) Thickness of the western mare basalts. *Proc Lunar Planet Sci Conf* 10:2935-2955
- DeHon RA, Waskom JD (1976) Geologic structure of the eastern mare basins. *Proc Lunar Sci Conf* 7:2729-2746
- Delano JW (1986) Pristine lunar glasses. *J Geophys Res* 91:D201-D215
- Delano JW, Livi K (1981) Lunar volcanic glasses and their constraints on mare petrogenesis. *Geochim Cosmochim Acta* 45:2137-2149
- Dombard AJ, Gillis JJ (2001) Testing the viability of topographic relaxation as a mechanism for the formation of lunar floor-fractured craters. *J Geophys Res* 106:27901-27910
- Dowty E, Prinz M, Keil K (1973) Composition, mineralogy, and petrology of 28 mare basalts from Apollo 15 rake samples. *Proc Lunar Planet Sci Conf* 4:423-444
- El-Baz F (1972) The Alhazen to Abul Wafa swirl belt: An extensive field of light-colored, sinuous markings. *Apollo 16 Preliminary Science Report*, NASA SP-315:29-93 – 29-97
- Elphic RC, Lawrence DJ, Feldman WC, Barraclough BL, Maurice S, Binder AB, Lucey PG (2000) Lunar rare earth element distribution and ramifications for FeO and TiO₂: Lunar Prospector neutron spectrometer observations. *J Geophys Res* 105:20,333-20,345
- Fagan TJ, Taylor GJ, Keil K, Bunch TE, Wittke JH, Korotev RL, Jolliff BL, Gillis JJ, Haskin LA, Jarosewich E, Clayton RN, Mayeda TK, Fernandes VA, Burgess R, Turner G, Eugster O, Lorenzetti S (2002) Northwest Africa 032: Product of lunar volcanism. *Meteorit Planet Sci* 37:371-394
- Feldman WC, Binder AB, Barraclough BL, Belian RD (1998) First results from the Lunar Prospector Spectrometers. *Lunar Planet Sci XXIX*:1936
- Feldman WC, Lawrence DJ, Maurice S, Elphic RC, Barraclough BL, Binder AB, Lucey PG (1999) Classification of lunar terranes using neutron and thorium gamma-ray data. *Lunar Planet Sci XXX*:2056
- Feldman WC, Maurice S, Lawrence DJ, Little RC, Lawson SL, Gasnault O, Wiens RC, Barraclough BL, Elphic RC, Prettyman TH, Steinberg JT, Binder AB (2001) Evidence for water ice near the lunar poles. *J Geophys Res* 106, E10:23,231-23,251
- Florenskiy KP, Bazilevskiy AT, Ivanov AV (1977) The role of exogenic factors in the formation of the lunar surface. In: The Soviet-American Conference on Cosmochemistry of the Moon and Planets. Moscow USSR, June 4-8, 1974. Pomeroy H, Hubbard NJ (eds) p 571-584

- Freed AM, Melosh HJ, Solomon SC (2001) Tectonics of mascon loading: Resolution of the strike-slip faulting paradox. *J Geophys Res* 106:20,603-20,620
- Freeman VF (1981) Regolith of the Apollo 16 site. In: *Geology of the Apollo 16 area, Central Highlands*. Ulrich GE, Hodges CA, Muehlberger WR (eds) USGS Prof Paper 1048:147-159
- French BM (1998) *Traces of Catastrophes: A Handbook of Shock-Metamorphic Effects in Terrestrial Meteorite Impact Structures*. LPI Contribution 954, Lunar and Planetary Institute
- Fujiwara A, Kadono T, Nakamura A (1993) Cratering experiments into curved surfaces and their implication for craters on small satellites. *Icarus* 105:345-350
- Gaddis LR, Pieters CM, Hawke BR (1985) Remote sensing of lunar pyroclastic mantling deposits. *Icarus* 61:461-489
- Gault DE, Wedekind JA (1969) The destruction of tektites by micrometeoroid impact. *J Geophys Res* 74:6780-6794
- Gault DE, Wedekind JA (1978) Experimental studies of oblique impact. *Lunar Planet Sci IX*:374-376
- Gerstenkorn H (1955) Über Gezeitenreibung beim Zweikörper-Problem. *Zeit Astrophys* 36:245-274
- Gibson RL, Reimold WU, Ashley AJ, Koehler C (2001) Granulitic melt breccias in the Vredefort impact structure, South Africa - A terrestrial analog for lunar granulites. *Lunar Planet Sci XXXII*:1013
- Gifford AW, El-Baz F (1978) Thickness of mare flow fronts. *Lunar Planet Sci IX*:382-384
- Giguere TA, Taylor GJ, Hawke BR, Lucey PG (2000) The titanium content of lunar mare basalts. *Meteorit Planet Sci* 35:193-200
- Giguere TA, Hawke BR, Blewett DT, Bussey DBJ, Lucey PG, Smith GA, Spudis PD, Taylor GJ (2003) Remote sensing studies of the Lomonosov-Fleming region of the Moon. *J Geophys Res* 108, doi 10.1029/2003JE002069
- Gillis JJ, Jolliff BL, Elphic RC (2003) A revised algorithm for calculating TiO_2 from Clementine UVVIS data: A synthesis of rock, soil, and remotely sensed TiO_2 concentrations. *J Geophys Res* 108, doi 10.1029/2001JE001515
- Goins NR, Toksöz MN, Dainty AM (1978) Seismic structure of the lunar mantle - An overview. *Proc Lunar Planet Sci Conf* 9:3575-3588
- Goins NR, Dainty AM, Toksöz MN (1981) Seismic energy release of the Moon. *J Geophys Res* 86:378-388
- Gold T (1966) The Moon's surface. In: *The Nature of the Lunar Surface*, Proc 1965 IAU-NASA Symp (WN Hess, DH Menzel, JA O'Keefe, eds.), 107-124. Johns Hopkins, Baltimore
- Golombek MP (1985) Fault type predictions from stress distributions on planetary surfaces - Importance of fault initiation depth. *J Geophys Res* 90:3065-3074
- Golombek MP, Anderson FS, Zuber MT (1999) Topographic profiles across wrinkle ridges indicate subsurface faults. *EOS Trans, Am Geophys Union*, 80:610
- Golombek MP, Anderson FS, Zuber MT (2000) Martian wrinkle ridge topography: Evidence for subsurface faults from MOLA. *Lunar Planet Sci XXXI*:1294
- Greeley R (1971) Lava tubes and channels in the lunar Marius Hills. *Earth, Moon, and Planets* 3:289
- Greeley R, Kadel SD, Williams DA, Gaddis LR, Head JW, McEwen AS, Murchie SL, Nagel E, Neukum G, Pieters CM, Sunshine JM, Wagner R, Belton MJS (1993) Galileo imaging observations of lunar maria and related deposits. *J Geophys Res* 98:17183-17206
- Greeley R, Sullivan R, Klemaszewski J, Homan K, Head JW, Pappalardo RT, Veverka J, Clark B, Johnson TV, Klaasen KP, Belton M, Moore J, Asphaug E, Carr MH, Neukum G, Denk T, Chapman CR, Pilcher CB, Geissler PE, Greenberg R, Tufts R (1998) Europa: Initial Galileo geological observations. *Icarus* 135:4-24
- Green DH, Ringwood AE, Hibberson WO, Ware NG (1975) Experimental petrology of Apollo 17 mare basalts. *Proc Lunar Sci Conf* 6:871-893
- Grier JA, McEwen AS, Lucey PG, Milazzo M, Strom RG (1999) The optical maturity of ejecta from large rayed craters: Preliminary results and implications. In: *Workshop on New Views of the Moon II: Understanding the Moon Through the Integration of Diverse Datasets*. LPI Contribution No. 980, 19
- Guest JE, Murray JB (1976) Volcanic features of the nearside equatorial lunar maria. *J Geol Soc Lond* 132:251-258
- Halekas JS, Mitchell DL, Lin RP, Frey S, Hood LL, Acuna MH, Binder AB (2001) Mapping of crustal magnetic anomalies on the lunar near side by the Lunar Prospector electron reflectometer. *J Geophys Res* 106, E11:27,841-27,852
- Hartmann WK (1971) Martian Cratering III: Theory of crater obliteration. *Icarus* 15:410-428
- Hartmann WK (1975) Lunar 'cataclysm' - A misconception. *Icarus* 24:81-187
- Hartmann WK, Kuiper GP (1962) Concentric structures surrounding lunar basins. *Commun Lunar Planet Lab* 1:51-66
- Hartmann WK, Davis DR (1975) Satellite-sized planetesimals and lunar origin. *Icarus* 24:504-515
- Hartmann WK, Strom RG, Weidenschilling SJ, Blasius KR, Woronow A, Dence MR, Grieve RAF, Diaz J, Chapman CR, Shoemaker EM, Jones KL (1981) Chronology of planetary volcanism by comparative studies of planetary craters. In: *Basaltic Volcanism on the Terrestrial Planets*. Pergamon Press, p 1050-1127
- Hartmann WK, Phillips RJ, Taylor GJ (1986) Origin of the Moon. *Lunar and Planetary Institute*
- Haskin LA (1998) The Imbrium impact event and the thorium distribution at the lunar highland surface. *J Geophys Res* 103(E1):1679-1689
- Haskin LA (2000) Basin impacts, especially large and late Imbrium. In: *Workshop on New Views of the Moon III: Synthesis of sample analysis, on-surface investigation, and remote sensing information*. Lunar and Planetary Institute, p 12

- Haskin LA, Warren P (1991) Lunar chemistry. In: The Lunar Sourcebook: A user's guide to the Moon. Heiken G, Vaniman D, French BM (eds) Lunar and Planetary Institute and Cambridge Univ Press 357-474
- Haskin LA, Jolliff BL (1998) On estimating provenances of lunar highland materials. In: Workshop on New Views of the Moon: Integrated Remotely Sensed, Geophysical, and Sample Datasets, 35
- Haskin LA, Korotev RL, Rockow KM, Jolliff BL (1998) The case for an Imbrium origin of the Apollo Th-rich impact-melt breccias. *Meteorit Planet Sci* 33:959-975
- Haskin LA, Gillis JJ, Korotev RL, Jolliff BL (2000a) The nature of mare basalts in the Procellarum KREEP Terrane. *Lunar Planet Sci XXXI*:#1661
- Haskin LA, Gillis JJ, Korotev RL, Jolliff BL (2000b) The materials of the lunar Procellarum KREEP Terrane: A synthesis of data from geomorphological mapping, remote sensing and sample analyses. *J Geophys Res* 105: 20,403-20,415
- Haskin LA, Korotev RL, Gillis JJ, Jolliff BL (2002) Stratigraphies of Apollo and Luna highland landing sites and provenances of materials from the perspective of basin impact ejecta modeling. *Lunar Planet Sci XXXIII*:#1364
- Haskin LA, Moss BE, McKinnon WB (2003) On estimating contributions of basin ejecta to regolith deposits at lunar sites. *Meteorit Planet Sci* 38(Nr 1):13-33
- Hawke BR, Head JW (1977) Pre-Imbrian history of the Fra Mauro region and Apollo 14 sample provenance. *Proc Lunar Sci Conf* 8: 2741-2761
- Hawke BR, Head JW (1978) Lunar KREEP volcanism - Geologic evidence for history and mode of emplacement. *Lunar Planet Sci IX*:3285-3309
- Hawke BR, Spudis PD (1980) Geochemical anomalies on the eastern limb and farside of the moon. Conference on the Lunar Highlands Crust, Houston, Tex., November 14-16, 1979, Proceedings. (A81-26201 10-91) Pergamon Press, 467-481
- Hawke BR, Bell JF (1981) Remote sensing studies of lunar dark-halo craters. *Bull Am Astron Soc* 13:712
- Hawke BR, Mac Laskey D, McCord TB, Adams JB, Head JW, Pieters CM, Zisk S (1979) Multispectral mapping of lunar pyroclastic deposits. *Bull Am Astron Soc* 12:582
- Hawke BR, Spudis PD, Clark PE (1985) The origin of selected lunar geochemical anomalies: Implications for early volcanism and the formation of light plains. *Earth, Moon and Planets* 32:257-273
- Hawke BR, Coombs CR, Gaddis LR, Lucey PG, Owensby PD (1989) Remote sensing and geologic studies of localized dark mantle deposits on the Moon. *Proc Lunar Planet Sci Conf* 19:255-268
- Hawke BR, Giguere TA, Lucey PG, Peterson CA, Taylor GJ, Spudis, PD (1998) Multidisciplinary studies of ancient mare basalt deposits. Workshop on New Views of the Moon, Lunar and Planetary Institute, 37-38
- Hawke BR, Blewett DT, Lucey PG, Peterson CA, Bell JF, Campbell BA, Robinson MS (1999) The composition and origin of selected lunar crater rays. Workshop on New Views of the Moon II: Understanding the Moon Through the Integration of Diverse Datasets, #8035
- Hawke BR, Blewett DT, Lucey PG, Smith GA, Taylor GJ, Lawrence DJ, Spudis PD (2001) Remote sensing studies of selected spectral anomalies on the Moon. *Lunar Planet Sci XXXII*:#1241,
- Hawke BR, Lawrence DJ, Blewett, DT, Lucey, PG, Smith GA, Taylor GJ, Spudis PD (2002a) Remote sensing studies of geochemical and spectral anomalies on the nearside of the Moon. *Lunar Planet Sci XXXIII*:#1598
- Hawke BR, Lawrence DJ, Blewett, DT, Lucey, PG, Smith GA, Taylor GJ, Spudis PD (2002b) Lunar highlands volcanism: The view from a millennium. In: The Moon Beyond 2002: Next Steps in Lunar Science and Exploration. LPI Contribution No. 1128, Lunar and Planetary Institute, p 22
- Hawke BR, Lawrence DJ, Blewett DT, Lucey PG, Smith GA, Spudis PD, Taylor GJ (2003) Hansteen Alpha: A volcanic construct in the lunar highlands. *J Geophys Res* 108(E7), doi:10.1029/2002JE002013
- Hawke BR, Gillis JJ, Giguere TA, Blewett DT, Lawrence DJ, Lucey PG, Smith GA, Spudis PD, Taylor GJ (2005) Remote sensing and geologic studies of the Balmer-Kapteyn region of the Moon. *J Geophys Res* 110, doi 10.1029/2004JE002383
- Head JW (1974) Lunar dark-mantle deposits: Possible clues to the distribution of early mare deposits. *Proc Lunar Sci Conf* 5:207-222
- Head JW (1975a) Lunar mare deposits: Areas, volumes, sequence, and implication for melting in source areas. In: Origins of Mare Basalts and their Implications for Lunar Evolution. Lunar and Planetary Institute, p 66-69
- Head JW (1975b) Some geologic observations concerning lunar geophysical models. Proc Soviet-American Conference on the Cosmochemistry of the Moon and Planets, Moscow 407-416
- Head JW (1976) Lunar volcanism in space and time. *Rev Geophys Space Phys* 14:265-300
- Head JW (1982) Lava flooding of ancient planetary crusts: Geometry, thickness, and volumes of flooded lunar impact basins. *Moon and Planets* 26:61-88
- Head JW (1999) Surfaces and interiors of the terrestrial planets. In: The New Solar System. Beatty JK, Petersen CC, Chaikin A (eds) Cambridge University Press, p 157-173
- Head JW, McCord TB (1978) Imbrian-age highland volcanism on the moon - The Gruithuisen and Mairan domes. *Science* 199:1433-1436
- Head JW, Wilson L (1979) Alphonsus-type dark-halo craters: Morphology, morphometry and eruption conditions. *Proc Lunar Planet Sci Conf* 10:2861-2897

- Head JW, Wilson L (1980) The formation of eroded depressions around the sources of lunar sinuous rilles: Observations. *Lunar Planet Sci XI*:426-428
- Head JW, Wilson L (1992) Lunar mare volcanism: Stratigraphy, eruption conditions, and the evolution of secondary crusts. *Geochim Cosmochim Acta* 56:2155-2175
- Head JW Wilson L (1999) Lunar Gruithuisen and Mairan Domes: Rheology and mode of emplacement. In: *Workshop on New Views of the Moon II: Understanding the Moon Through the Integration of Diverse Datasets*. LPI Contribution 980, Lunar and Planetary Institute, p 23
- Head JW, Pieters C, McCord TB, Adams J, Zisk SH (1978a) Definition and detailed characterization of lunar surface units using remote observations. *Icarus* 33:145-172
- Head JW, Adams JB, McCord TB, Pieters C, Zisk A (1978b) Regional stratigraphy and geologic history of Mare Crisium. In: *Mare Crisium: The view from Luna 24*. Merrill RB, Papike JJ (eds) *Geochim Cosmochim. Acta Suppl.* 9. Pergamon Press, New York, 727
- Head JW, Murchie S, Mustard JF, Pieters CM, Neukum G, McEwen A, Greeley R, Nagel E, Belton MJS (1993) Lunar impact basins: New data for the western limb and far side (Orientale and South Pole-Aitken basins) from the first Galileo flyby. *J Geophys Res* 98:17149-17182
- Head JW, Reed JS, Weitz C (1998) Lunar Rima Parry IV: Dike emplacement processes and consequent volcanism. *Lunar Planet Sci XXIX*:#1914
- Head JW, Wilson L, Robinson M, Hiesinger H, Weitz C, Yingst A (2000) Moon and Mercury: Volcanism in Early Planetary History. In: *Environmental Effects on Volcanic Eruptions: From Deep Oceans to deep Space*. Zimbelman JR, Gregg TKP (eds) Kluwer Academic Press, p 143-178
- Head JW, Wilson L, Weitz CM (2002) Dark ring in southwestern Orientale Basin: Origin as a single pyroclastic eruption. *J Geophys Res* 107(E1), doi:10.1029/2000JE001438
- Heather DJ, Dunkin SK, Wilson L (2003) Volcanism on the Marius Hills plateau: Observational analyses using Clementine multispectral data. *J Geophys Res* 108, doi:10.1029/2002JE001938
- Heiken G, McEwen MC (1972) The geologic setting of the Luna 20 site. *Earth Planet Sci Lett* 17:3-6
- Heiken G, McKay DS, Brown RW (1974) Lunar deposits of possible pyroclastic origin. *Geochim Cosmochim Acta* 38:1703-1718
- Heiken G, Vaniman D, French BM (eds) (1991) *The Lunar Sourcebook: A User's Guide to the Moon*. Lunar and Planetary Institute and Cambridge Univ Press
- Hiesinger H, Head JW, Jaumann R, Neukum G (1999) Lunar mare volcanism. *Lunar Planet Sci XXX*:#1199
- Hiesinger H, Jaumann R, Neukum G, Head JW, Wolf U (2000) Ages and stratigraphy of mare basalts on the lunar nearside. *J Geophys Res* 105:29,239-29,275
- Hiesinger H, Head JW, Wolf U, Neukum G (2001) New age determinations of lunar mare basalts in Mare Cognitum, Mare Nubium, Oceanus Procellarum, and other nearside mare. *Lunar Planet Sci XXXII*:#1815
- Hiesinger H, Head JW, Wolf U, Jaumann R, Neukum G (2002) Lunar mare basalt flow units: Thicknesses determined from crater size-frequency distributions. *Geophys Res Lett* 29, doi:10.1029/2002GL014847
- Hiesinger H, Head JW, Wolf U, Jaumann R, Neukum G (2003) Ages and stratigraphy of mare basalts in Oceanus Procellarum, Mare Nubium, Mare Cognitum, and Mare Insularum. *J Geophys Res* 108, doi 10.1029/2002JE001985
- Hinners NW (1972) Apollo 16 site selection. *Apollo 16 Preliminary Science Report*, NASA-SP315: 1-1 – 1-3
- Hood LL (1987) Magnetic field and remanent magnetization effects of basin-forming impacts on the moon. *Geophys Res Lett* 14:844-847
- Hood LL, Williams CR (1989) The lunar swirls - Distribution and possible origins. *Lunar Planet Sci XIX*:99-113
- Hood LL, Zubee MT (2000) Recent refinement in geophysical constraints on lunar origin and evolution. In: *Origin of the Earth and Moon*. Canup RM, Righter K (eds) University of Arizona Press, p 397-409
- Hood LL, Mitchell DL, Lin RP, Acuna MH, Binder AB (1999) Initial measurements of the lunar induced magnetic dipole moment using Lunar Prospector magnetometer data. *Geophys Res Lett* 26:2327-2330
- Hood LL, Zakharian A, Halekas J, Mitchell DL, Lin RP, Acuna MH, Binder AB (2001) Initial mapping and interpretation of lunar crustal magnetic anomalies using Lunar Prospector magnetometer data. *J Geophys Res* 106, E11:27,825-27,839
- Hornemann U, Müller WF (1971) Shock-induced deformation twins in clinopyroxene. *Neues Jb Min, Mh* 6: 247-256
- Hörz F (1978) How thick are lunar mare basalts? *Proc Lunar Planet Sci Conf* 9:3311-3331
- Hörz F, Morrison DA, Gault DE, Oberbeck VR, Quaide WL, Vedder JF, Brownlee DE, Hartung JB (1977) The micrometeoroid complex and evolution of the lunar regolith. In: *The Soviet-American Conference on Cosmochemistry of the Moon and Planets*, 605-635
- Hörz F, Grieve R, Heiken G, Spudis P, Binder A (1991) Lunar surface processes. In: *Lunar Sourcebook - A User Guide to the Moon*. Heiken G, Vaniman D, French B (eds) Cambridge University Press, p 61-120
- Howard KA, Head JW, Swann GA (1973) Geology of Hadley Rille. *Proc Lunar Sci Conf* 3:1-14
- Hubbard NJ, Minear JW (1975) A chemical and physical model for the genesis of lunar rocks: Part II mare basalts. In: *Lunar Planet Sci XI*:405
- Hulme G (1973) Turbulent lava flows and the formation of lunar sinuous rilles. *Mod Geol* 4:107-117

- Ivanov BA (1992) Impact craters. In: Venus Geology, Geochemistry, and Geophysics - Research results from the USSR. Barsukov V, Basilevsky A, Volkov V, Zharkov V (eds) Univ. Arizona Press, p 113-128
- Ivanov BA, Melosh HJ (2003) Impacts do not initiate volcanic eruptions: Eruptions close to the crater. *Geology* 31: 869-872
- James OB (1981) Petrologic and age relations in Apollo 16 rocks: Implications for subsurface geology and the age of the Nectaris basin. *Proc Lunar Planet Sci Conf* 12B:209-233
- James OB, Wright TL (1972) Apollo 11 and 12 mare basalts and gabbros: Classification, compositional variations, and possible petrogenetic relations. *Bull Geol Soc Am* 83:2357-2382
- James OB, Hötz F (eds) (1981) Workshop on Apollo 16. LPI Technical Report 81-01, Lunar and Planetary Institute
- Jessberger EK, Huncke JC, Podosek FA, Wasserburg GJ (1974) High-resolution argon analysis of neutron-irradiated Apollo 16 rocks and separated minerals. *Proc Lunar Sci Conf* 5:1419-1449
- Johnson JR, Larson SM, Singer RB (1991) Remote sensing of potential lunar resources. I - Near-side compositional properties. *J Geophys Res* 96:18,861-18,882
- Jolliff BL (1999) Clementine UVVIS multispectral data and the Apollo 17 landing site: What can we tell and how well? *J Geophys Res* 104:14123-14148
- Jolliff BL, Korotev RL, Haskin LA (1991) Geochemistry of 2-4-mm particles from Apollo 14 soil (14161) and implications regarding igneous components and soil-forming processes. *Proc Lunar Planet Sci Conf* 21:193-219
- Jolliff BL, Gillis JJ, Haskin LA, Korotev RL, Wieczorek MA (2000) Major lunar crustal terrains: Surface expression and crust-mantle origins. *J Geophys Res* 105(E2):4197-4216
- Khan A, Mosegaard K, Rasmussen KL (2000) A new seismic velocity model for the Moon from a Monte Carlo inversion of the Apollo lunar seismic data. *Geophys Res Lett* 27:1591-1594
- Khan A, Mosegaard K, Williams JG, Logonne P (2004) Does the Moon possess a molten core? Probing the deep lunar interior using results from LLR and Lunar Prospector. *J Geophys Res* 109, doi 10.1029/2004JE002294
- Kieffer SW, Schaal RB, Gibbons RV, Hötz F, Milton DJ, Dube A (1976) Shocked basalt from Lonar impact crater, India, and experimental analogues. *Proc Lunar Science Conference* 7:1391-1412
- Kipp ME, Melosh HJ (1986) Origin of the Moon: A preliminary numerical study of colliding planets. *Lunar Planet Sci XVII*:420-421
- Köhler U, Head JW, Neukum G, Wolf U (1999) North-polar lunar light plains: Ages and compositional observations. In: Workshop on New Views of the Moon II: Understanding the Moon Through the Integration of Diverse Datasets, 34
- Köhler U, Head JW, Neukum G, Wolf U (2000) Lunar light plains in the northern nearside latitudes: Latest results on age distributions, surface composition, nature, and possible origin. *Lunar Planet Sci XXXI*:#1822
- Kokubo E, Canup RM, Ida S (2000) Lunar accretion from an impact-generated disk. In: *Origin of the Earth and Moon* (Canup RM, Righter K, eds.) Univ. Arizona Press, 145-163
- Konopliv AS, Binder AB, Hood LL, Kucinskas AB, Sjogren WL, Williams JC (1998) Improved gravity field of the Moon from Lunar Prospector. *Science* 281:1476-1480
- Konopliv AS, Asmar SW, Yuan DN (2001) Recent gravity models as a result of the Lunar Prospector mission. *Icarus* 150:1-18
- Korotev RL (1987) The nature of the meteoritic components of Apollo 16 soil as inferred from correlations of iron, cobalt, iridium, and gold with nickel. *Proc Lunar Planet Sci Conf* 17:447-461
- Korotev RL (1990) Cobalt and nickel concentrations in the 'komatiite component' of Apollo 16 polymict samples. *Earth Planet Sci Lett* 96:481-489.
- Korotev RL (2000) The great lunar hot spot and the composition and origin of the Apollo mafic ("LKFM") impact-melt breccias. *J Geophys Res* 105:4317-4345
- Korotev RL, Jolliff BL (2001) The curious case of the lunar magnesian granulitic breccias. *Lunar Planet Sci XXXII*: #1455
- Korotev RL, Gillis JJ (2001) A new look at the Apollo 11 regolith and KREEP. *J Geophys Res* 106:12339-12353
- Korotev RL, Jolliff BL, Rockow KM (1996) Lunar meteorite Queen Alexandra Range 93069 and the iron concentration of the lunar highlands surface. *Meteorit Planet Sci* 31:909-924
- Korotev RL, Jolliff BL, Zeigler RA, Haskin LA (2003a) Compositional constraints on the launch pairing of three brecciated lunar meteorites of basaltic composition. *Antarctic Met Res* 16:152-175
- Korotev RL, Jolliff BL, Zeigler RA, Gillis JJ, Haskin LA (2003b) Feldspathic lunar meteorites and their implications for compositional remote sensing of the lunar surface and the composition of the lunar crust. *Geochim Cosmochim Acta* 67(24):4895-4923
- Kring DA, Cohen BA (2002) Cataclysmic bombardment throughout the inner solar system 3.9-4.0 Ga. *J Geophys Res* 107, doi 10.1029/2001JE001529
- Kuskov OL, Konrod VA (2000) Resemblance and difference between the constitution of the Moon and Io. *Planet Space Sci* 48:717-726
- Kuzmin RO, Bobina NN, Zabalueva EV, Shashkina VP (1988) The Structure of the martian cryolithosphere upper levels. In: *Workshop on Mars Sample Return Science*. LPI Technical Report 88-07, Lunar and Planetary Institute, p 108

- Lammlein DR, Latham GV, Dorman J, Nakamura Y, Ewing M (1974) Lunar seismicity, structure and tectonics. *Rev Geophys Space Phys* 12:1-21
- Langseth MG, Keihm SJ, Peters K (1976) Revised lunar heat-flow values. *Proc Lunar Sci Conf* 7:3143-3171
- Lawrence DJ, Feldman WC, Barraclough BL, Binder AB, Elphic RC, Maurice S, Thomsen DR (1998) Global elemental maps of the Moon: The Lunar Prospector gamma-ray spectrometer. *Science* 281:1484-1489
- Lawrence DJ, Feldman WC, Barraclough BL, Binder AB, Elphic RC, Maurice S, Miller MC, Prettyman TH (2000) Thorium abundances on the lunar surface. *J Geophys Res* 105(E8):20,307-20,331
- Lawrence DJ, Feldman WC, Blewett DT, Elphic RC, Lucey PG, Maurice S, Prettyman TH, Binder AB (2001) Iron abundances on the lunar surface as measured by the Lunar Prospector gamma-ray spectrometer. *Lunar Planet Sci XXXII*:#1830
- Lawrence DJ, Feldman WC, Elphic RC, Little RC, Prettyman TH, Maurice S, Lucey PG, Binder AB (2002) Iron abundances on the lunar surface as measured by the Lunar Prospector gamma-ray and neutron spectrometers. *J Geophys Res* 107, doi:10.1029/2001JE001530
- Lawrence DJ, Hawke BR, Hagerty JJ, Elphic RC, Feldman WC, Prettyman TH, Vaniman DT (2005) Evidence for a high-Th_{2O} evolved lithology on the Moon at Hansteen Alpha. *Geophys Res Lett* 32, doi 10.1029/2004GL022022
- Lawson SL, Feldman WC, Lawrence DJ, Moore KR, Maurice S, Belian RD, Binder AB (2002) Maps of Lunar Radon-222 and Polonium-210. *Lunar Planet Sci XXXIII*:#1835
- Lemoine FG, Smith DE, Zuber MT, Neumann GA, Rowlands DD (1997) A 70th degree lunar gravity model (GLGM-2) from Clementine and other tracking data. *J Geophys Res* 102:16339-16359
- Levison HF, Dones L, Chapman CR, Stern SA, Duncan MJ, Zahnle K (2001) Could the lunar "Late Heavy Bombardment" have been triggered by the formation of Uranus and Neptune? *Icarus* 151:286-306
- Li L, Mustard JF (2000) The compositional gradients and lateral transport by dark-halo and dark-ray craters. *Lunar Planet Sci XXXI*:#2007
- Li L, Mustard JF (2003) Highland contamination in lunar mare soils: Improved mapping with multiple end-member spectral mixture analysis (MESMA). *J Geophys Res* 108, doi 10.1029/2002JE001917
- Lin RP, Anderson KA, Hood LL (1988) Lunar surface magnetic field concentrations antipodal to young large impact basins. *Icarus* 74:529-541
- Lindstrom MM, Lindstrom DJ (1986) Lunar granulites and their precursor anorthositic norites of the early lunar crust. *J Geophys Res* 91:D263-D276
- Lognonné P, Gagnepain-Beyneix J, Chenet H (2003) A new seismic model of the Moon: Implications for structure, thermal evolution and formation of the Moon. *Earth Planet Sci Lett* 211:27-44
- Longhi J (1980) A model of early lunar differentiation. *Proc Lunar Planet Sci Conf* 11:289-315
- Longhi J (1992a) Origin of picritic green glass magmas by polybaric fractional fusion. *Proc Lunar Planet Sci Conf* 22: 343-353
- Longhi J (1992b) Experimental petrology and petrogenesis of mare volcanics. *Geochim Cosmochim Acta* 56:2235-2252
- Longhi J (1993) Liquidus equilibria of lunar analogs at high pressure. *Lunar Planet Sci XXIV*:895-896
- Love SG, Hörz F, Brownlee DE (1993) Target porosity effects in impact cratering and collisional disruption. *Icarus* 105:216-224
- Lucchitta BK (1976) Mare ridges and related highland scarps - Result of vertical tectonism. *Proc Lunar Sci Conf* 7: 2761-2782
- Lucchitta BK (1977) Crater clusters and light mantle at the Apollo 17 site - A result of secondary impact from Tycho. *Icarus* 30:80-96
- Lucey PG, Spudis PD, Zuber M, Smith D, Malaret E (1994) Topographic compositional units on the Moon and the early evolution of the lunar crust. *Science* 266:1855
- Lucey PG, Taylor GJ, Malaret E (1995) Abundance and distribution of iron on the Moon. *Science* 268:1150-1153
- Lucey PG, Blewett DT, Johnson JL, Taylor GJ, Hawke BR (1996) Lunar titanium content from UV-VIS measurements. *Lunar Planet Sci XXVII*:781-782
- Lucey PG, Taylor GJ, Malaret E (1997) Global abundance of FeO on the Moon - Improved estimates from multispectral imaging and comparisons with the lunar meteorites. *Lunar Planet Sci XXVIII*:849-850
- Lucey PG, Blewett DT, Hawke BR (1998) Mapping the FeO and TiO₂ content of the lunar surface with multispectral imagery. *J Geophys Res* 103:3679-3699
- Lucey PG, Blewett DT, Jolliff BL (2000) Lunar iron and titanium abundance algorithms based on final processing of Clementine ultraviolet-visible images. *J Geophys Res* 105:20297-20305
- Ma M-S, Schmitt RA, Nielsen RL, Taylor GJ, Warner RD, Keil K. (1979) Petrogenesis of Luna 16 aluminous mare basalts. *Geophys Res Lett* 6:909-912
- Mackin JH (1964) Origin of lunar maria. *Geol Soc Am Bull* 80:735-747
- Malin MC (1974) Lunar red spots: Possible pre-mare materials. *Earth Planet Sci Lett* 21:331-341
- Maurer P, Eberhardt P, Geiss J, Grogler N, Stettler A, Brown GM, Peckett A, Krähenbühl U (1978) Pre-Imbrian craters and basins - Ages, compositions and excavation depths of Apollo 16 breccias. *Geochim Cosmochim Acta* 42: 1687-1720

- Maurice S, Feldman WC, Lawrence DJ, Elphic RC, Johnson JR, Chevrel S, Genetay I, Binder AB (2001) A maturity parameter of the lunar regolith from neutron data. *Lunar Planet Sci XXXII*:#2033
- Maxwell TA (1978) Origin of multi-ring basin ridge systems: An upper limit to elastic deformation based on a finite-element model. *Proc Lunar Planet Sci Conf* 9:3541-3559
- Maxwell TA, El-Baz F (1978) The nature of rays and sources of highland material in Mare Crisium. In: *Mare Crisium: The View from Luna 24*. *Geochim Cosmochim Acta Suppl.* 9, p 89-103
- McCauley JH (1967) Geologic map of the Hevelius Region of the Moon. USGS Misc. Inv. Map I-491
- McCauley JF, Scott DH (1972) The geologic setting of the Luna 16 landing site. *Earth Planet Sci Lett* 13:225-232
- McEwen AS, Gaddis LR, Neukum G, Hoffmann H, Pieters CM, Head JW (1993) Galileo observations of post-Imbrium lunar craters during the first Earth-Moon flyby. *J Geophys Res* 98:17207-17234
- McEwen AS, Robinson MS, Eliason EM, Lucey PG, Duxbury TC, Spudis PD (1994) Clementine observations of the Aristarchus region of the Moon. *Science* 266:1858-1862
- McEwen AS, Moore JM, Shoemaker EM (1997) The Phanerozoic impact cratering rate: Evidence from the farside of the Moon. *J Geophys Res* 102:9231-9242
- McKay DS, Heiken G, Basu A, Blanford G, Simon S, Reedy R, French B, Papike J (1991) The lunar regolith. In: *The Lunar Source Book: A user's guide to the Moon*. Heiken G, Vaniman D, French B (eds) Cambridge Univ. Press, p 285-356
- McSween HY (1999) Meteorites and Their Parent Planets. Cambridge University Press
- Melendrez DE, Johnson JR, Larson SM, Singer RB (1994) Remote sensing of potential lunar resources. 2: High spatial resolution mapping of spectral reflectance ratios and implications for nearside mare TiO_2 content. *J Geophys Res* 99:5601-5619
- Melosh HJ (1975) Large impact craters and the moon's orientation. *Earth Planet Sci Lett* 26:353-360
- Melosh HJ (1978) The tectonics of mascon loading. *Proc Lunar Planet Sci Conf* 9:3513-3525
- Melosh HJ (1989) Impact Cratering: A Geological Process. Oxford University Press
- Melosh HJ (2001) Can impacts induce volcanic eruptions? In: *International Conference on Catastrophic Events and Mass Extinctions: Impacts and Beyond*, Vienna, 3144
- Merrill RB, Papike JJ (eds) (1978) *Mare Crisium: The View from Luna 24*. *Geochim Cosmochim Acta Suppl.* 9. Pergamon Press
- Morrison RH, Oberbeck VR (1975) Geomorphology of crater and basin deposits—emplacement of the Fra Mauro formation. *Proc Lunar Sci Conf* 6:2503-2530
- Muehlberger WR (1974) Structural history of southeastern Mare Serenitatis and adjacent highlands. *Proc Lunar Sci Conf* 5:101-110
- Muehlberger WR, Hörz F, Sevier JR, Ulrich GE (1980) Mission objectives for geological exploration of the Apollo 16 landing site. In: *Proc Conf Lunar Highlands Crust*. JJ Papike, RB Merrill (eds) Pergamon Press, p 1-49
- Müller PM, Sjogren WL (1968) Mascons: Lunar mass concentrations. *Science* 161:680-684
- Müller PM, Sjogren WL (1969) Lunar gravimetry and mascons. *Appl Mech Rev* 22:955-959
- Müller WF, Hornemann U (1969) Shock-induced planar deformation structures in experimentally shock-loaded olivines and in olivines from chondritic meteorites. *Earth Planet Sci Lett* 7:251-264
- Murase T, Mc Birney AR (1970) Viscosity of lunar lavas. *Science* 167:1491-1493
- Mustard JF, Head JW (1996) Buried stratigraphic relationships along the southwestern shores of Oceanus Procellarum: Implications for early lunar volcanism. *J Geophys Res* 101:18913-18926
- Nakamura Y (1983) Seismic velocity structure of the lunar mantle. *J Geophys Res* 88:677-686
- Nakamura Y (2003) New identification of deep moonquakes in the Apollo lunar seismic data. *Physics Earth Planet Int* 139:197-205
- Nakamura Y (2005) Farside deep moonquakes and deep interior of the Moon. *J Geophys Res* 110, doi 10.1029/2004JE002332
- Nakamura Y, Lammlein D, Latham G, Ewing M, Dorman J, Press F, Toksöz N (1973) New seismic data on the state of the deep lunar interior. *Science* 181:49-51
- Neal CR, Taylor LA (1992) Petrogenesis of mare basalts - A record of lunar volcanism. *Geochim Cosmochim Acta* 56: 2177-2211
- Neal CR, Hacker MD, Snyder GA, Taylor LA, Liu Y-G, Schmitt RA (1994a) Basalt generation at the Apollo 12 site, Part 1: New data, classification, and re-evaluation. *Meteoritics*, 29:334-348
- Neal CR, Hacker MD, Snyder GA, Taylor LA, Liu Y-G, Schmitt RA (1994b) Basalt generation at the Apollo 12 site, Part 2: Source heterogeneity, multiple melts, and crustal contamination. *Meteoritics* 29:349-361
- Neukum G (1977) Different ages of lunar light plains. *The Moon* 17:383-393
- Neukum G (1983) Meteoritenbombardement und Datierung planetarer Oberflächen. *Habilitationsschrift*, Univ. München, Munich, Germany
- Neukum G, Wise DU (1976) Mars - A standard crater curve and possible new time scale. *Science* 194:1381-1387
- Neukum G, Ivanov BA (1994) Crater size distributions and impact probabilities on Earth from lunar, terrestrial-planet, and asteroid cratering data. In: *Hazard Due to Comets and Asteroids*. Gehrels T (ed) Univ. of Ariz. Press, p 359-416

- Neukum G, Ivanov BA, Hartmann WK (2001) Cratering records in the inner solar system in relation to the lunar reference system. *Space Sci Rev* 96:55-86
- Neumann GA, Zuber MT, Smith DE, Lemoine FG (1996) The lunar crust: Global structure and signature of major basins. *J Geophys Res* 101:16841-16843
- Nozette S, and the Clementine team (1994) The Clementine mission to the Moon: Scientific overview. *Science* 266: 1835-1839
- Nozette S, Lichtenberg CL, Spudis P, Bonner R, Ort W, Malaret E, Robinson M, Shoemaker EM (1996) The Clementine bistatic radar experiment. *Science* 274:1495-1498
- Nozette S, Spudis PD, Robinson MS, Bussey DBJ, Lichtenberg C, Bonner R (2001) Integration of lunar polar remote-sensing data sets: Evidence for ice at the lunar south pole. *J Geophys Res* 106:23,253-23,266
- Nunes PD, Tatsumoto M, Unruh DM (1974) U-Th-Pb and Rb-Sr systematics of Apollo 17 boulder 7 from the North Massif of the Taurus-Littrow valley. *Earth Planet Sci Lett* 23:445-452
- Nyquist LE, Shih C-Y (1992) The isotopic record of lunar volcanism. *Geochim Cosmochim Acta* 56:2213-2234
- Nyquist LE, Bogard DD, Shih C-Y (2001) Radiometric chronology of the Moon and Mars. In: *The Century of Space Science*. Bleeker JA, Geiss J, Huber M (eds) Kluwer Academic Publishers, p 1325-1376
- Oberst J, Mizutani H (2002) A new inventory of deep moonquake nests visible in the Apollo 12 area. *Lunar Planet Sci XXXIII*:#1704
- O'Keefe JD, Ahrens TJ (1993) Planetary cratering mechanics. *J Geophys Res* 98:17,011-17,028
- O'Keefe JD, Ahrens TJ (1994) Impact-induced melting of planetary surfaces. In: *Large Meteorite Impacts and Planetary Evolution*. Dressler BO, Grieve RAF, Sharpton VL (eds), Special Paper 293, The Geological Society of America, Boulder, p 103-109
- Ostertag R (1983) Shock experiments on feldspar crystals. *J Geophys Res (Suppl.)* 88:B364-B376
- Ostertag R, Stöfller D, Borchardt R, Palme H, Spettel B, Wänke H (1987) Precursor lithologies and metamorphic history of granulitic breccias from North Ray crater, Station 11, Apollo 16. *Geochim Cosmochim Acta* 51:131-142
- Oberbeck VR (1975) The role of ballistic erosion and sedimentation in lunar stratigraphy. *Rev Geophys Space Phys* 13:337-362
- Oberbeck VR, Quaide WL, Gault DE, Morrison RH, Hörr F (1974) Smooth plains and continuous deposits of craters and basins. *Proc Lunar Sci Conf* 5:111-136
- Papike JJ, Vaniman DT (1978) The lunar mare basalt suite. *Geophys Res Lett* 5:433-436
- Papike JJ, Hodges FN, Bence AE, Cameron M, Rhodes JM (1976) Mare basalts: Crystal chemistry, mineralogy, and petrology. *Rev Geophys Space Phys* 14:475-540
- Papike JJ, Ryder G, Shearer CK (1998) Lunar samples. *Rev Mineral* 36:5-1-5-234
- Parmentier EM, Zhong S, Zuber MT (2000) On the relationship between chemical differentiation and the origin of lunar asymmetries. *Lunar Planet Sci XXXI*:#1614
- Petro NE, Pieters CM (2004) Surviving the heavy bombardment: Ancient material at the surface of South Pole-Aitken Basin. *J Geophys Res* 109, doi 10.1029/2003JE002182
- Pieters CM (1978) Mare basalt types on the front side of the Moon. *Proc Lunar Planet Sci Conf* 9:2825-2849
- Pieters CM (1993b) Compositional diversity and stratigraphy of the lunar crust derived from reflectance spectroscopy. In: *Topics in Remote Sensing 4 - Remote geochemical analysis: elemental and mineralogical composition*. Pieters CM, Englert PAJ (eds) Cambridge Univ. Press, p 309-339
- Pieters CM, Head JW, Adams JB, McCord TB, Zisk SH, Whitford-Stark JL (1980) Late high-titanium basalts of the western maria: Geology of the Flamsteed Region of Oceanus Procellarum. *J Geophys Res* 85:3919-3938
- Pieters CM, Sunshine JM, Fischer EM, Murchie SL, Belton M, McEwen A, Gaddis L, Greeley R, Neukum G, Jaumann R, Hoffmann H (1993a) Crustal diversity of the Moon: Compositional analyses of Galileo solid state imaging data. *J Geophys Res* 98:17,127-17,148
- Pieters CM, Staid MI, Fischer EM, Tompkins S, He G (1994) A sharper view of impact craters from Clementine data. *Science* 266:1844
- Pieters CM, Head JW, Gaddis L, Jolliff B, Duke M (2001) Rock types of South Pole-Aitken basin and extent of basaltic volcanism. *J Geophys Res* 106(E11):28,001-28,022
- Pike RJ (1977) Apparent depth/apparent diameter relation for lunar craters. *Proc Lunar Planet Sci* 8:3427-3436
- Pike RJ (1980) Geometric interpretation of lunar craters. U.S. Geol. Survey Prof. Paper, 1046-C
- Pike RJ (1988) Geomorphology of impact craters on Mercury. In: *Mercury*. Vilas F, Chapman CR, Matthews MS (eds), Univ. Arizona Press, p 165-273
- Prettyman TH, Feldman WC, Lawrence DJ, McKinney GW, Binder AB, Elphic RC, Gasnault OM, Maurice S, Moore KR (2002) Library least squares analysis of lunar Prospector gamma ray spectra. *Lunar Planet Sci XXXIII*: #2012
- Pritchard ME, Stevenson DJ (2000) The thermochemical history of the Moon: Constraints and major questions. *Lunar Planet Sci XXXI*:#1878
- Rhodes JM (1977) Some compositional aspects of lunar regolith evolution. *Phil Trans A* 285, 1327:293-301
- Rhodes JM, Hubbard NJ (1973) Chemistry, classification, and petrogenesis of Apollo 15 mare basalts. *Proc Lunar Sci Conf* 4:1127-1148

- Rhodes JM, Brannon JC, Rodgers KV, Blanchard DP, Dungan MA (1977) Chemistry of Apollo 12 mare basalts - Magma types and fractionation processes. Proc Lunar Sci Conf 8:1305-1338
- Richmond NC, Hood LL, Mitchell DL, Lin RP, Acuña MH, Binder AB (2005) Correlations between magnetic anomalies and surface geology antipodal to lunar impact basins. J Geophys Res 110, doi 10.1029/2005JE002405
- Ringwood AF, Essene E (1970) Petrogenesis of Apollo 11 basalts, internal constitution, and origin of the Moon. Proc Apollo 11 Lunar Sci Conf:769-799
- Ringwood AF, Kesson SE (1976) A dynamic model for mare basalt petrogenesis, Proc Lunar Sci Conf 7:1697-1722
- Robinson MS, Jolliff BL (2002) Apollo 17 landing site: Topography, photometric corrections, and heterogeneity of the surrounding highland massifs. J Geophys Res 107, doi 10.1029/2001JE001614
- Ryan MR (1987) Elasticity and contractancy of Hawaiian olivine tholeiite and its role in the stability and structural evolution of subcaldera magma reservoirs and rift systems. In: Volcanism in Hawaii I. Decker RW, Wright TL, Stauffer PH (eds) USGS Prof. Paper 1350:1395-1447
- Ryder G (1990) Accretion and bombardment in the early Earth-Moon system: The lunar record. LPI Contribution 746: 42, Lunar and Planetary Institute
- Ryder G (2002) Mass flux in the ancient Earth-Moon system and benign implications for the origin of life on Earth. J Geophys Res 107, doi 10.1029/2001JE001583
- Ryder G, Spudis PD (1980) Volcanic rocks in the lunar highlands. In: Proc of the Conference on the Lunar Highlands Crust. Pergamon Press, p 353-375
- Ryder G, Schmitt HH, Spudis PD (eds) (1992) Workshop on Geology of the Apollo 17 Landing Site, LPI Tech. Rpt. 92-09, Part 1, Lunar and Planetary Institute
- Ryder G, Koeberl C, Mojzsis SJ (2000) Heavy bombardment of the Earth at ~3.85 Ga: The search for petrographic and geochemical evidence. In: Origin of the Earth and Moon. Canup RM, Righter K (eds) Univ. of Arizona Press, p 475-492
- Schaal RB, Hörz F (1977) Shock metamorphism of lunar and terrestrial basalts. Proc Lunar Science Conference 8: 1697-1729
- Schaal RB, Hörz F, Thompson TD, Bauer JF (1979) Shock metamorphism of granulated lunar basalt. Proc Lunar Planet Sci Conf 10:2547-2571
- Schaber GG (1973) Lava flows in Mare Imbrium: Geologic evaluation from Apollo orbital photography. Proc Lunar Planet Sci Conf 4:73-92
- Schaber GG, Boyce JM, Moore HJ (1976) The scarcity of mapable flow lobes on the lunar maria: Unique morphology of the Imbrium flows. Proc Lunar Sci Conf 7:2783-2800
- Schaefer OA, Husain L (1974) Chronology of lunar basin formation and ages of lunar anorthositic rocks. Lunar Planet Sci V:663-665
- Schmidt OY (1959) A theory of the origin of the Earth. Lawrence and Wishart
- Schmitt HH (1973) Apollo 17 report on the valley of Taurus-Littrow. Science 182:681-690
- Schmitt HH (2000a) Source and implications of large lunar basin-forming objects. Lunar Planet Sci XXXI:#1821
- Schmitt HH (2001) Lunar cataclysm? Depends on what "cataclysm" means. Lunar Planet Sci XXXII:#1133
- Schmitt RT (2000) Shock experiments with the H6 chondrite Kernoué: Pressure calibration of microscopic shock effects. Meteoritics 35:545-560
- Schubert G, Lingenfelter RE, Peale SJ (1970) The morphology, distribution, and origin of lunar sinuous rilles. Rev Geophys Space Phys 8:199-224
- Schultz PH (1976) Floor-fractured lunar craters. The Moon 15:241-273
- Schultz PH, Gault DE (1975) Seismic effects from major basin formations on the Moon and Mercury. The Moon 12: 159-177
- Schultz PH, Gault DE (1979) Atmospheric effects on martian ejecta emplacement. J Geophys Res 84:7669-7687
- Schultz PH, Spudis PD (1979) Evidence for ancient mare volcanism. Proc Lunar Planet Sci Conf 10:2899-2918
- Schultz PH, Srnka LJ (1980) Cometary collisions on the Moon and Mercury. Nature 284:22-26
- Schultz PH, Spudis PD (1983) Beginning and end of lunar mare volcanism. Nature 302:233-236
- Schultz PH, Gault DE (1990) Prolonged global catastrophes from oblique impacts. Geol Soc Am Spec Paper 247: 239-261
- Schultz PH, Anderson RR (1996) Asymmetry of the Manson impact structure: Evidence for impact angle and direction. Geol Soc Am Special Paper 302:397-417
- Schultz RA, Zuber MT (1994) Observations, models, and mechanisms of failure of surface rocks surrounding planetary surface loads. J Geophys Res 99:14,691-14,702
- Sharpton VL (1994) Evidence from Magellan for unexpectedly deep complex craters on Venus. In: Large Meteorite Impacts and Planetary Evolution. Dressler BO, Grieve RAF, Sharpton VL (eds), Special Paper 293, The Geological Society of America, Boulder, p 19-27
- Shearer CK, Newsom HE (2000) W-Hf abundances and the early origin and evolution of the Earth-Moon system. Geochim Cosmochim Acta 64:3599-3613
- Shervais JW, Taylor LA, Lindstrom MM (1985a) Apollo 14 mare basalts: Petrology and geochemistry of clasts from consortium breccia 14321. J Geophys Res 90:C375-C395

- Shervais JW, Taylor LA, Laul JC, Shih C-Y, Nyquist LE (1985b) Very high potassium (VHK) basalt: Complications in mare basalt petrogenesis. Proc Lunar Planet Sci Conf 16:D3-D18
- Shkuratov YG, Kaydash VG, Opanasenko NV (1999) Iron and titanium abundance and maturity degree distribution on the lunar nearside. Icarus 137:222-234
- Shkuratov YG, Bondarenko NV (2001) Regolith layer thickness mapping of the Moon by radar and optical data. Icarus 149:329-338
- Shoemaker EM (1964) The geology of the Moon. Scientific American 211:38-47
- Shoemaker EM (1970) Origin of fragmental debris on the lunar surface and history of bombardment of the Moon. Presentation at I Seminario de Geología Lunar, Univ. of Barcelona (Rev. January 1971)
- Shoemaker EM, Hackman R (1962) Stratigraphic basis for a lunar time scale. In: The Moon: Symposium 14 of the International Astronomical Union. Kopal Z, Mikhailov ZK (eds), Academic, p 289-300
- Shoemaker EM, Bailey NG, Batson RM, Dahlem DH, Foss TH, Grolier MJ, Goddard EM, Hait MH, Holt HE, Larson KB, Rennilson JJ, Schaber GG, Schleicher DL, Schmitt HH, Sutton RL, Swann GA, Waters AC, West MN (1970a) Geologic setting of the lunar samples returned by the Apollo 11 mission. In: Apollo 11 Preliminary Science Report 41-84, NASA SP-214
- Shoemaker EM, Batson RM, Bean AL, Conrad C Jr., Dahlem D, Goddard EN, Hait MT, Larson KB, Schaber GG, Schleicher DL, Sutton RL, Swann GA, Waters AC (1970b) Preliminary geologic investigation of the Apollo 12 landing site. Part A Geology of the Apollo 12 landing site. In: Apollo 12 Preliminary Science Report 113-182, NASA SP-235
- Shoemaker EM, Robinson MS, Eliason EM (1994) The south pole region of the Moon as seen by Clementine. Science 266:1851-1854
- Short NM, Foreman ML (1972) Thickness of impact crater ejecta on the lunar surface. Mod Geol 3:69-91
- Simonds CH, Phinney WC, Warner JL, McGee PE, Geeslin J, Brown RW, Rhodes JM (1977) Apollo 14 revisited, or breccias aren't so bad after all. Proc Lunar Sci Conf 8:1869-1893
- Simpson RA, Tyler GL (1999) Reanalysis of Clementine bistatic radar data from the lunar south pole. J Geophys Res 104:3845-3862
- Slade MA, Butler BJ, Muhleman DO (1992) Mercury radar imaging - Evidence for polar ice. Science 258:635-640
- Smith DE, Zuber MT, Neumann GA, Lemoine FG (1997) Topography of the Moon from the Clementine LIDAR. J Geophys Res 102:1591-1611
- Smith DE, Zuber MT, Solomon SC, Phillips RJ, Head JW, Garvin JB, Banerdt WB, Muhleman DO, Pettengill GH, Neumann GA, Lemoine FG, Abshire JB, Aharonson O, Brown DC, Hauck SA, Ivanov AB, McGovern PJ, Zwally HJ, Duxbury TC (1999) The global topography of Mars and implications for surface evolution. Science 284: 1495-1503
- Smith JV, Anderson AT, Newton RC, Olson EJ, Wyllie PJ, Crewe AV, Isaacson MS, Johnson D (1970) Petrologic history of the Moon inferred from petrography, mineralogy, and petrogenesis of Apollo 11 rocks. Proc Apollo 11 Lunar Sci Conf:897-925.
- Snee LW, Ahrens TJ (1975) Shock-induced deformation features in terrestrial peridot and lunar dunite. Proc Lunar Sci Conf 6:833-842
- Solomon SC (1978) The nature of isostasy on the Moon: How big of a Pratt-fall for Airy methods. Proc Lunar Planet Sci Conf 9:3499-3511
- Solomon SC, Chaiken J (1976) Thermal expansion and thermal stress in the Moon and terrestrial planets: Clues to early thermal history. Proc Lunar Sci Conf 7:3229-3243
- Solomon SC, Longhi J (1977) Magma oceanography 1: Thermal evolution. Proc Lunar Sci Conf 8:583-599
- Solomon SC, Head JW (1979) Vertical movement in mare basins: Relation to mare emplacement, basin tectonics, and lunar thermal history. J Geophys Res 84:1667-1682
- Solomon SC, Head JW (1980) Lunar mascon basins: Lava filling, tectonics, and evolution of the lithosphere. Rev Geophys Space Phys 18:107-141
- Solomon SC, Head JW (1982) Mechanisms for lithospheric heat transport on Venus: Implications for tectonic style and volcanism. J Geophys Res 87:9236-9246
- Spohn T, Konrad W, Breuer D, Ziethe R (2001) The longevity of lunar volcanism: Implications of thermal evolution calculations with 2D and 3D mantle convection models. Icarus 149:54-65
- Spudis PD (1978) Composition and origin of the Apennine Bench Formation. Lunar Planet Sci IX:1086-1088
- Spudis PD (1984) Apollo 16 site geology and impact melts: Implications for the geologic history of the lunar highlands. Proc Lunar Planet Sci Conf 15:C95-C107
- Spudis PD (1993) The Geology of Multi-ring Impact Basins. Cambridge Planet. Sci Ser. 8, Cambridge Univ. Press
- Spudis PD (1996) The Once and Future Moon. Smithsonian Institution Press
- Spudis PD, Ryder G (1981) Apollo 17 impact melts and their relation to the Serenitatis basin. In: Multi-Ring Basins, Proc Lunar Planet Sci Conf 12, Part A. Schultz PH, Merrill RB (eds) Pergamon, p 133-148
- Spudis PD, Ryder G (1985) Geology and petrology of the Apollo 15 landing site - Past, present, and future understanding. EOS 66:721, 724-726
- Spudis PD, Ryder G (eds) (1986) Geology and petrology of the Apollo 15 landing site, LPI Tech. Rpt. 86-03, Lunar and Planetary Institute

- Spudis PD, Pieters CM (1991) Global and regional data about the Moon. In: *Lunar Sourcebook*. Heiken G, Vaniman D, French B (eds) Cambridge University Press, p 595-632
- Spudis PD, Swann GA, Greeley R (1988) The formation of Hadley Rille and implications for the geology of the Apollo 15 region. *Proc Lunar Planet Sci Conf* 18:243-254
- Spudis PD, Hawke BR, Lucey PG (1989) Geology and deposits of the lunar Nectaris basin. *Proc Lunar Planet Sci Conf* 19:51-59
- Spudis PD, Reisse RA, Gillis JJ (1994) Ancient multiring basins on the Moon revealed by Clementine laser altimetry. *Science* 266:1848-1851
- Spurr JE (1944) Geology applied to selenology, Vol. I The Imbrian plain region of the Moon. Science Press
- Spurr JE (1945) Geology applied to selenology, Vol. II The features of the Moon. Science Press
- Spurr JE (1948) Geology applied to selenology, Vol. III Lunar catastrophic history. Rumford
- Spurr JE (1949) Geology applied to selenology, Vol. IV The shrunken Moon. Rumford
- Stadermann FJ, Heusser E, Jessberger EK, Lingner S, Stöffler D (1991) The case for a younger Imbrium basin - New Ar-40 - Ar-39 ages of Apollo 14 rocks. *Geochim Cosmochim Acta* 55:2339-2349
- Staid MI, Pieters C (2001) Mineralogy of the last lunar basalts: Results from Clementine, *J Geophys Res* 106:27887-27900
- Staid MI, Pieters C, Head JW (1996) Mare Tranquillitatis: Basalt emplacement history and relation to lunar samples. *J Geophys Res* 101:23213-23228
- Stöffler D (1972) Deformation and transformation of rock-forming minerals by natural and experimental shock processes: I. Behavior of minerals under shock compression. *Fortschr Miner* 49:50-113
- Stöffler D (1974) Deformation and transformation of rock-forming minerals by natural and experimental shock processes: II. Physical properties of shocked minerals. *Fortschr Miner* 51:256-289
- Stöffler D (1984) Glasses formed by hypervelocity impact. *J Non-Crystalline Solids* 67:465-502
- Stöffler D (1990) Die Bedeutung des Rieskraters für die Planeten- und Erdwissenschaften, In: *Rieskrater-Museum Nördlingen*, Hrsg. von der Stadt Nördlingen, Verlag F. Steinmeier, Nördlingen, 2. Auflage 1991, 97-114
- Stöffler D, Hornemann U (1972) Quartz and feldspar glasses produced by natural and experimental shock. *Meteoritics* 7:371-394
- Stöffler D, Reimold (1978) Experimental shock metamorphism of dunite. *Proc Lunar Planet Sci Conf* 9:2805-2824
- Stöffler D, Grieve RAF (1994) Classification and nomenclature of impact metamorphic rocks: A proposal to the IUGS Subcommission on the Systematics of Metamorphic Rocks. *Lunar Planet Sci XXV*:1347-1348. *Lunar Planet Sci Institute*
- Stöffler D, Langenhorst F (1994) Shock metamorphism of quartz in nature and experiment: I. Basic observation and theory. *Meteoritics* 29:155-181
- Stöffler D, Grieve RAF (1996) IUGS classification and nomenclature of impact metamorphic rocks: Towards a final proposal. International Symposium on the Role of Impact Processes in the Geological and Biological Evolution of Planet Earth, Postojna, Slovenia, 27.9.-2.10.1996, Abstract
- Stöffler D, Ryder G (2001) Stratigraphy and isotope ages of lunar geologic units: Chronological standard for the inner solar system. In: *Chronology and Evolution of Mars*. Kallenbach R, Geiss J, Hartmann WK (eds), Space Science Series of ISSI, Kluwer Academic Publishers, Dordrecht, *Space Science Rev* 96:9-54
- Stöffler D, Knöll HD, Marvin UB, Simonds CH, Warren PH (1980) Recommended classification and nomenclature of lunar highland rocks, In: *Proc Conf Lunar Highland Crust*. Papike JJ, Merrill RB (eds) Pergamon Press, 51-70
- Stöffler D, Bischoff A, Borchardt R, Burghelle A, Deutsch A, Jessberger EK, Ostertag R, Palme H, Spettel B, Reimold WU (1985) Composition and evolution of the lunar crust in the Descartes highlands, Apollo 16. *J Geophys Res* 90:C449-C506
- Stöffler D, Ostertag R, Jammes C, Pfannschmidt G, Sen Gupta PR, Simon SB, Papike JJ, Beauchamp RM (1986) Shock metamorphism and petrography of the Shergotty achondrite. *Geochim Cosmochim Acta* 50:889-903
- Stöffler D, Bischoff A, Buchwald U, Rubin AE (1988) Shock effects in meteorites. In: *Meteorites and the Early Solar System*. Kerridge JF, Matthews MS (eds) University of Arizona Press, p 165-205
- Stöffler D, Keil K, Scott ERD (1991) Shock metamorphism of ordinary chondrites. *Geochim Cosmochim Acta* 55:3845-3867
- Strom RG (1964) Analysis of lunar lineaments, I: Tectonic maps of the Moon. *Univ. of Arizona Lunar Planet Lab Comm* 2:205-216
- Strom RG, Neukum G (1988) The cratering record on Mercury and the origin of impacting objects. In: *Mercury*. Vilas F, Chapman CR, Matthews MS (eds), Univ. Arizona Press, p 336-373
- Stuart-Alexander DE, Wilhelms DE (1975) The Nectarian system, a new time-stratigraphic unit. *USGS Journal of Research* 3:53-58
- Swann GA, Trask NJ, Hait MH, Sutton RL (1971) Geologic setting of the Apollo 14 samples. *Science* 173:716-719
- Swann GA, Bailey NG, Batson RM, Freeman VL, Hait MH, Head JW, Holt HE, Howard KA, Irwin JB, Larson KB, Muehlberger WR, Reed VS, Rennilson JJ, Schaber GG, Scott DR, Silver LT, Sutton RL, Ulrich GE, Wilshire HG, Wolfe EW (1972) Preliminary geologic investigation of the Apollo 15 landing site. In: *Apollo 15 Preliminary Science Report* 5-1 – 5-112, NASA-SP289

- Swann GA, Bailey NG, Batson RM, Eggleton RE, Hait MH, Holt HE, Larson KB, Reed VS, Schaber GG, Sutton RL, Trask NI, Ulrich GE, Wilshire HG (1977) Geology of the Apollo 14 landing site in the Fra Mauro highlands. USGS Prof. Paper 800:103
- Taylor GJ, Drake MJ, Wood JW, Marvin UB (1973) The Luna 20 lithic fragments, and the composition and origin of the lunar highlands. *Geochim Cosmochim Acta* 37:1087-1106
- Taylor GJ, Warren P, Ryder G, Delano J, Pieters C, Lofgren G (1991) Lunar rocks. In: *The Lunar Source Book: A User's Guide to the Moon*. Heiken G, Vaniman D, French B (eds) Cambridge Univ. Press, 183-284
- Taylor LA (2002) Origin of nanophase Fe⁰ in agglutinates: A radical new concept. In: *The Moon Beyond 2002: Next Steps in Lunar Science and Exploration*, LPI Contribution No. 1128, Lunar and Planetary Institute, p 62
- Taylor LA, Shervais JW, Hunter RH, Shih C-Y, Bansal BM, Wooden J, Nyquist LE, Laul LC (1983) Pre-4.2 AE mare-basalt volcanism in the lunar highlands. *Earth Planet Sci Lett* 66:33-47
- Taylor SR (1982) Planetary Science. Lunar and Planetary Institute
- Taylor SR, Norman MD, Esat T (1993) The lunar highland crust: The origin of the Mg suite. *Meteoritics* 28:448
- Tera F, Papanastassiou DA, Wasserburg GJ (1974) Isotopic evidence for a terminal lunar cataclysm. *Earth Planet Sci Lett* 22:1-21
- Thompson AC, Stevenson DJ (1983) Two-phase gravitational instabilities in thin disks with application to the origin of the Moon. *Lunar Planet Sci XIV*:787-78
- Thurber CH, Solomon SC (1978) An assessment of crustal thickness variations on the lunar near side: Models, uncertainties, and implications for crustal differentiation. *Proc Lunar Planet Sci Conf* 9:3481-3497
- Toksöz MN, Dainty AM, Solomon SC, Anderson KR (1973) Velocity structure and evolution of the Moon. *Proc Lunar Sci Conf* 4:2529
- Tompkins S, Pieters CM, Mustard JF, Pinet P, Chevrel S (1994) Distribution of materials excavated by the lunar crater Bullialdus and implications of the geologic history of the Nubium Region. *Icarus* 110:261-274
- Tompkins S, Margot JL, Pieters CM (2000) Effects of topography on interpreting the composition of materials within the crater Tycho. *Lunar Planet Sci XXXI*:#1401
- Tonks WB, Melosh HJ (1992) Core formation by giant impacts. *Icarus* 100:326-346
- Tonks WB, Melosh HJ (1993) Magma ocean formation due to giant impacts. *J Geophys Res* 98:5319-5333
- Touma J (2000) The phase space adventure of the Earth and Moon. In: *Origin of the Earth and Moon*. Canup RM, Righter K (eds) University of Arizona Press, p 165-178
- Ulrich GE, Hodges CA, Muehlberger WR (1981) Geology of the Apollo 16 area, central lunar highlands. USGS Prof. Paper 1048:539
- Urey HC (1966) The capture hypothesis of the origin of the Moon. In: *The Earth-Moon system*. Marsden BG, Cameron AGW (eds) Plenum Press, p 210-212
- Vinogradov AP (1971) Preliminary data on lunar ground brought to Earth by automatic probe "Luna-16". *Proc Lunar Sci Conf* 2:1-16
- Vinogradov AP (1973) Preliminary data on lunar soil collected by the Luna 20 unmanned spacecraft. *Geochim Cosmochim Acta* 37:721-729
- von Frese RRB, Tan L, Potts LV, Kim JW, Merry CJ, Bossler JD (1997) Lunar crustal analysis of Mare Orientale from topographic and gravity correlations. *J Geophys Res* 102:25,657-25,676
- Vondrak RR and Crider DH (2003) Ice at the lunar poles. *American Scientist* 91(4):322-329
- Wagner RJ, Head JW, Wolf U, Neukum G (1996) Age relations of geologic units in the Gruithuisen region of the Moon based on crater size-frequency measurements. *Lunar Planet Sci XXVII*:1367-1368
- Wagner R, Head JW, Wolf U, Neukum G (2002) Stratigraphic sequence and ages of volcanic units in the Gruithuisen region of the Moon. *J Geophys Res* 107, doi 10.1029/2002JE001844
- Warner JL (1970) Apollo 12 Lunar sample information. NASA TR-R-353:391
- Warner JL, Simonds CH, Phinney WC (1976) Genetic distinction between anorthosites and Mg-rich plutonic rocks: New data from 76255. *Lunar Planet Sci VII*:915-917
- Warner JL, Phinney WC, Bickel CE, Simonds CH (1977) Feldspathic granulitic impactites and pre-final bombardment lunar evolution. *Proc Lunar Sci Conf* 8:2051-2066
- Warner RD, Taylor GJ, Mansker WL, Keil K (1978) Clast assemblages of possible deep-seated (77517) and immiscible-melt (77538) origins in Apollo 17 breccias. *Proc Lunar Planet Sci Conf* 9:941-958
- Warren PH (1993) A concise compilation of petrologic information on possibly pristine nonmare moon rocks. *Am Mineral* 78:360-376
- Warren PH (1994) Lunar and martian meteorite delivery services. *Icarus* 111:338-363
- Warren PH (2001) Early lunar crustal genesis: The ferroan anorthosite epsilon-neodymium paradox as a possible result of crustal overturn. *Meteoritics* 36:219
- Warren PH, Wasson JT (1979) The origin of KREEP. *Rev Geophys Space Phys* 17:73-88
- Warren PH, Kallemeyn GW, Kyte FT (1997) Siderophile element evidence indicates that Apollo 14 high-Al mare basalts are not impact melts. *Lunar Planet Sci XXVIII*:1501-1502
- Wentworth SJ, McKay DS, Lindstrom DJ, Basu A, Martinez RR, Bogard DD, Garrison DH (1994) Apollo 12 ropy glasses revisited. *Meteoritics* 29:323-333

- Weitz C, Head JW (1998) Diversity of lunar volcanic eruptions at the Marius Hills complex. *Lunar Planet Sci XXIX*: #1229
- Weitz C, Head JW (1999) Spectral properties of the Marius Hills volcanic complex and implications for the formation of lunar domes and cones. *J Geophys Res* 104:18933-18956
- Weitz CM, Head JW, Pieters CM (1998) Lunar regional dark mantle deposits: Geologic, multispectral, and modeling studies. *J Geophys Res* 103:22725-22760
- Whitford-Stark JL, Head JW (1977) The Procellarum volcanic complexes: Contrasting styles of volcanism. *Proc Lunar Sci Conf* 8:2705-2724
- Whitford-Stark JL, Head JW (1980) Stratigraphy of Oceanus Procellarum basalts: Sources and styles of emplacement. *J Geophys Res* 85:6579-6609
- Wichman RW, Schultz PH (1995) Floor-fractured impact craters on Venus: Implications for igneous crater modification and local mechanism. *J Geophys Res* 100:3233-3244
- Wichman RW, Schultz PH (1996) Crater-centered laccoliths on the Moon: Modeling intrusion depth and magmatic pressure at the crater Taruntius. *Icarus* 122:193-199
- Wieczorek MA (2003) The thickness of the lunar crust: How low can you go? *Lunar Planet Sci XXXIV*:#1330
- Wieczorek MA, Phillips RJ (1998) Potential anomalies on a sphere: Applications to the thickness of the lunar crust. *J Geophys Res* 103:1715-1724
- Wieczorek MA, Phillips RJ (2000) The Procellarum KREEP Terrane: Implications for mare volcanism and lunar evolution. *J Geophys Res* 105:20,417-20,430
- Wieczorek MA, Zuber MT, Phillips RJ (2001) The role of magma buoyancy on the eruption of lunar mare basalts. *Earth Planet Sci Lett* 185:71-83
- Wilhelms DE (1970) Summary of lunar stratigraphy – Telescopic observations. USGS Prof. Paper 599:F1-F47
- Wilhelms DE (1984) Moon. In: *The Geology of the Terrestrial Planets* 107-206, NASA SP-469
- Wilhelms DE (1987) The geologic history of the Moon. U. S. Geol. Survey Prof. Paper 1348
- Williams DA, Kadel SD, Greeley R, Lesser CM (2001) Erosion by flowing lava: Geochemical evidence in the Cave Basalt, Mount St. Helens, Washington. American Geophysical Union abstract #V22B-1046
- Williams JG, Boggs DH, Yoder CF, Ratcliff JT, Dickey JO (2001a) Lunar rotational dissipation in solid body and molten core. *J Geophys Res* 106:27,933-27,968
- Williams KK, Zuber MT (1998) Measurement and analysis of lunar basin deposits from Clementine altimetry. *Icarus* 131:107-122
- Wilson L, Head JW (1981) Ascent and eruption of basaltic magma on the Earth and Moon. *J Geophys Res* 86:2971-3001
- Wilson L, Head JW (1983) A comparison of volcanic eruption processes on Earth, Moon, Mars, Io, and Venus. *Nature* 302:663-669
- Wilson L, Head JW (1990) Factors controlling the structures of magma chambers in basaltic volcanoes. *Lunar Planet Sci XXI*:1343-1344
- Wilson L, Head JW (2003) Deep generation of magmatic gas on the Moon and implications for pyroclastic eruptions. *Geophys Res Lett* 30, doi:10.1029/2002GL016082
- Wilson L, Head JW (2003b) Lunar Gruithuisen and Mairan domes: Rheology and mode of emplacement. *J Geophys Res* 108, doi 10.1029/2002JE001909
- Wolfe EW, Bailey NG, Lucchitta BK, Muehlberger WR, Scott DH, Sutton RL, Wilshire HG (1981) The geologic investigation of the Taurus-Littrow valley: Apollo 17 landing site. USGS Prof. Paper 1080:280
- Wood CA, Head JW (1975) Geologic setting and provenance of spectrally distinct pre-mare material of possible volcanic origin. In: *Conference on Origins of Mare Basalts and their Implications for Lunar Evolution*. LPI Contribution number 234:189
- Wood JA, Dickey JS, Marvin UB, Powell BN (1970) Lunar anorthosites and a geophysical model of the Moon. *Proc Apollo 11 Science Conference* 965-988
- Wu SSC, Moore HJ (1980) Experimental photogrammetry of lunar images – Apollo 15-17 orbital investigations. USGS Prof. Paper 1046:D1-D23
- Yingst RA, Head JW (1997) Volumes of lunar lava ponds in South Pole-Aitken and Orientale Basins: Implications for eruption conditions, transport mechanisms, and magma source regions. *J Geophys Res* 102(E5):10909-10932
- Yingst RA, Head JW (1998) Characteristics of lunar mare deposits in Smythii and Marginis basins: Implications for magma transport mechanisms. *J Geophys Res* 103(E5):11,135-11,158
- Zisk SH (1978) Mare Crisium area topography: A comparison of Earth-based radar and Apollo mapping camera results. In: *Mare Crisium: The View from Luna 24*. *Geochim Cosmochim Acta Suppl.* 9, Lunar and Planetary Institute. Pergamon Press, p 75-80
- Zuber MT, Smith DE, Lemoine FG, Neumann GA (1994) The shape and internal structure of the Moon from the Clementine mission. *Science* 266:1839-1843